

**miR-322/503 Cluster Drives Cardiac Differentiation by
Inhibiting CUG-binding Protein 1**

A Dissertation Presented to
the Faculty of the Department of Biology and Biochemistry
University of Houston

In Partial Fulfillment
of the Requirements for the Degree
Doctor of Philosophy

By
Xiaopeng Shen
December 2014

**miR-322/503 Cluster Drives Cardiac Differentiation by
Inhibiting CUG-binding Protein 1**

Xiaopeng Shen

APPROVED:

Dr. Robert J. Schwartz, Chairman

Dr. Yu Liu

Dr. Preethi Gunaratne

Dr. William Widger

Dr. Austin J. Cooney

**Dean, College of Natural Sciences and
Mathematics**

Acknowledgments

I accomplished this study under Dr. Schwartz, in the department of Biology and Biochemistry, at the University of Houston. I would like to express my sincere gratitude to my advisor, Dr. Robert Schwartz. When I joined this lab Dr. Schwartz and Dr. Yu Liu selected me to work on screening microRNAs which promote cardiac differentiation. I was honored to work on a project that is both innovative and significant, and increases our understanding of heart development. The research outcomes of this project might be applied to therapies against heart defects. While working on this project, I was trained in not only experimental skills but scientific thought. Dr. Schwartz's novel theories and enthusiasm for science inspires me in my work. He has provided me with patient guidance and support in my research. Through this guidance I have been able to become a competent researcher from a naive student. In addition, I am eternally grateful to Dr. Yu Liu, a member of my Ph.D. dissertation committee, who supported me with direct guidance and advice in my research. My project is derived from his preliminary work on microRNAs enriched in Mesp1 positive progenitor cells. Since I began working on this project, Dr. Yu Liu has devoted his time and attention to not only my project, but to my progress as an independent researcher. Whenever I was faced with challenges, he made every effort to help me to solve the problems. Dr. Yu Liu supported and encouraged me when I was frustrated. Due to the complex and novel nature of this project, I required

guidance and direction when I was faced with multiple avenues of research. Dr. Yu Liu always helped me to devise clear work strategies. To be honest, I occasionally felt conceited when I got positive results. It was Dr. Yu Liu who made me know who I was and how far I still had to go. I would like to express my sincere thanks to Dr. Austin Cooney, Dr. Preethi Gunaratne, and Dr. William Widger for their guidance and input as members of my dissertation committee member. Dr. Cooney and Dr. Gutanaratne not only provided me with suggestions on my research, but offered recommendation letters for my application for the American Heart Association pre-doctoral fellowship. Dr. Widger assisted me with insightful suggestions for my qualify proposal. Without their help, I could not be a true Ph.D. student.

I also want to express my gratitude to all other members in the lab. I would like to thank Dr. Wei Yu for her assistance and guidance in mouse work and in situ hybridization. I would like to thank Dr. David Stewart for his direction in mouse work and instrumentation. I would like to thank Dr. Ashley Benham and Dr. Benjamin Soibam's for their assistance in microarray, sequencing, and bioinformatic studies. I would like to thank Mani Chopra for direction with VALA microscopy. I would like to thank Rui Liang, Sian Behrendt, and Dr. Xiaoping Peng for generous help and sharing of preparations. I would like to thank Christina Ulrich for language editing of my Ph.D. dissertation. I would like to thank Dr. Hua Zhang for assistance with my personal affairs. I would like to thank

Paul Swinton for generating and culturing knockout and transgenic mice. I would like to thank Cindy Beery for assistance with my payroll and paperwork. I would like to thank Dr. Dinakar Iyer for efficient management of the Schwartz lab. All the assistance from those mentioned above was very important to me.

Finally, I want to express my thanks to my family, including my parents, my future wife, and my future parents-in-law. It is all of your support and understanding that made me brave enough and confident enough to study here. I was so driven to graduate as soon as possible because I miss you all a lot. I know you all miss me too. I know the experience I gained here will make me able to ensure a better life for us.

Houston, 2014, Xiaopeng Shen

**miR-322/503 Cluster Drives Cardiac Differentiation by
Inhibiting CUG-binding Protein 1**

An Abstract of a Dissertation

Presented to

the Faculty of the Department of Biology and Biochemistry

University of Houston

In Partial Fulfillment

of the Requirements for the Degree

Doctor of Philosophy

By

Xiaopeng Shen

December 2014

ABSTRACT

Understanding the mechanisms of early cardiac fate determination may lead to better approaches in promoting heart regeneration after injury. MicroRNAs (miRNAs) involved in the process are particularly interesting due to their small profile and relatively shorter path to clinic. With *Mesp1* as the marker, we used a *Mesp1-Cre/Rosa-EYFP* reporter system to track the earliest cardiac progenitors, and identified the miRNAs enriched in these cells. Among them, the miR-322/503 cluster is found to be a powerful regulator of the cardiac program: (1) in a screening of more than 20 cardiac progenitor cell (CPC) enriched miRNAs, miR-322/503 was the most powerful in driving calcium flux activity in mouse embryonic stem cells (mESCs) differentiation; (2) induced ectopic expression of miR-322/503 to mimic the natural course in mESCs led to α -actinin expression and significant increases of cardiac transcription factors (*Tbx5*, *Mef2C*, *Nkx2-5* and α -MHC); and (3) inhibitors of miR-322 and miR-503 significantly reduced expression of α -actinin and the above cardiac TFs. Remarkably, miR-322/503 regulates the cardiac program by inhibiting an RNA-alternative splicing/decay factor, CUG-binding protein 1 (*Celf1*), which is also known for a role in myotonic dystrophy pathogenesis. The evidences include: (i) miR-322 and miR-503 had a shared target site at the 3'UTR of *Celf1*; (ii) expression patterns of miR-322/503 and *Celf1* were mutually exclusive, with the highest *Celf1* expression in the brain; (iii) miR-322/503 repressed *Celf1* protein expression in a dose-dependent

manner; (iv) Celf1-shRNA induced up-regulation of cardiac transcription factors and α -actinin, mimicking the function of miR-322/503; and (v) the ectopic expression of Celf1 repressed expression of cardiac transcription factors, while promoted expressions of early neural markers, including Sox1, Notch3, Nestin and Pax6. In summary, we have identified a miR-322/503-Celf1 pathway that promotes cardiac differentiation by preventing activation of other lineages. This new regulatory mechanism may be used to direct cardiac regeneration after heart injury, and treat myotonic dystrophy where Celf1 up-regulation is responsible for skeletal muscle wasting and other symptoms.

CONTENTS

ABSTRACT.....	VII
CONTENTS.....	IX
LIST OF FIGURES.....	XI
LIST OF TABLES	XIII
1 INTRODUCTION	1
1.1 Heart development.....	1
1.1.1 Overview of embryogenesis	1
1.1.2 Heart development and cardiac differentiation	4
1.2 Heart failure and therapy strategies.....	10
1.2.1 Heart failure	10
1.2.2 Therapy strategies against heart failure	12
1.3 microRNA.....	15
1.3.1 Overview of microRNA	15
1.3.2 microRNAs involved in heart development and diseases	17
1.3.3 microRNA as a therapeutic approach against cardiovascular diseases	20
2 MATERIAL AND METHODS	23
2.1 Cell culture and lentivirus production	23
2.2 Ectopic microRNA expression clones construction and cardiac-driving screening	24
2.3 Inducible ectopic gene expression ES cell lines	27
2.4 Total RNA extraction and Real-Time Quantitative RT-PCR	28
2.5 microarray analysis	32
2.6 Immunostaining	32
2.7 microRNA inhibitors	33
2.8 Celf1 knockdown.....	33
2.9 Western Blots	34
2.10 Luciferase assay	34
2.11 Whole mount <i>in situ</i> hybridization	37
2.12 Transgenic miR-322/503 promoter-LacZ embryo generation and Salmon gal staining.....	40
2.13 RNA decay assay	41
3 RESULTS.....	42
3.1 miR-322/503 displayed the highest cardiac-driving potential	42

3.1.1 miR-322 and miR-503 were the top enriched microRNAs in Mesp1 positive progenitor cells.....	42
3.1.2 miR-322/503 cluster showed the highest cardiac differentiation promoting potential in screening	45
3.1.3 Expression pattern of miR-322/503 in mouse embryos	48
3.1.4 Expression pattern of miR-322/503 during ES differentiation	50
3.2 Ectopic miR-322/503 expression promoted cardiac differentiation	52
3.2.1 Inducible ectopic miR-322/503 expression cell line.....	52
3.2.2 Ectopic miR-322/503 expression promoted cardiac differentiation	54
3.2.3 Effect of ectopic miR-322/503 expression on other lineage specifications	56
3.2.4 Microarray analysis of ectopic miR-322/503 expression's effect on differentiation	58
3.3 Inhibitors of miR-322 and miR-503 blocked cardiac differentiation	61
3.4 Celf1 is a target of miR-322/503 cluster	63
3.4.1 miR-322/503 repressed Celf1 expression	63
3.4.2 miR-322/503 verse Celf1 in various tissues	66
3.4.3 miR-322/503 verse Celf1 during wild type ES differentiation	68
3.4.4 Celf1 is proven to be a miR-322/503 target by luciferase assay	70
3.4.5 Celf family expression patterns during embryo development.....	72
3.5 Celf1 knockdown mimicked the function of ectopic miR-322/503 expression on differentiation	74
3.6 Ectopic Celf1 expression inhibited cardiac and promoted neural differentiation	76
3.6.1 Inducible Celf1 overexpression ES cell line.....	76
3.6.2 Ectopic Celf1 expression inhibited cardiac differentiation	79
3.6.3 Ectopic Celf1 expression promoted neural differentiation	81
3.6.4 Celf1 promoted mRNA decay of several cardiac factors.....	83
4 DISCUSSION AND CONCLUSION	85
4.1 Discussion	85
4.1.1 Cardiac-driving microRNA screening	85
4.1.2 Effect of ectopic miR-322/503 expression on differentiation	91
4.1.3 Losses of miR-322 and miR-503 impair cardiac differentiation.....	93
4.1.4 Celf1 as a direct target of miR-322/503 in regulating cardiac differentiation.....	96
4.1.5 Celf1 inhibits cardiac differentiation and promotes neural differentiation	99
4.2 Conclusion.....	102
BIBLIOGRAPHY	105

LIST OF FIGURES

Figure 1. The plasmids used for producing <i>in situ</i> probes of Celf1, Celf2, Celf4 and Celf6.	39
Figure 2. miR-322 and miR-503 were the top enriched microRNAs in Mesp1 positive progenitor cells.	44
Figure 3. miR-322/503 displayed the highest cardiac differentiation promoting potential. .	47
Figure 4. Expression pattern of miR-322/503 in mouse embryos.	49
Figure 5. Expression patterns of miR-322 and miR-503 along wild type E14 differentiation.	51
Figure 6. Inducible ectopic miR-322/503 expression cell line.	53
Figure 7. Ectopic miR-322/503 expression promoted cardiac differentiation.	55
Figure 8. Influence of ectopic miR-322/503 expression on skeletal muscle, endothelia, endoderm and smooth muscle differentiation.	57
Figure 9. Microarray analysis of ectopic miR-322/503 expression's effect on differentiation.	60
Figure 10. Inhibitors of miR-322 and miR-503 blocked cardiac differentiation.	62
Figure 11. miR-322/503 repressed Celf1 expression.	65
Figure 12. miR-322/503 verse Celf1 in various tissues.	67
Figure 13. miR-322/503 verse Celf1 along wild type ES differentiation.	69
Figure 14. Celf1 was proven to be a miR-322/503 target.	71
Figure 15. Celf family expression patterns along embryo development.	73
Figure 16. Celf1 knockdown mimicked the function of ectopic miR-322/503 expression on differentiation.	75
Figure 17. Inducible Celf1 overexpression cell line.	78

Figure 18. Ectopic Celf1 expression inhibited cardiac differentiation.	80
Figure 19. Ectopic Celf1 expression promoted neural differentiation.....	82
Figure 20. Celf1 promoted mRNA decay of several cardiac factors.....	84
Figure 21. miR-322 and miR-503 on mouse genome.....	90
Figure 22. Working model of miR-322/503 in regulating cardiac and neural differentiations.	104

LIST OF TABLES

Table 1. Ectopic microRNA expression clones.	26
Table 2. Customized RT-qPCR Taqman primers and probes used in this study.	30
Table 3. Taqman MicroRNA and Gene Expression Assays purchased from Life Technologies.	31
Table 4. Primers used to produce luciferase assay clones.	36
Table 5. Primers and templates used to make in situ probes of Celf1, Celf2, Celf4, and Celf6.	38

1 INTRODUCTION

1.1 Heart development

1.1.1 Overview of embryogenesis

Embryogenesis is the embryo development process, which starts at fertilization. After fertilization, an egg cell and a sperm cell merge to form a zygote. The zygote then conducts mitotic division. After the first four divisions, the zygote becomes a 16-cell ball, which is known as morula. At late morula stage, the cells are separated into two groups: (1) the outer layer, called the trophoblast, which does not form an embryo; and (2) the inner cell mass (ICM), which finally develops into the embryo (1). After seven divisions, the embryo enters the blastula stage. Mammalian embryos in this stage form a blastocyst structure, in which the ICM part can be easily distinguished from the rest of the blastula. The embryo in the blastula stage has a cavity structure, the amniotic cavity, which is formed by the outer stratum derived from the trophoblast and the deep surface of the ICM as well as the primitive ectoderm and endoderm layers derived from the rest of ICM (2, 3). Then a non-transparent streak structure, known as the primitive streak, appears at the middle of the primitive ectoderm and endoderm (4). The primitive streak comes from the invagination of the ectoderm's axial part, which then grows deep into and mixes with the primitive endoderm (5, 6). The mesoderm layer then appears at the both sides of the primitive streak and grows

between the ectoderm and endoderm. At this point, the embryo has developed into three layers, the ectoderm, mesoderm, and endoderm. The embryo in this stage is called gastrula. The three layers shown in this stage will develop into different tissues and organs. For instance, the ectoderm mainly contributes to the nervous system, whereas part of the mesoderm will develop into cardiomyocytes of the heart. In mammalian animals, embryos also need formation of somites, which are derived from mesoderm and finally develop into skeletal muscle, vertebra, and other tissues. In the later stage, the embryo undergoes organogenesis and even metamorphosis, which marks the accomplishment of embryogenesis.

In murine embryonic development, the pre-natal embryogenesis process is about nineteen days. On embryonic day 1 (E1.0), fertilization is completed and the zygote divides into 2~4 cells. On E2.0, the morula structure appears. On E3.0, the blastocyst appears and the ICM structure is visible. On E5.0, rapid growth of the ICM cells leads to the formation of the epiblast. Nodal signaling pathway functions in the epiblast of this stage to induce distal visceral endoderm (DVE), which will define the anterior-posterior axis of the embryo (7). On E6.0, gastrulation begins and the mesoderm layer appears. On E6.5, the 50 earliest heart precursor cells are identified on both sides of the epiblast (8). On E7.0, amniotic cavity structure is apparent. At this stage, the heart precursors migrate towards the midline of the epiblast and form a linear heart tube. On E8.0, somites

start to appear and the embryo tail is rotating from posterior to anterior. The heart tube is also looping at this stage. On E9.0, posterior neuropore forms and closes. On E10.0, a representative feature of the embryo is deep lens indentation. At E11.0, the most obvious feature is lens vesicle closure. On E12.0, embryos display the earliest finger structure. On E15.0, the toes of embryos separate clearly. On E17.0, skin of embryos gets thickened and wrinkled. On E19.0, embryos are born and start post-natal development.

1.1.2 Heart development and cardiac differentiation

The heart is the first organ formed during embryonic development (9). The heart is comprised of several cell lineages, including cardiomyocytes, conduction system cells, smooth muscle cells, and endothelia cells (10). All cells of the heart are derived from three precursor cell populations: cardogenic mesoderm cells (CMCs), the proepicardium (PE), and cardiac neural crest cells (CNCCs) (11). CMCs forms the first heart field (FHF) and the second heart field (SHF) (10, 12), which finally develop into the main part of the myocardium of ventricular, atrial and outflow tract (OFT) (13, 14). CMCs also contribute to the formation of the endocardium (15, 16) and conduction system (17, 18). PE differentiates into cardiac fibroblasts, some cardiomyocytes, smooth muscle cells (19), and endothelia cells of coronary (20). CNCCs finally differentiate into aortic smooth muscle cells and heart nervous system (21) and contribute to the formation of cardiac valves and septation (22).

CMCs are the first population that migrates from the primitive streak (PS) to the splanchnic mesoderm, from which the cardiac crescent develops (13). At murine embryo E8.0, the bilateral cardiac crescents fuse at the midline and form the FHF linear heart tube, which then undergoes looping and further development (23). The FHF heart tube cells then recruit other CMCs to build the SHF. FHF cells

mainly contribute to the left ventricle, whereas SHF cells mainly contribute to the atria, OFT, and right ventricle (13, 24-27).

PE is a population of cells that first appears at the septum transversum's coelomic mesenchyme, which is located close to the venous pole of the E8.5 embryo's linear heart tube (28). PE gives rise to the cardiac fibroblasts, some cardiomyocytes, smooth muscle cells, and endothelial cells of coronary. In murine embryo development, PE cells migrate from the PE angle to the naked myocardium formed by CMCs and form the epicardium at E9.5~11.5 stage. The epicardium performs diverse and crucial functions in heart development, such as facilitating myocardium growth and giving rise to coronary vessels and epicardium-derived cells, which can further differentiate into other cardiac cell lineages, like cardiac fibroblasts (29-31).

CNCCs are the third heart precursor cell population. CNCCs arise from the dorsal neural tube and initially belong to cranial neural crest cells (22). After migration to the heart, CNCCs contribute to the formation of aortic smooth muscle cells, the heart conduction system, cardiac valve, and septum. Loss of CNCCs leads to abnormal development of aortic arch, OFT septation, and conduction system. Moreover, ablation of CNCCs also results in abnormal function of myocardium (32).

Cardiomyocytes, also called cardiac muscle cells, are the functional unit of heart contraction and beating. Cardiomyocytes have a relatively low self-regenerative ability (33). Therefore, if cardiomyocytes get damaged, for example in heart failure, the heart cannot repair itself easily. Moreover, the remaining cardiomyocytes respond to a decreased pumping ability caused by injured cardiomyocytes with excessive growth, which finally leads to hypertrophy and even lower pumping function. Cardiomyocytes mainly arise from differentiation of the CMCs. The differentiation process from embryonic stem cells to CMCs and finally to cardiomyocytes is termed cardiac differentiation. The cardiac differentiation is regulated by many pathways. From embryonic stem cells to mesoderm precursor cells, the process is positively regulated by bone morphogenetic protein (BMP), Activin /Nodal, Wnt/ β -catenin, and fibroblast growth factor (FGF) pathways (34, 35). As a target of Wnt/ β -catenin pathway, Brachyury /T (T) serves as a marker of mesoderm precursor cells (36). T⁺ mesodermal precursor cells display two waves of Flk-1 expressions. The first wave of T⁺ /Flk-1⁺ cells contribute to the differentiation of the hematopoietic system; the second wave of T⁺ /Flk-1⁺ cells then differentiates into cardiac mesoderm cells (16, 37, 38). From T⁺ /Flk-1⁺ mesoderm precursor cells to cardiogenic mesoderm cells, T is down regulated and Mesp1 is initially expressed as a result of transcription regulation by Eomesodermin and Wnt/ β -catenin (39-41). Mesp1, a basic helix-loop-helix (HLH) transcription factor, is expressed in the early mesoderm (42). Mesp1 is expressed at the onset of

gastrulation (E6.25 stage of mouse embryos); after Mesp1 positive cells exit the PS, Mesp1 expression dramatically drops (42, 43). Mesp1 is expressed in the progenitor cells of both FHF and SHF cells. However, the expressions of Mesp1 in FHF and SHF occur at distinct times, E6.25 for FHF and E7.25 for SHF in mouse embryo development, which indicates that FHF and SHF cells are derived from two different Mesp1 positive progenitor populations (44). Mesp1 knockout in mice causes lethal development defects, including abnormal heart morphology, cardia bifida, and abnormal developed smaller head folds (45). With the injection of Mesp1 overexpression plasmid into two-cell stage *xenopus laevis* embryos, beating region as well as myosin light chain expression could be induced in different regions of the embryos other than the region that generate heart, which indicated that Mesp1 could promote cardiac differentiation individually at early embryo stage (46). ES cells with Mesp1 overexpression, either constitutive (46) or inducible by doxycycline treatment (47), displayed precocious beating and cardiac troponin T expression (cTnT), and significant increases of cTnT and α -MHC (46-48). The descendant cells of Mesp1 overexpressing ES cells could differentiate into all kinds of cardiomyocytes in the heart (46-48). Through hanging drop differentiation of Mesp1 overexpressing ES cells, wild type ES cells and a mixture of the both cells, people found that Mesp1 promoted cardiac differentiation in a cellular autonomous mode and has no remarkable influence on surrounding cells (47). Mesp1, a pivotal transcription regulator of cardiac mesoderm, promotes expressions of downstream cardiac factors, including Tbx5

(49), Mef2c (50), Nkx2-5 (51) and Myocd (40, 52). Therefore, the appearance of Mesp1 is the earliest marker of cardiac mesoderm and the start of further cardiac differentiation. As to further differentiation from cardiac mesoderm, regulatory mechanisms of differentiations towards the FHF and SHF cells are different. Differentiation towards FHF cells is promoted by BMP (53) and FGF (54) pathways and inhibited by the Wnt pathway (55). Cardiomyocytes, as a result of FHF cell differentiation, are marked by Nkx2-5, Gata-4 (56), Tbx5 and cardiomyocyte structure proteins, including MLC2a (57) and α -MHC (58). Differentiation towards the SHF cells is promoted by BMP, FGF, Wnt, Shh and TGF- β pathways (59, 60). Isl-1, regulated by the canonical Wnt pathway (61, 62), serves as a marker of the SHF cells to differ from the FHF cells. Although Isl-1 was reported to be expressed in the early embryo development stage, Isl-1 is only expressed in SHF cells and not expressed in FHF cells in later cardiac differentiation process (60, 63). Isl-1⁺ /Nkx2-5⁺ /Flk-1⁺ SHF cells, a pool of SHF progenitor cells (15, 16, 64, 65), then differentiate into two populations: Isl-1⁺ /Flk-1⁺ SHF cells, which finally differentiate into endothelial and smooth muscle cells (64); Isl-1⁺ /Nkx2-5⁺ cells, which finally differentiate into cardiomyocytes and smooth muscle cells (66-68).

Since Mesp1 is the marker of cardiac mesoderm and promotes the expressions of downstream cardiac transcription factors, it is logical to propose that the regulators enriched in Mesp1 positive progenitor cells, such as transcription

factors and non-coding RNAs (microRNAs, LncRNAs), might promote cardiac differentiation as well. Transcription factors involved cardiac differentiation regulatory pathways are well documented as described above. However, non-coding RNAs (microRNAs, LncRNAs) involved cardiac pathways are still elusive. LncRNAs were discovered recently and described to be important regulators of various biological processes as well, but the function mechanisms of LncRNAs are still unclear. Compared to LncRNAs, microRNAs have a universal working mechanism, which makes the studies and applications of microRNAs easy and controllable. microRNAs are a group of small non-coding RNAs that regulate almost all biological processes. microRNAs are potential to be applied into therapy against diseases because they are endogenous and easily delivered. Although several microRNAs were reported to regulate heart development and diseases, those microRNAs were mostly function in the later cardiac differentiation stage or in heart disease conditions. The microRNAs that regulate earlier cardiac differentiation, especially immediately after cardiac mesoderm formation, were rarely reported. To discover those microRNAs, we performed cardiac differentiation promoting screening on the microRNAs enriched in Mesp1 expressing cells and did further studies on the microRNAs that showed the highest cardiac promoting potential.

1.2 Heart failure and therapy strategies

1.2.1 Heart failure

Heart failure is the leading cause of mortality in developed countries. In those countries, the incidence of heart failure is about 2% among adults and 6~10% among adults over 65 years old (69, 70). The incidence of heart failure is higher in men than in women. Heart failure is a disease in which the heart loses the ability to pump enough blood to meet body needs (71). Heart failure can be caused by many heart-related diseases, such as myocardial infarction and high blood pressure (69, 72). The fundamental cause of heart failure is massive injury and loss of cardiomyocytes. As cardiomyocytes lack the ability of self-regeneration, cardiomyocytes are unable to undergo proliferation to generate fresh cardiomyocytes to replace the injured ones. Heart failure is divided into three types based on which ventricle is affected: left-sided failure, right-sided failure, and biventricular failure. The symptoms of left-sided failure include the increase of breathing rate and work, displaced apex beat, and gallop rhythm. The symptoms of right-sided failure include enhanced hepatojugular reflux and obvious parasternal heave. Biventricular failure is usually characterized by pleural effusion. As a result of heart failure, the damaged heart experiences reduced contraction force and reduced ability to accommodate increased oxygen need. To compensate for the loss of contraction force, the heart then increases

heart rate and displays hypertrophy as a result of excessive growth of fibers. In heart failure, heart usually displays ventricle enlargement as compensation of contraction force loss. Researchers are seeking therapeutic approaches for heart failure. Recently, researchers have proposed a new concept – cell-based therapy against heart failure, using cardiomyocytes induced from cardiac progenitor cells, embryonic stem cells, or induced pluripotent stem cells (iPSC) to repair the injured heart (73-76). The aim of my project is to discover novel microRNAs that drive cardiac differentiation, which might then be applied into therapy against heart failure.

1.2.2 Therapy strategies against heart failure

Presently, there are two main therapeutic strategies for heart failure: drug-based therapy and cell-based therapy. Currently, drug-based therapy is unable to correct the fundamental cause of heart failure and cannot repair the injured heart. The function of drug-based therapy is mostly to relieve the symptoms caused by heart failure. Therefore, the lethal rate from heart failure is still relatively high regardless of drug-based therapy. As a response, a new therapeutic strategy – cell-based therapy has been proposed (77-79). Cell-based therapy intends to replace damaged cardiomyocytes with cardiomyocytes either induced from cardiac progenitor cells, embryonic stem cell, or iPS *in vitro* or reprogrammed from other endogenous cell lineages *in vivo* (80). In order to efficiently induce cardiomyocytes from other cell lineages, understanding the mechanisms of cardiac differentiation and reprogramming is of top priority. Currently, researchers are attempting to apply newly discovered cardiac differentiation and reprogramming regulatory pathways into cell-based therapy against heart failure.

In drug-based therapy, four major strategies have been used: vasodilators, diuretics, beta blockers, and positive inotropic agents. Vasodilators decrease either preload to lead to pooling of increased amount of blood (81, 82) or afterload to increase cardiac output (83). Diuretics improve tissue perfusion and pulmonary function (84). Beta blockers rescue some repressed nervous system

activation to strengthen heart beating and cardiac output (85). Positive inotropic agents also strengthen contractile force to increase cardiac output (86).

In cell-based therapy, two main strategies are employed. One is inducing cardiomyocytes *in vitro* and transplanting the cardiomyocytes back into damaged heart region (75); the other is directly reprogramming cardiomyocytes *in vivo*, especially directly in the damaged heart region. For both strategies, two major cell sources were used, extra-cardiac stem cells and endogenous cardiac stem cells. Extra-cardiac stem cells include embryonic stem cells, iPS, and other non-cardiac progenitor cells; endogenous cardiac stem cells include Isl-1+ cardiac stem cells, c-kit+ cardiac stem cells, Sca-1+ cardiac stem cells, epicardium derived cells, and so on (87). Currently, numerous protocols for inducing cardiomyocytes from human Pluripotent Stem Cells (hPSC) have been reported (75, 88). However, therapy against heart failure by transplanting hPSC-derived cardiomyocytes back into the body is hindered by safety problems and low engraftment to heart after injection (76). Nowadays, hPSC cells are substituted by other progenitor cells from the corresponding heart failure patients. Therefore, the safety problem, which mainly refers to immune rejection, is solved. However, there still a risk of arrhythmias if the transplanted cells cannot communicate well with heart conduction system (89). Moreover, low engraftment efficiency is still a problem. In clinical trials, transplanted cardiomyocytes are finally eliminated after a relatively long period. As a result, the majority of the patients that received the

therapy display no significant improvement. In contrast to the first strategy, the second strategy, reprogramming cardiomyocytes *in vivo*, does not have the problem of low engraftment efficiency or the safety problem. It was recently reported that cardiomyocytes could be induced from cardiac fibroblasts *in vivo* by either overexpressions of Tbx5, Mef2c, Gata4, and Hand2 or overexpressions of miR-1, miR-133, miR-208, and miR-499 (90-92). Those studies provide us with an idea that we may deliver those regulators directly into the damaged heart region to induce cardiomyocytes from residential cardiac fibroblasts and the newly generated cardiomyocytes are able to repair the damaged heart. Since microRNAs are small non-coding RNAs, they can be delivered in to bodies by more variable methods, including viral and nonviral delivery methods (93). The variety of delivery methods makes microRNAs a hopeful therapy approach against heart failure. In this study, we propose to discover novel microRNAs that can be candidates to be used to induce cardiomyocytes from other cell lineages and applied into heart failure therapy.

1.3 microRNA

1.3.1 Overview of microRNA

microRNAs (also termed as miRNA or miR) are a group of 20~22 nucleotides (nt) small non-coding RNAs. The function of microRNAs is to repress mRNA translation or induce mRNA degradation (94, 95). Mature microRNAs are produced through several steps: transcription, nuclear processing, nuclear export, and cytoplasmic processing. microRNA coding genes are mainly transcribed from genomic DNA with RNA polymerase II (96). The initial transcripts containing microRNAs are called pri-miRNAs. Pri-miRNAs are usually about 80 nt hairpin-loop RNAs that have 5' cap and 3' poly (A) end (96, 97). Pri-miRNAs then are cut by Drosha /DGCR8 complex to generate pre-miRNAs in the nucleus. Pre-miRNAs keep the hairpin-loop structure with 2 nt overhang at 3' end but do not have 5' cap and 3' poly(A) end structure (98). Pre-miRNAs then are exported into cytoplasm through Exportin-5, a nucleocytoplasmic shuttler (99). Pre-miRNAs are cleaved by Dicer to remove the loop structure that connects 5' and 3' double strand arms and in this way to generate duplexes of miRNA-5p:miRNA-3p pairs in the cytoplasm (100, 101). miRNA-5p:miRNA-3p pairs then are dissociated and one of the two strands is incorporated into RNA-induced silencing complexes (RISC). miRNA incorporated RISC then interacts with its target mRNAs to repress translation or induce mRNA degradation (102, 103). To function, miRNA

should bind to its fully or partially complementary mRNAs and in this way drives RISC to its target mRNAs. In mammals, the binding of miRNA to its target mRNAs is partially complementary but binding of a 7 nt region of miRNA, called seed sequence, to target mRNAs should be fully complementary (104). There are many bioinformatic tools for miRNA target prediction, for example RNA22 (105). By bioinformatic prediction, each miRNA could target hundreds of mRNAs because of the relative short recognition sequence, which is also proved by experiments (106-108). By targeting mRNAs, microRNAs regulate almost all biological processes, including cell differentiation, cell proliferation, insulin secretion, development timing, and apoptosis. In this project, we were studying the function of microRNAs in promoting embryonic stem cell differentiation towards cardiomyocytes.

1.3.2 microRNAs involved in heart development and diseases

microRNAs are a group of small but important regulators that function in almost all biological processes. The important role of microRNAs in heart development was shown by global deletion of all microRNAs in cardiovascular cells through conditional knockout (CKO) of Dicer in cardiovascular cells of mice. As a result, the CKO mice died due to the knockout of Dicer in cardiovascular cells (109). It is proved that microRNAs played a crucial role in the cardiovascular system. Recently, many microRNAs were reported to function in both cardiovascular development and diseases.

The heart is composed of various types of cells, including cardiomyocytes, fibroblasts, conduction system cells, vascular endothelia and smooth muscle cells (SMCs), and epicardial and endocardial cells. Regulatory microRNAs vary among differentiation processes of those cell types. For cardiomyocyte differentiation, miR-1 and miR-133 are two well-known microRNAs, and were reported to have important regulatory function during differentiation. The expressions of miR-1 and miR-133 are regulated by SRF and MEF2 (110, 111). miR-1 and miR-133 work jointly in facilitating mesoderm formation and inhibiting ectoderm and endoderm formations. However, miR-1 still promotes cardiomyocyte formation from mesoderm cells, while miR-133 inhibits this process (112). 50% of mice survived with the knockout of either miR-1 and miR-

133 Concurrently, miR-210 was reported to repress cardiac differentiation by targeting Shh pathway (113). For conduction system cell differentiation, miR-208a, a microRNA encoded by α -MHC intron, is reported to inhibit the differentiation process through repressing several important transcription factors, such as Gata4, and the gap junction protein connexin 40 (114). Beyond their functions in heart development, microRNAs also play important roles in heart diseases. miR-208a induces heart hypertrophy through targeting thyroid hormone-associated protein 1 and myostatin (114). miR-23a promotes hypertrophy by repressing ubiquitin proteolysis (115). miR-21 was shown to induce cardiac hypertrophy and fibrosis after cellular stress (116). miR-29 protects the heart from fibrosis by inhibiting the expression of extracellular matrix proteins (117).

The vascular system is composed of endothelial cells and SMCs. Angiogenesis is the process of vascular formation, in which endothelial cells form tube structure and recruit SMCs to endothelial plexus to generate new vasculature. miR-126 promotes angiogenesis by activating vascular endothelial growth factor (VEGF) signaling (118). miR-218 promotes angiogenesis by targeting SLIT-ROBO pathway (119). miR-145 is reported to be crucial for SMC differentiation. Besides angiogenesis, microRNAs also regulate vascular diseases (120). miR-21 promotes excessive SMC proliferation and restenosis; whereas, miR-145 promotes SMC differentiation and inhibits restenosis (121, 122).

Therefore, microRNAs are important regulators in almost all fields of cardiovascular development and diseases. Although many microRNAs were reported to regulate cardiac differentiation and heart disease, almost all of them worked in relatively late stage of cardiac differentiation and the disease of adult heart. For example, the fact that miR-208a is a microRNA encoded by α -MHC intron, which is expressed at late stage of cardiac differentiation, indicates miR-208a may function in relatively late stage of cardiac differentiation. In order to apply microRNAs into cell-based therapy against heart failure, we are eager to discover microRNAs functioned in relatively early cardiac differentiation stage, for example cardiac mesoderm, so that the microRNAs could be used to induce cardiomyocytes from cardiac progenitor cells or other cell lineages.

1.3.3 microRNA as a therapeutic approach against cardiovascular diseases

microRNAs are important regulators in cardiovascular development and diseases (123-126). The unique expression patterns of certain microRNAs in cardiovascular diseases make the microRNAs promising diagnostic markers (127-129). Dysregulated microRNAs are closely associated with cardiovascular diseases. As both ectopic expression and inhibition of microRNAs can now be easily introduced into cells or tissues, microRNAs are unquestionable therapeutic targets. Ectopic expression and inhibition of microRNAs can be achieved with microRNA mimics and antimiRs. Currently, antimiR-based therapy has been performed on non-human primates (130, 131). For example, the antimiR against miR-122, a microRNA that is important for hepatitis C virus (HCV) pathology, was used to treat chronically HCV-infected chimpanzees (131). The antimiR was an oligonucleotide that was complementary to miR-122 and modified with locked nucleic acids (LNAs), which increased its binding strength to miR-122. With the antimiR treatment, the chimpanzees showed weakened HCV symptoms. The application of antimiR-based therapy into human clinical trials is in process.

The fact that each microRNA targets hundreds of mRNAs is a “double-edged sword”. microRNAs commonly regulate cardiovascular diseases through synergistically targeting several genes in the same regulatory pathways, undergoing an altered mechanism when compared to classical drugs. An

individual microRNA's effect on one target is usually relatively weak, but the microRNA's effects on several synergistic targets are amplified (132). This complexity in microRNA targets allows microRNAs to overcome a common defect of classical drugs, which is cells or tissues' insensitivity to drugs after therapy for a period of time. However, this complexity may also introduce unpredicted off-target effects in different cells or tissues. For example, miR-17/92 cluster have been reported to facilitate lung cancer as well as promote cardiac differentiation (133, 134). If miR-17/92 mimics are used for heart failure therapy, potential increases in the incidence of lung cancer in patients will be a problem. Therefore, we need to find ways to take advantage of the complexity of microRNA targets and avoid off-target effects at the same time when using microRNA-involved therapies.

Meanwhile, delivery methods and safety concerns are two main challenges for microRNA-involved therapy. When introducing ectopic microRNA expression, adeno-associated virus (AAV) is the most ideal delivery method now to maintain stable and relatively high level microRNA expression level (135, 136). Currently, a cardiac-specific AAV subtype is under development. One AAV subtype – AAV9 was thought to be only cardiac affinitive (137-140) but finally proved to exist in other tissues (141, 142). In addition, the AAV delivery method might cause random insertions into genomic DNA, which is a hidden safety risk. At the same time, AAV could cause immune resistance from bodies (143). Therefore, there

are lots of concerns about AAV delivery method. Also, when introducing microRNA inhibitors to down-regulate microRNA levels, the synthetic microRNA inhibitors might be recognized as foreign antigens by the body and instigate the immune response, thereby causing inflammation (144).

In summary, microRNAs are promising diagnostic markers and therapeutic targets in spite of some challenges. As to heart failure, cell-based therapy, as a promising therapy approach, needs to induce cardiomyocytes from non-cardiomyocyte cells via certain ways, for example the treatment of microRNAs. Before applying microRNAs into heart failure therapy, it is necessary to understand how and which microRNAs regulate cardiac differentiation. Considering that microRNA involved cardiac regulatory pathways in earlier cardiac differentiation stage were still elusive, we performed this study to discover novel microRNAs that functioned in that stage. Since *Mesp1* is a pivotal regulator and the earliest marker of cardiac mesoderm (47), we performed cardiac-driving screening on the microRNAs that were enriched in *Mesp1* positive progenitor cells and did further study on the microRNAs that showed the highest cardiac-driving potential to find their functional mechanisms.

2 MATERIAL AND METHODS

2.1 Cell culture and lentivirus production

E14 cells, as mouse embryonic stem cells, were cultured on plates coated with 0.1% gelatin in KNOCKOUT™ DMEM (Gibco) supplemented with 15% embryonic certified FBS, 2 mM L-Glutamin, 100 U/mL penicillin, 100 µg/mL streptomycin, 100 nM 2-Mercaptonol, and 1.0×10^3 U/mL Leukemia inhibitory factor (LIF) (EMD Millipore). Upon differentiation, E14 cells were cultured on the plates coated with 0.5 mg/mL collagen IV (Sigma) in 70.9% Iscove's Modified Dulbecco's Medium (Gibco), 23.6% Ham's F-12 Nutrient Mix, 0.05% BSA, 100 U/mL penicillin, 100 µg/mL streptomycin, 0.45 mM 1-thioglycerol, 2 mM L-Glutamine, 0.5X B27 Supplement (Gibco), and 0.5X N2 Supplement (Gibco). The initial cell density for differentiation was 1.0×10^5 . To specify cardiac differentiation, 10 ng/mL activin (R&D) was added for the first 4 days. To specify neural differentiation, 10 µM SB431542 (TOCRIS) and 12 ng/mL FGF2 (R&D) were added.

293FT cells were cultured in Dulbecco's Modified Eagle's Medium (DMEM/HIGH) (Fisher Scientific) supplemented with 10% FBS, 100 U/mL penicillin, 100 µg/mL streptomycin and 2 mM L-Glutamine. For lentiviral production, 6×10^6 293FT cells were plated onto 10 cm plate 24 hours prior to transfection. During transfection, 8 µg lentiviral plasmid, 4 µg pMD2.G, and 6 µg psPAX2 were mixed thoroughly in

1 mL serum free DMEM. Then 36 μ L Fugene HD (Promega) was added to the plasmids mixture in serum-free DMEM. The plasmids and Fugene HD were mixed thoroughly by vortexing and incubated at room temperature for 30 minutes. The transfection mixture was then added to the 293FT cells drop-wise over the plate. The cells were then incubated at 37°C and 5% CO₂ for 72 hours. The culture medium was changed 24 hours after transfection. Then 293FT cells' medium was collected at 48 and 72 hours. The collected media was centrifuged at 2000 rpm, 4 °C for 7 minutes. Finally, the supernatant was collected and stored at -80 °C for future use.

2.2 Ectopic microRNA expression clones construction and cardiac-driving screening

microRNA inserts were amplified through PCR from G4 mouse genome using Phusion High-Fidelity DNA Polymerase (New England BioLabs). The backbone vector chosen was PII-3.8, a GFP expressing vector.. For single microRNA clones, we used T4 Polynucleotide Kinase (New England BioLabs) to add phosphates to the ends of PCR products and then cut the inserts with restriction enzymes, XhoI and HpaI. For microRNA cluster clones, the inserts were cut using EcoRI. The pII-3.8 vector was cut by XhoI and HpaI for single microRNA clones and EcoRI for microRNA clusters. We then used Rapid DNA Dephos & Ligation Kit (Roche) to dephosphorylate and ligate the single and cluster clones into the PII-3.8 backbone. All clones were sequenced to be correct. Constructed

microRNA expression clones are shown in Table 1. We then produced lentiviruses from the microRNA clones by the method described in 2.1. E14 cells were infected with the constructed lentiviruses and sorted for GFP positive cells by FAC sorting to generate stable transfection cell lines. While screening, the stable cell lines were cultured in the described cardiac differentiation medium and planted into glass bottom 96-well plates. The medium was changed every 48 hours during the differentiation period. On differentiation days 5 to 8, the cells were stained with Fluo-4 calcium indicator (Life technologies) and scanned by the Vala microscope to monitor calcium flux activities following electrical pulses. The control group used lentivirus containing blank PII-3.8 plasmid.

Table 1. Ectopic microRNA expression clones. Ectopic microRNA expression clones were constructed for cardiac-driving screening. This table includes 11 microRNA clusters and 12 single microRNAs.

Clone Name	Included microRNAs
miR-322/503 cluster	miR-322, miR-503
miR-17/92 cluster	miR-17, miR-18a, miR19a, miR19b-1, miR92a-1
miR-130b cluster	miR-130b, miR-301b
miR-369 cluster	miR-369, miR-409, miR-410, miR-412
miR-382 cluster	miR-382, miR-134
miR-27a cluster	miR-27a, miR-23a, miR-24-2
miR-99b cluster	miR-99b, let-7e
miR-192 cluster	miR-192, miR-194-2
miR-96 cluster	miR-96, miR-183
miR-141 cluster	miR-141, miR-200c
miR-425 cluster	miR-425, miR-191
miR-21	miR-21
miR-152	miR-152
miR-542	miR-542
miR-26a1	miR-26a1
miR-340	miR-340
miR-28	miR-28
miR-335	miR-335
miR-708	miR-708
miR-378	miR-378
miR-26a2	miR-26a2
miR-31	miR-31
miR-126	miR-126

2.3 Inducible ectopic gene expression ES cell lines

Inducible ectopic gene expression system was purchased from Clontech. To construct pLVX-miR-322/503 plasmid, miR-322/503 insert was PCR amplified as described above, cut by EcoRI, and ligated into pLVX-Tight-Puro vector that were cut by EcoRI using Rapid DNA Dephos & Ligation Kit (Roche). To construct pLVX-Celf1 plasmid, 3.1FlagCUGBP plasmid (contributed by Dr. Thomas A. Cooper, Balyor College of Medicine) was cut by NheI, then blunted by T4 DNA polymerase (New England BioLabs), and finally cut by NotI to release Celf1 ORF. pLVX-Tight-Puro was first cut by BamHI, then blunted by T4 DNA polymerase (New England BioLabs), and finally cut by NotI. Ligation was performed with Rapid DNA Dephos & Ligation Kit (Roche).

pLVX-miR-322/503, pLVX-Celf1, and pLVX-Tet-On Advanced vector were individually co-transfected with pMD2.G and psPAX2 into 293FT cells to generate their corresponding lentiviruses. E14 cells were first infected by pLVX-Tet-On Advanced lentivirus and selected by 200 µg/mL Neomycin from 72 hours after infection for 10 days to generate stable E14 Tet-On Advanced cell line. E14 Tet-On Advanced cells were then infected with pLVX-miR-322/503 or pLVX-Celf1 lentiviruses. These cells were then selected for successful infection by supplementing their medium with 1 µg/mL Puromycin post-infection days 3 until 5 to generate stable E14 Tet-On Advanced/ pLVX-miR-322/503 or E14 Tet-On Advanced/ pLVX-Celf1 cell lines. . After the two cell lines were established, each

line was then differentiated as described above. During differentiation, doxycycline was added from differentiation day 3 for E14 Tet-On Advanced/pLVX-miR-322/503 cells and differentiation day 4 for E14 Tet-On Advanced/pLVX-Celf1 cells to induce ectopic expressions of the corresponding genes.

2.4 Total RNA extraction and Real-Time Quantitative RT-PCR

Cells were homogenized in Tripure Isolation Reagent (Roche). 0.2 mL chloroform/ 1mL Tripure was added to the homogenized cells and the mixture was shaken vigorously for 15 seconds. The mixture was left at room temperature for 3 minutes and then centrifuged at 12000 g, 4 °C for 15 minutes. The aqueous phase of the mixture was transferred to a nuclease free tube and precipitated with isopropanol at room temperature for 10 minutes. After centrifugation, the supernatant was discarded and the pellet washed in 70% ethanol. The pellet was air-dried and dissolved in nuclease-free water. RNA concentration was determined by Nanopure measurement (General Electric).

Real-Time Quantitative RT-PCR (RT-qPCR) was used to measure the expression levels of microRNA or mRNA in total RNA samples. Taqman MicroRNA Assay systems (Life Technologies) (Table 3) and 7900HT Fast Real-Time PCR System (Applied Biosystems) were used for microRNA measurement. microRNA expression levels were related to 18s rRNA (Table3). Customized Taqman primers and probes (Table 2), TaqMan Gene Expression Assay systems

(Table 3), EuroScript RT-PCR kit (Euroclone Cytogenetics) and 7900HT Fast Real-Time PCR System (Applied Biosystems) were used to determine mRNA levels. Each well contained a 20 μ L total mixture. This mixture consisted of 10 μ L 2X buffer, 0.5 μ L 4uM forward primer, 0.5 μ L 4uM reverse primer, 0.5 μ L probe, 0.1 μ L RT enzyme, and 7.4 μ L nuclease-free water for customized Taqman primers and probes. For TaqMan Gene Expression Assays 10 μ L 2*buffer, 1 μ L primer and probe mix, 0.1 μ L RT enzyme, and 7.9 μ L nuclease-free water were used. mRNA expression levels were related to GAPDH. At least three biological replicates were performed for each condition, and then analyzed with the student's T-test.

Table 2. Customized RT-qPCR Taqman primers and probes used in this study.

Gene	Forward Primer	Probe	Reverse Primer
Oct4	CACGAGTGGAAAGCAACTC AGA	CTCTGAGCCCTGTGCCGACC G	TCTCCAACCTCACGGCATTG
Sox2	TGGACAGCTACGCGC ACA	CTGCCGTTGCTCCAG CCGTTCC	GCTGCTCCTGCATCAT GCT
Eomes	GCCGTCTGCGATTCTG CT	AGCATGCAGTTGGGA GAGCA	GGGCAGGTTCCACCGA GCT
Mesp1	GGCACCTTCGGAGGG AGTAG	TCCTGGAAGAGGCGG CAGTGATACC	CCCGGGATGCCATGT
Gsc	CTGGCCAGGAAGGTG CAC	TTCGGGAGGAGAAGG TGGAGGTCTG	CTTGGCTCGGCGGTT CTTA
Tbx5	CAGGCTGCCTTCACC CAG	AGGGCATGGAAGGAA TCAAGGTGTTTCT	CAGCCACAGTTCACG TTCATG
Mef2C	TCCACTCCCCCATTGG ACT	ACCAGACCTTCGCCG GACGAAAG	TGCGCTTGACTGAAG GACTTT
Nkx2-5	CCTCGGGCGGATAAAA AAAGA	CGCGCTGCAGAAGGC AGTGG	GCCATCCGTCTCGGC TT
α-MHC	GAATGACGGACGCC AGATG	TTGTCATCAGGCACGA AGCACTCCG	ACGACCTTGGCCTTAA CATACTC
Myf5	AGCAGCTTTGACAGC ATCTACTGT	TGCTGCAGATAAAAAGC TCCGTGTCCA	AATGCTGGACAAGCA ATCCAA
Pax3	CCAGAGGGCGAAGCT TACC	TCTGGTTTAGCAACCG CCGTGCA	GTTGATTGGCTCCAG CTTGTTT
Sox17	TCGGTCTGGAGAGCC ATGAG	TACGCCAGTGACGAC CAGAGCCAGC	CCACCACCTCGCCTTT CAC
Flk1	ACTGCAGTGATTGCCA TGTTCT	CTGGCTCCTTCTTGTC ATTGTCCTACGGA	TCATTGGCCCCGCTTAA CG
Pecam 1	CGAAGTTAGAGTTCTC CTCCAGTC	TGTCACTCTCCTCGGC GATCTTGCT	GCCGATGCCTGCAGT ACAG
Acta2	GCCCTGCCTCATGCC ATC	CACGGACAATCTCAC GCTCGGCAGT	AAGTCCAGAGCTACAT AGCACAG
myocd	CGAGAAAACAATTGGA TAGTGCC	AAGGGCAGAAACAGG TCCGACCGT	AATGTGCATAGTAACC AGGCTGG
Notch3	CTGGGAATGAAGAACATG	CATTCAAGTCTGTGAC CACCTCC	CTACCTTCAGTCTCTTGG
Sox1	ACCGCCTTGCTAGAA GTTGC	AAGCCGCCAAGGAAG CCAGCACAG	GTTGCTGCCTCCTCT TGTC
Pax6	GACTGCCAGCTTCCAT CCAC	CCTCGCCTCCAGCCT CAGCCC	AACACACCAACTTTTCG CAAGATAG
Gapdh	ACTGGCATGGCCTTC CG	TTCTACCCCAATGT GTCCGTCGT	CAGGCGGCACGTCAG ATC

Table 3. Taqman MicroRNA and Gene Expression Assays purchased from Life Technologies.

Gene	Assay ID	Catalog Number
miR-322 (424)	001076	4427975
miR-503	002456	4427975
18s rRNA	N/A	4333760F
Wnt5a	Mm00437347_m1	4331182
Hdac5	Mm01246076_m1	4453320
Tbx3	Mm01195726_m1	4453320
Celf1	Mm04279608_m1	4351372
Celf2	Mm01336295_m1	4351372
Celf4	Mm01164640_mH	4351372
Celf6	Mm01176134_m1	4351372
Nestin	Mm00450205_m1	4453320

2.5 microarray analysis

Total RNA samples were sent to Phalanx Biotech Company (CA, USA) for Mouse OneArray microarray analysis. Each sample was performed in triplicate. Data were initially statistically analyzed by Phalanx. Further analysis in the form of gene ontology (GO) was completed in our lab with the assistance from Benjamin Soibam to determine gene changes in each biological process.

2.6 Immunostaining

The cells on plates or slides were fixed with 4% Paraformaldehyde (PFA) and blocked with Phosphate-Buffered Saline (PBS) + 0.1% Triton-100 + 10% normal goat or donkey serum, dependent on the primary antibody source. The cells were then incubated in primary antibodies at room temperature overnight. The primary antibodies included mouse monoclonal antibody against sarcomeric α -Actinin (1:100, Novus Biologicals), mouse monoclonal antibody against SM-actin (1:100, Santa Cruz), goat antibody against VE-Cadherin (1:50, Santa Cruz), and mouse monoclonal antibody against TuJ1 (1:100, Thermo). On the following day, the cells were incubated in fluorescence conjugated secondary antibodies for 90 minutes. The secondary antibodies included Alexa Fluor 488 Goat Anti-Mouse IgG (H+L) Antibody (1:500, Life Technologies), Alexa Fluor 488 Donkey Anti-Goat IgG (H+L) Antibody (1:300, Life Technologies), and Alexa Fluor 594 Goat Anti-Mouse IgG (H+L) Antibody (1:500, Life Technologies). Lastly, the cells were

stained with DAPI for 5 minutes. The cells were imaged using a Nikon fluorescent microscope.

2.7 microRNA inhibitors

miRZip-424 and miRZip-503 (System Biosciences) were secured to act as inhibitors of miR-322 (also called miR-424) and miR-503. The plasmids were packaged for lentiviral production as described in 2.1. E14 cells were infected with the lentiviruses individually and selected by 1ug/mL Puromycin 72 hrs after infection for 5 days to generate stable cell lines. The lentivirus produced from lentiviral scramble shRNA (Thermo Fisher) was used as control. The stable inhibitors and control infected E14 cell lines were used in differentiation experiments.

2.8 Celf1 knockdown

Lentiviral Celf1 shRNA (Thermo Fisher) was secured to perform Celf1 knockdown. The plasmid was packaged for lentiviral production as described in 2.1. E14 cells were infected with the lentiviruses individually and selected by 1ug/mL Puromycin 72 hrs after infection for 5 days to generate stable cell lines. The lentivirus produced from lentiviral scramble shRNA (Thermo Fisher) was used as control. The Celf1 shRNA and scramble shRNA infected E14 cell lines were used in differentiation experiments.

2.9 Western Blots

Cells were lysed with RIPA buffer (50mM Tris-HCl pH 8.0, 150 mM NaCl, 1% Nonidet –P40, 0.5% sodium deoxycholate, 0.1% SDS) containing protease inhibitor. Cell lysate concentration was then calculated and normalized protein samples were then applied to 4-12% Bis-Tris gels (Life Technologies) for electrophoresis. Following electrophoresis, the separated proteins were transferred onto nitrocellulose membranes. The membranes were blocked in 3% milk in PBST, and then incubated with primary antibodies at 4 °C overnight. The primary antibodies used were mouse monoclonal antibody against Celf1 (1:1000, Santa Cruz), mouse monoclonal antibody against FLAG (1:1000, Sigma), and goat monoclonal antibody against β -Actin conjugated with HRP (1:2000, Santa Cruz). On the following day, the membranes were incubated with HRP conjugated secondary antibodies for 90 minutes. The secondary antibody used was Rabbit Anti-Mouse IgG – HRP (1:2000, Life Technologies). Chemiluminescence reagents (Amersham Biosciences) were applied to the membranes for 5 minutes at room temperature. Lastly the membranes were exposed to film. β -actin was used as the internal control.

2.10 Luciferase assay

To construct luciferase assay vectors, we obtained cDNA samples from total RNA collected from E14 cells and constructed a cDNA library as the template for PCR amplification of predicted miR-322/503 target regions. cDNA samples were

obtained using SuperScript III Reverse Transcriptase (Invitrogen). We then performed PCR amplification with Phusion High-Fidelity DNA Polymerase (New England BioLabs) using the template cDNA library and the designed primers (Table4). This allowed us to amplify out the predicted miR-322/503 target regions on Celf1 mRNA. We ligated the amplified fragments into Promega's pmirGLO vector using Clontech's In-Fusion HD Cloning kit to generate luciferase assay plasmids. All plasmids were sequenced to confirm correct insertions. Luciferase assay were performed utilizing the Dual-Luciferase Reporter Assay System (Promega). Final firefly luciferase activities were normalized to Renilla luciferase activities. At least three biological replicates were performed for each condition, and then analyzed according to the student's T-test.

Table 4. Primers used to produce luciferase assay clones.

Clone	Forward Primer	Reverse Primer
Luc1	GCTCGCTAGCCTCGAGAGCCA AAACCCTCCTCAGAG	CGACTCTAGACTCGAGAGCCA GGTTTCCCCACACAG
Luc2	GCTCGCTAGCCTCGAGTGGTC TGAACACACTTGGAC	CGACTCTAGACTCGAGCAGTAA GTCCTGGTCTCCAAAC
Luc3	GCTCGCTAGCCTCGAGGCAGA TGTTTATGCCCTTG	CGACTCTAGACTCGAGGGCTG CTCTGAGACAGTTAC

2.11 Whole mount *in situ* hybridization

Whole mount *in situ* hybridization was performed as described previously.⁽¹⁴⁵⁾ Whole mount *in situ* hybridization against Celf1, Celf2, Celf4, and Celf6 was performed on E7.5, E8.5, E9.5, and E10.5 embryos. *in situ* probes of Celf1, Celf2, Celf4, and Celf6 were created using the primers and templates listed in the Table 4. PCR amplification with Taq enzyme (Life Technologies) for each target was performed and the resulting DNA was ligated into pGEMT-easy vector (Promega) according to manufacturer's protocol. The produced plasmids were sequenced to be correct. The *in situ* probes of Celf1, Celf2, Celf4, and Celf6 were produced with the promoters and enzyme sites labeled on their corresponding plasmid maps. (Figure 1)

Table 5. Primers and templates used to make *in situ* probes of Celf1, Celf2, Celf4, and Celf6

Gene	Forward Primer	Reverse Primer	PCR template
CELF 1	GGGAAACCTTGCTGGTC TAA	GACATTCCCAAAGGGCATA AAC	3.1 FLAG CUGBP1
CELF 2	CAGGGTGATGTTCTCTC CATT	CGCCATACCTGAGAGCATT T	3.1 FLAG ETR3
CELF 4	ATGTCTGGATGGAGCTG TTTAG	GAGTGAAGCAGAGGTGAG AAG	G4 Mouse Genome
CELF 6	GGAAGCCCAGACTTACT TTGT	TCTCTCTCTCTCTCTCT CTCT	G4 Mouse Genome

Celf family *in situ* probe plasmid maps

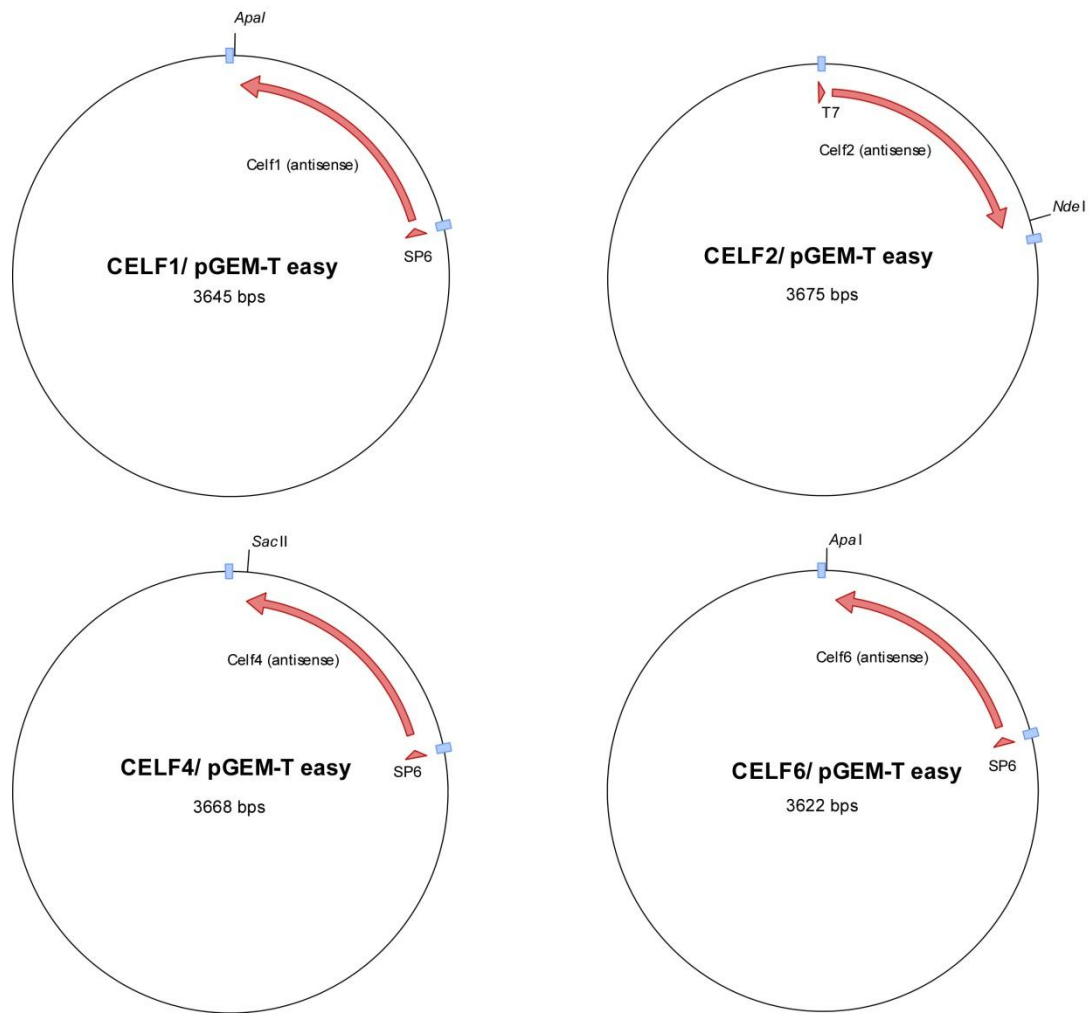


Figure 1. The plasmids used for producing *in situ* probes of Celf1, Celf2, Celf4 and Celf6. The *in situ* probes of Celf1, Celf2, Celf4, and Celf6 were produced with the promoters and enzyme sites labeled on their corresponding plasmids. For example, Celf1 *in situ* probe was produced with SP6 promoter and *Apal* site. Red arrows stand for the final probes.

2.12 Transgenic miR-322/503 promoter-LacZ embryo generation and Salmon gal staining

The promoter region of miR-322/503 was determined by searching evolutionary conserved region on vista.dcode.org website. We PCR amplified the promoter region with forward primer (5'-CGACGGTATCGATAAGCTCAAGATCATCC TCACCTACAAAACAAAATTGAG-3') and reverse primer (5'-GGATCATC GCGAGCCATGGCCCAGTGGTCCGCAG-3') from G4 mouse genome DNA. The resulting PCR fragment was ligated into HindIII and NcoI double cut Hsp68-LacZ vector using In-Fusion HD Cloning kit (Clontech). The plasmid was extracted with Maxi-Prep Kit (Qiagen), cut by XhoI and NotI, and applied onto 0.8% agarose gel for electrophoresis. The target 9810 bp band was cut and purified with QIAquick Gel Extraction Kit (Qiagen). The DNA was purified again with Elutip-d DNA purification minicolumn (Whatman). A pronuclear injection of the purified DNA was performed to generate transgenic embryos.

Transgenic embryos were fixed for 15 minutes in the fixation buffer: 0.2% glutaraldehyde, 2% formalin, 5 mM EGTA, and 2 mM MgCl₂ in 0.1 M phosphate buffer (pH 7.3). The embryos were then washed for 20 minutes three times with wash buffer (0.1% sodium deoxycholate, 0.2% IGEPAL, 2 mM MgCl₂, and 0.1 M phosphate buffer (pH 7.3)). The embryos were stained at 37 °C with staining solution: 1 mg/ml Salmon gal and 0.4 mM TNBT wash buffer. The staining was checked every 10 minutes and stopped at proper time to avoid over staining. (146)

2.13 RNA decay assay

ES cell differentiation was performed as described in 2.1. 10 µg/mL actinomycin d (Sigma) was added at 120 hours past differentiation. Total RNA samples were collected at 0, 2.5, 8 and 12 hours after the addition of actinomycin d. RT-qPCR was performed on the total RNA samples. All relative expression levels were normalized to their corresponding 0 hour relative expression levels.

3 RESULTS

3.1 miR-322/503 displayed the highest cardiac-driving potential

3.1.1 miR-322 and miR-503 were the top enriched microRNAs in Mesp1 positive progenitor cells.

Mesp1 is a pivotal cardiac mesoderm marker, which promotes the expressions of many cardiac lineage transcription factors, including Tbx5, Mef2C, and Nkx2-5.(52) Therefore, microRNAs enriched in Mesp1 positive cells are likely to promote cardiac differentiation. In order to discover microRNAs that promote cardiac differentiation, we performed screening on the miRNAs that were enriched in Mesp1 positive cells. Mesp1 lineage tracing cell line -- Mesp1^{cre/+}/ROSA EYFP/+ ESC was used to label Mesp1 ever expressing cells, which were then separated from the whole population. While Mesp1 was expressed, Cre would also be expressed. Cre then cut off one LoxP and Stop, allowing expression of EYFP. Totally, cell showed constant green fluorescence if Mesp1 was ever expressed (Figure 2A). The Mesp1 lineage-tracing cells were also verified in E9 mouse embryos. The area of the E9 embryos presenting green fluorescence was understood to be descended from Mesp1 positive cells. (Figure 2B) After 3 days hanging drop differentiation, Mesp1^{cre/+}/ROSA EYFP/+ ESCs were subjected to FACS sorting for GFP positive cells, resulting in obtaining Mesp1 positive and negative cells from the differentiating cell population (Figure

2B). Through RNA sequencing on the total RNAs extracted from FACS sorted Mesp1 positive and negative cells, we generated a list of microRNAs that were enriched in Mesp1 positive cells. The top 20 enriched microRNAs are shown in Figure 2C. In the list, miR-322 and miR-503 were the top two enriched microRNAs in Mesp1 positive cells. After consideration of enrichment level, degree of conservation between species, and whether they function as clusters or singles, 23 microRNA overexpression clones were constructed in pI3.8 vector. These vectors included 11 cluster clones and 12 single clones, to be used in cardiac-driving screening.

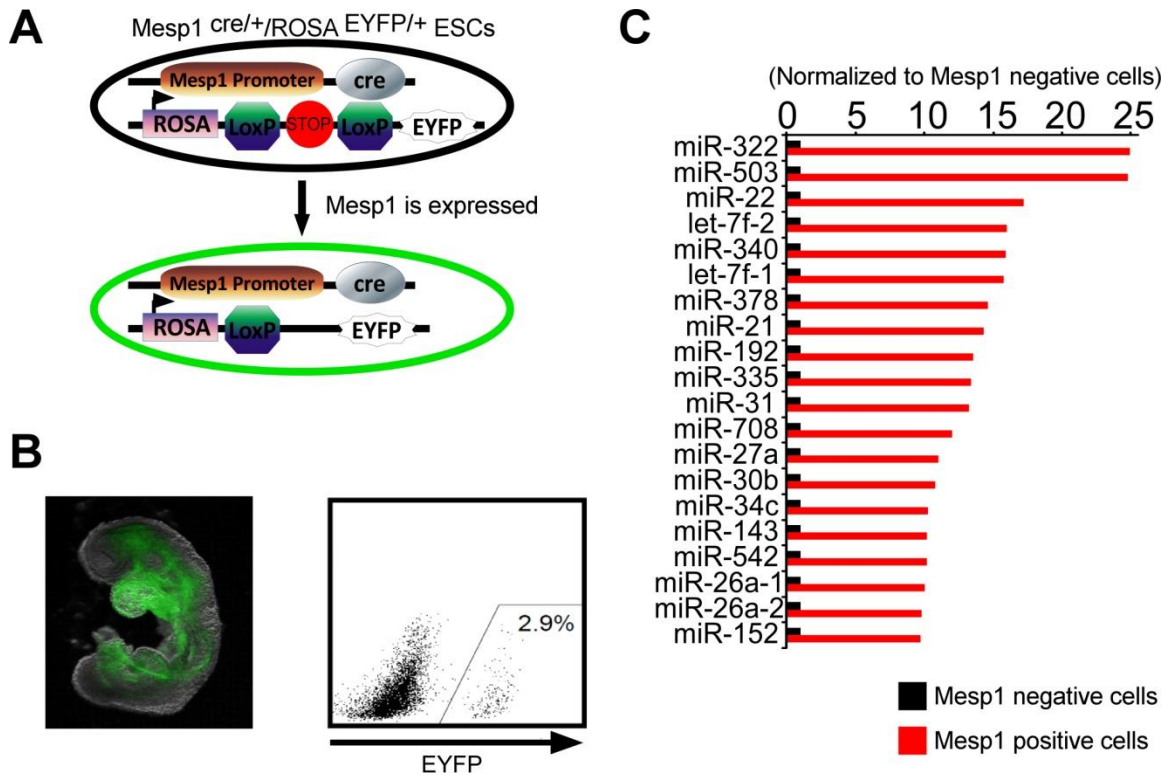


Figure 2. miR-322 and miR-503 were the top enriched microRNAs in Mesp1 positive progenitor cells. (A) Schematic diagram of Mesp1 lineage tracing cell line – Mesp1 $cre^{+/+}/Rosa\ EYFP^{+/+}$ ESCs. Mesp1 positive cells showed green fluorescence; Mesp1 negative cells showed no fluorescence. (B) Mesp1 positive cells showed EYFP fluorescence with the reporter cell line. In the left panel, Mesp1 ever expressed cells in E9 embryo were EYFP positive. In the right panel, Mesp1 positive and negative cells were separated by FACS sorting. The cells in the right corner were Mesp1 positive cells. (C) Top 20 microRNAs enriched in Mesp1 positive cells. All microRNA expressions were normalized to their corresponding expressions in Mesp1 negative cells.

3.1.2 miR-322/503 cluster showed the highest cardiac differentiation promoting potential in screening

In the screening process for cardiac-driving mRNAs, E14 cells were subcultured into collagen IV-coated 96-well glass bottom plates for monolayer differentiation as described above. Various microRNA overexpressing lentiviruses were added into each well to test the cardiac differentiation driving potential of the corresponding microRNAs. At day 5, a calcium dye, Fluo4, was added to each well in the 96-well plate. The plate was then inspected with a Vala microscope to measure the calcium flux activities of each well. Calcium flux activity was used as an indicator of cardiac differentiation. (Figure 3A) Here we defined four levels of calcium flux activity to represent four various levels of cardiac differentiation: “+++” for more than 3 peaks after one pulse and be consistent; “++” for 1~3 peaks after one pulse and be consistent; “+” for 1~3 peaks after one pulse and be inconsistent; and “-” for no observed peaks after one pulse. In the screening at differentiation day 5, miR-322/503 cluster and miR-17/92 cluster were “+++”; 8 clones were “++”; 6 clones were “+”; and 1 clone and the control were “-”. (Figure 3B) 16 out of 17 clones showed cardiac-driving potential, indicating that the majority of microRNAs enriched in Mesp1 positive progenitor cells might potentially promote cardiac differentiation. miR-17/92 cluster were reported to be a cardiac facilitating microRNA cluster (134). Since the miR-322/503 cluster induced an identical

calcium activity level as miR-17/92 cluster, the miR-322/503 cluster is potentially another cardiac-driving microRNA cluster. (Figure 3C)

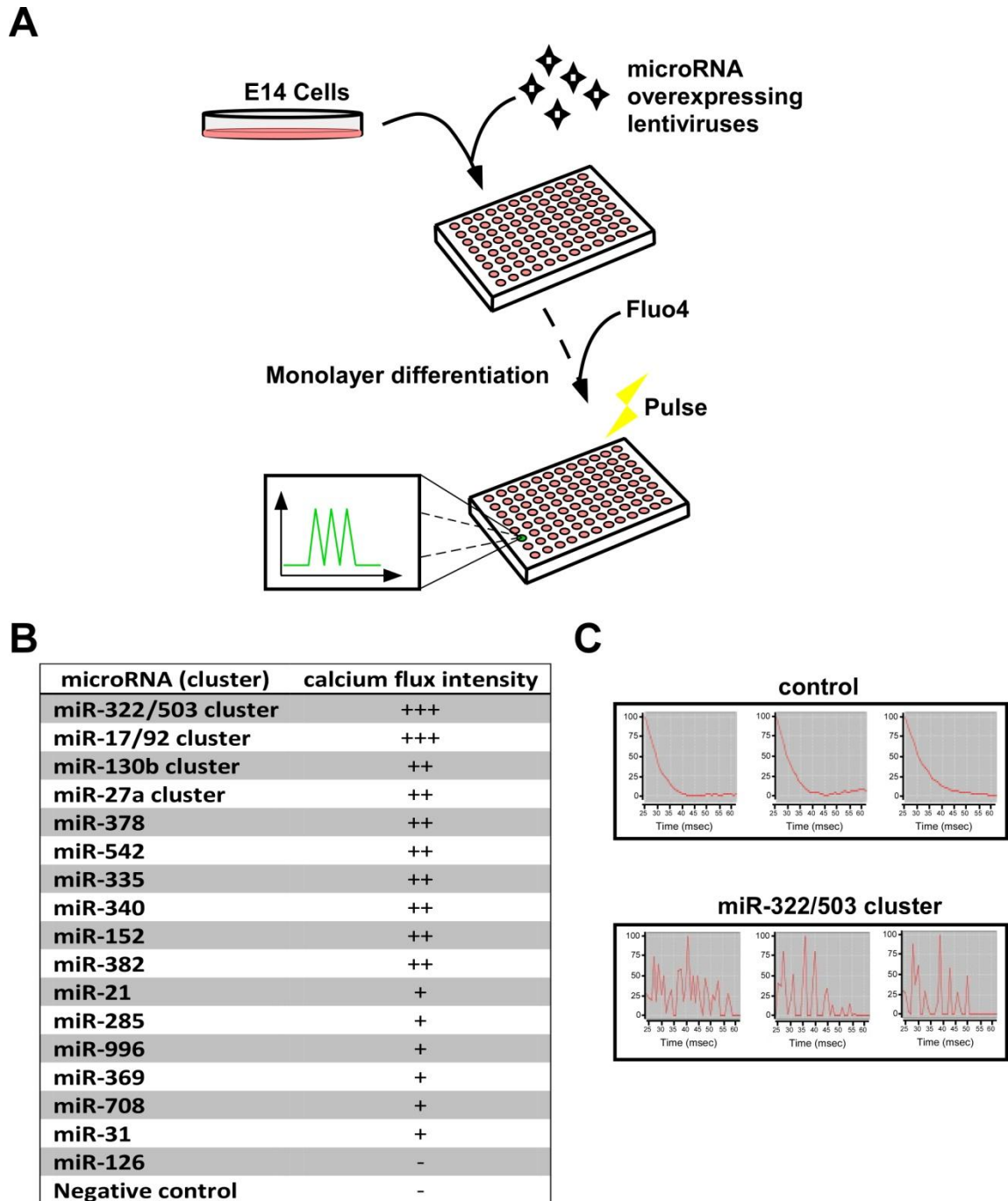


Figure 3. miR-322/503 displayed the highest cardiac differentiation promoting potential. (A) Schematic map of cardiac driving screening. (B) The calcium flux activities of differentiated E14 cells that were treated with various microRNA overexpression lentiviruses at day 5. +++: >3 peaks and consistent; ++: 1~3 peaks and consistent; +: 1~3 peaks and inconsistent; -: no peaks. (C) Calcium flux patterns of control and miR-322/503 cluster at differentiation day 5.

3.1.3 Expression pattern of miR-322/503 in mouse embryos

After discovering that miR-322/503 had the highest potential in driving cardiac differentiation, we studied the expression pattern of miR-322/503 in murine embryos. The miR-322/503 cluster, consisting of miR-322 and miR-503, is located on the murine X chromosome. Expressions of miR-322 and miR-503 are regulated by the same promoter region, which is located upstream of miR-322 and miR-503 on the chromosome through evolutionary conservation study. In order to study where miR-322/503 was expressed in murine embryo development, we constructed a LacZ promoter controlled by the miR-322/503 promoter. After injection of miR-322/503 promoter-LacZ into mouse embryos, we harvested E8.5 stage transgenic miR-322/503 promoter-LacZ embryos. Through salmon gal staining and genotyping of the E8.5 embryos, we obtained stained embryos of both transgenic LacZ positive and negative groups. After comparing LacZ positive to negative embryos, we observed that miR-322/503 was highly enriched in the heart and somites. (Figure 4A) As to E15.5 embryos, we dissected the embryos to harvest various tissues. We then extracted total RNA from those tissues and performed RT-qPCR on the RNA samples to detect miR-322 and miR-503 expressions in different tissues. We found that miR-322 and miR-503 were highly enriched in heart and tongue. (Figure 4B) To conclude, miR-322/503 was enriched in heart and skeletal muscle during murine embryo development.

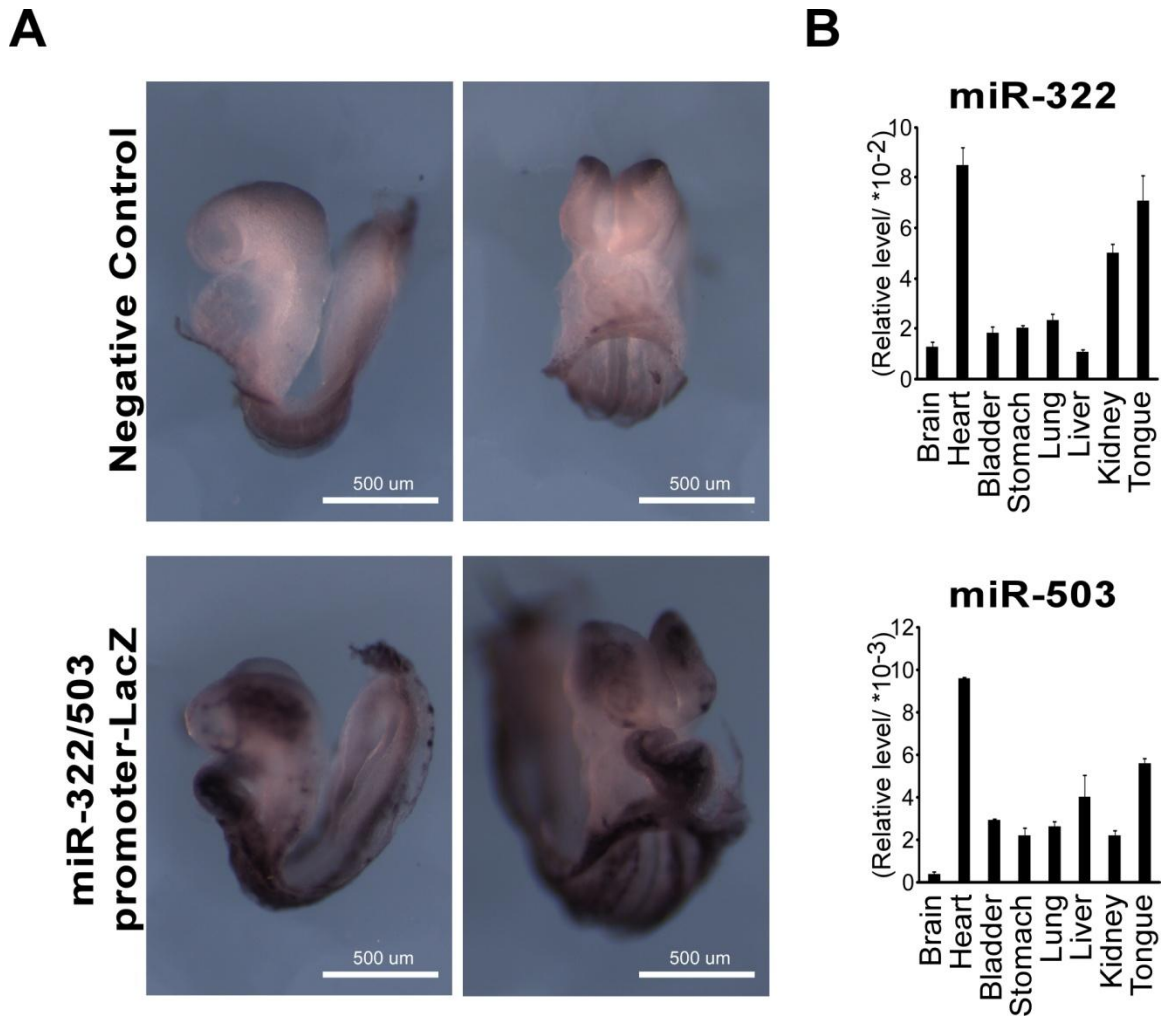


Figure 4. Expression pattern of miR-322/503 in mouse embryos. (A) Salmon gal staining of transgenic miR-322/503 promoter-LacZ embryos. The upper two panels showed the stained LacZ-negative genotyping embryos; the lower two panels showed the stained LacZ-positive genotyping embryo. The embryos were E8.5 littermates. (B) RT-qPCR of miR-322 and miR-503 in various tissues of E15.5 embryos. Expression levels were related to 18s rRNA.

3.1.4 Expression pattern of miR-322/503 during ES differentiation

Monolayer differentiation was performed on wild type E14 cells. Through RT-qPCR on the total RNAs extracted from cells collected at differentiation days 2, 3, 4, 5, 6, and 8, we observed the expression pattern of miR-322/503 during wild type E14 cell differentiation. From differentiation start point to differentiation day 3, both miR-322 and miR-503 maintained almost undetectable expression levels. The expression of both microRNAs steadily increased from day 3 until it reached peak expression levels at day 5. Following day 5, the expression of both microRNAs returned to similar values as their initial levels. (Figure 5) As previously stated, miR-322 and miR-503 were the top two enriched microRNAs in Mesp1 positive progenitor cells. Mesp1 was reported to display peak around day 3~4 (147). Therefore, the expression patterns of miR-322 and miR-503 were identical to Mesp1 expression during differentiation, but the changes in expressions of miR-322 and miR-503 were delayed when compared to Mesp1. As expressions of miR-322 and miR-503 initially increased at differentiation day 3, an inducible overexpression system was applied to allow induction of overexpression at day 3 to study the “gain-of-function” effects of miR-322/503.

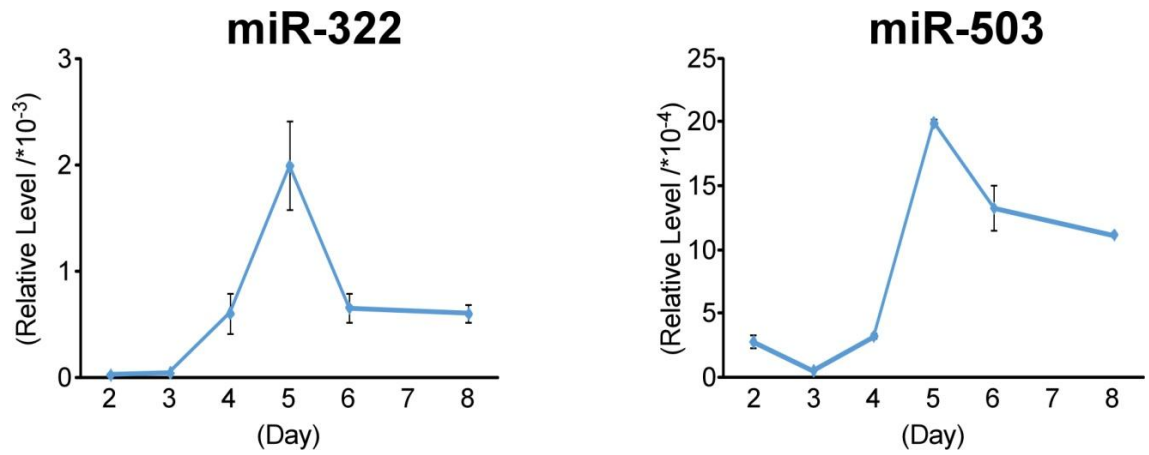


Figure 5. Expression patterns of miR-322 and miR-503 during wild type E14 differentiation. RT-qPCR was performed on total RNA samples extracted from wild type E14 differentiation day 2, 3, 4, 5, 6 and 8 cells. Expression levels are related to 18s rRNA.

3.2 Ectopic miR-322/503 expression promoted cardiac differentiation

3.2.1 Inducible ectopic miR-322/503 expression cell line

In wild type E14 differentiation, both miR-322 and miR-503 started to rise at day 3 and reached peak expression level at day 5. This indicates that miR-322 and miR-503 potentially have significant function starting from day 3 in E14 differentiation. Therefore, we would like to induce ectopic expressions of miR-322 and miR-503 from day 3. This allowed us to mimic the wild type expression patterns of both microRNAs. As miR-322 and miR-503 form the miR-322/503 cluster and are regulated by the same promoter, they were studied in tandem. Here, we used an inducible miR-322/503 overexpression E14 cell line – E14/ Tet-On Advanced/ pLVX-miR-322/503 cell to perform monolayer differentiation. Doxycycline was added from day 3 to induce ectopic miR-322/503 overexpression. The differentiation lasted for 8 days. (Figure 6A) To confirm doxycycline induced ectopic expression of miR-322/503, we treated cells with 1 ug/mL doxycycline for 24 hours, extracted total RNA from the cells and performed RT-qPCR to test the expression levels of miR-322 and miR-503 with and without doxycycline treatment. In comparison to non-treated group, expression levels of both miR-322 and miR-503 increased over 10-fold. (Figure 6B) Thus, ectopic miR-322/503 expression could be induced by doxycycline treatment on E14/ Tet-On Advanced/ pLVX-miR-322/503 cells.

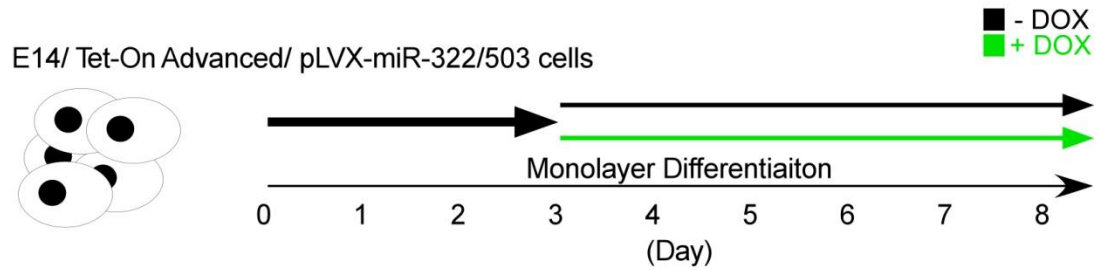
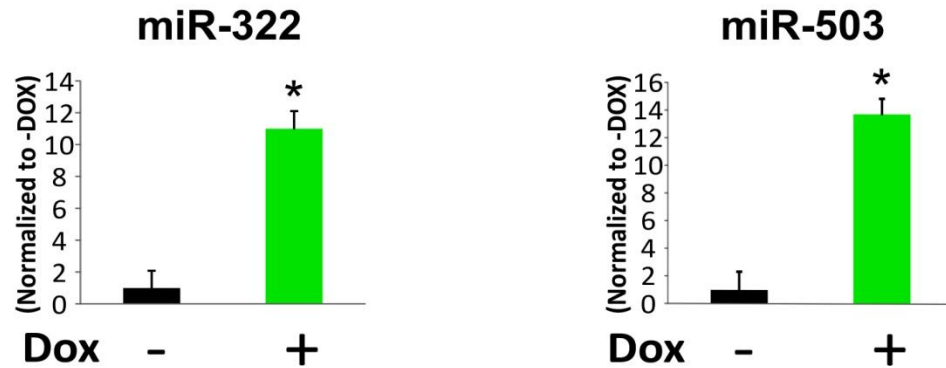
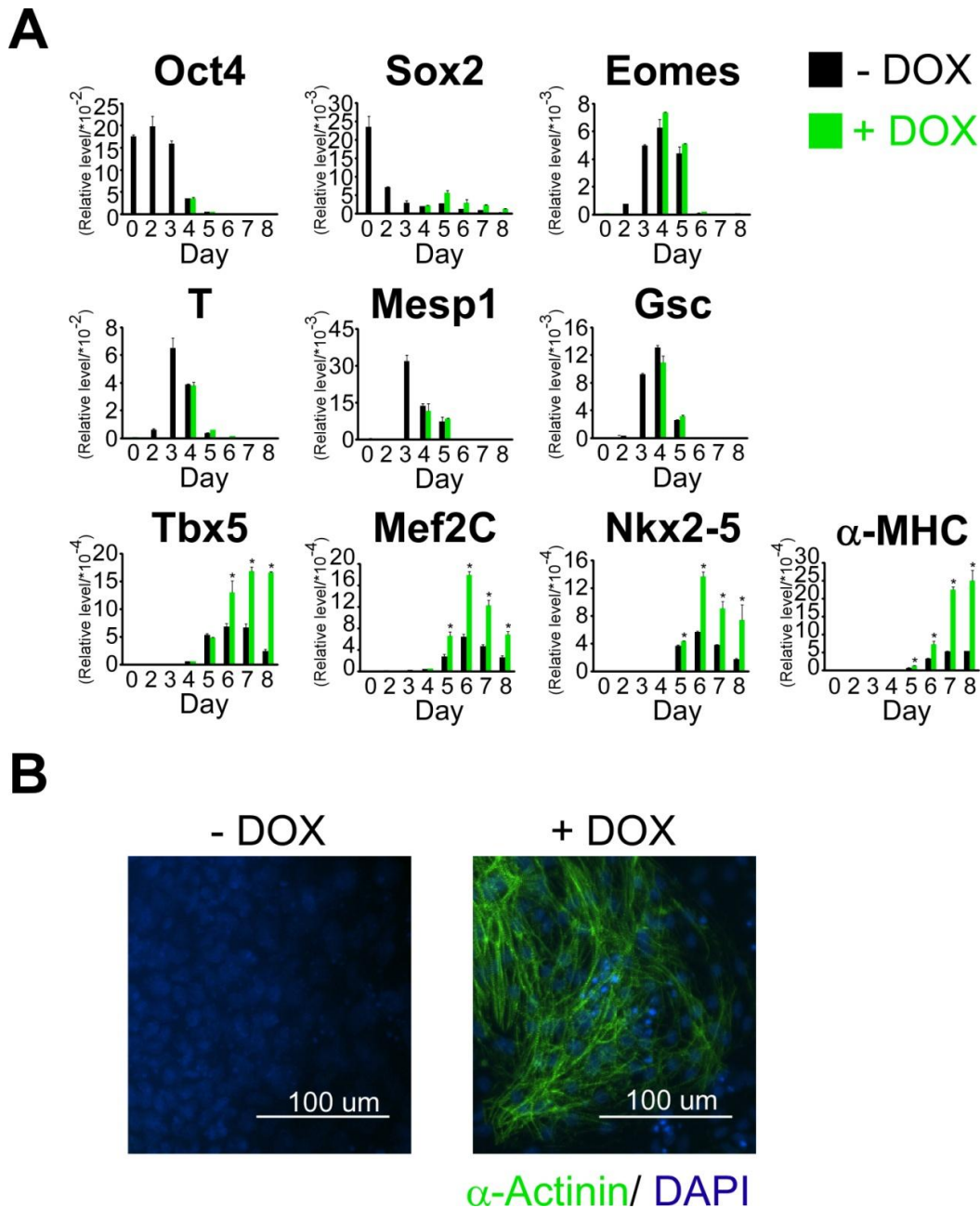
A**B**

Figure 6. Inducible ectopic miR-322/503 expression cell line. (A) Schematic diagram of monolayer differentiation of E14/ Tet-On Advanced/ pLVX-miR-322/503 cells. Doxycycline treatment started from differentiation day 3. **(B)** Verification of inductions of miR-322 and miR-503 with doxycycline treatment on E14/ Tet-On Advanced/ pLVX-miR-322/503 cells. RT-qPCR of miR-322 and miR-503 was performed on the total RNAs extracted from the cells treated with doxycycline for 24 hours and non-treated cells. Expression levels were related to 18s rRNA. *: $p < 0.05$ in t-test.

3.2.2 Ectopic miR-322/503 expression promoted cardiac differentiation

E14/ Tet-On Advanced/ pLVX-miR-322/503 cells were used for monolayer differentiation as described in the Figure 6A. These cells were then supplemented with doxycycline to induce ectopic expression of miR-322/503 from differentiation day 3 onward. Through RT-qPCR on the total collected RNAs collected during differentiation, we observed that levels of pluripotency markers (Oct4 and Sox2) and mesoderm markers (Eomes, T, Gsc and Mesp1) were not affected by doxycycline treatment. However, cardiac factors (Tbx5, Mef2C, Nkx2-5 and α -MHC) showed significant increases following doxycycline treatment. (Figure 7A) At differentiation day 6.5, we observed spontaneous beating and sarcomeric α -Actinin expression in doxycycline-treated cells, but we were unable to find similar instances in the control group. (Fig. 7A, 7B) Therefore, ectopic miR-322/503 expression significantly enhanced cardiac differentiation and induced precocious beating, but had no effect on pluripotency stage and mesoderm formation.



3.2.3 Effect of ectopic miR-322/503 expression on other lineage specifications

In order to test whether ectopic miR-322/503 expression affected differentiations of lineages besides the cardiomyocyte lineage, we performed RT-qPCR to test expression changes of other lineage makers during differentiation as described in Figure 6A. These lineages included skeletal muscle, endothelia, endoderm and smooth muscle. For skeletal muscle, early skeletal muscle markers (Pax3 and Myf5) were significantly up-regulated following doxycycline treatment, whereas later skeletal markers (MyoG, MyoD and Myf6) displayed no signal in the RT-qPCR of both doxycycline-treated and non-treated groups. (Figure 8A) This could be attributed to not favorable skeletal muscle differentiation conditions. Therefore, we discontinued the study of miR-322/503's function on differentiation towards skeletal muscle. For endothelia lineage, endothelial markers (Flk1 and Pecam1) showed remarkable increase after doxycycline treatment. (Figure 8B) However, another endothelia marker, VE-cardherin displayed no significant change with miR-322/503 overexpression. (Figure 8C) For endodermal lineage, the endoderm marker, Sox17, also showed remarkable increase following doxycycline treatment. (Figure 8B) Finally, for smooth muscle lineage, smooth muscle markers (Acta2 and SM-actin) showed no significant changes. (Figure 8B, 8C)

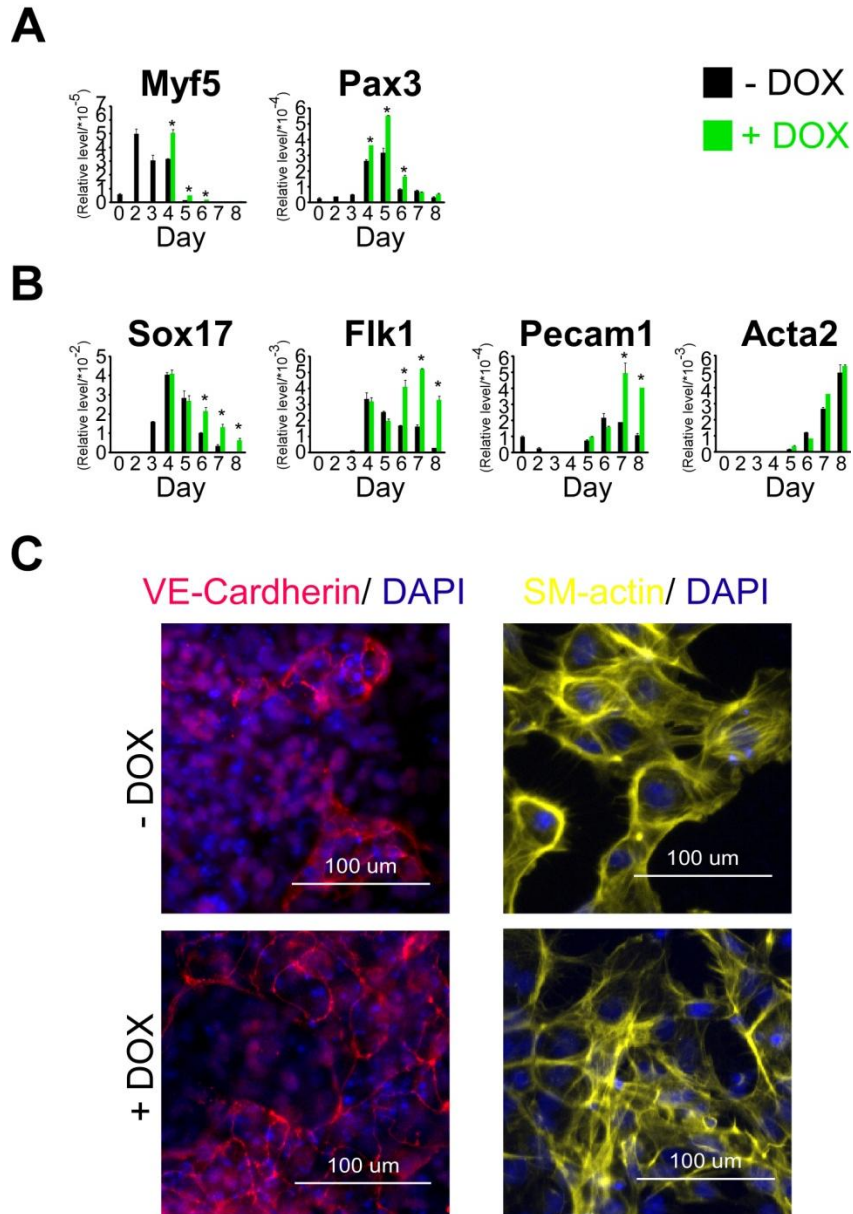


Figure 8. Influence of ectopic miR-322/503 expression on skeletal muscle, endothelia, endoderm and smooth muscle specification. (A, B) RT-qPCR of Myf5, Pax3, Sox17, Flk1, Pecam1 and Acta2 was performed on the total RNAs extracted from doxycycline-treated and non-treated monolayer differentiations of E14/ Tet-On Advanced/ pLVX-miR-322/503 cells. Doxycycline treatment started from differentiation day 3. Expression levels were related to GAPDH. *: $p < 0.05$ in t-test. **(C)** Immunostaining of VE-Cardherin and SM-actin on doxycycline treated and non-treated groups at differentiation D7.5.

3.2.4 Microarray analysis of ectopic miR-322/503 expression's effect on differentiation

In order to study the transient effects of miR-322/503 overexpression on the specifications of all lineages, we performed microarray analysis on the total RNA extracted from differentiation day 4 cells of doxycycline-treated and non-treated groups. After microarray data come out, we did gene ontology (GO) analysis on the data. Genes involved in ectoderm specification were significantly down-regulated. Genes involved in endoderm and mesoderm specifications were significantly up-regulated. Among all subgroups listed in Figure 9, neural differentiation related (ectoderm development, neural tube development), cardiac differentiation-related (heart development) and skeletal muscle-related (skeletal system development, striated muscle tissue development, skeletal muscle tissue/organ development) subgroups were most promising. Previously, we had found miR-322/503 was highly enriched in heart and skeletal muscle, but relatively low expressed in the brain. In the gain-of-function assay, ectopic miR-322/503 expression was shown to promote cardiac and skeletal muscle differentiation. These results agreed with the microarray results here. Meanwhile, we could make a hypothesis that ectopic miR-322/503 expression might inhibit neural differentiation. We also noticed that vascular formation related subgroups (blood vessel development, vasculature development) were both significantly up-regulated and down-regulated. This indicates that some genes in these

subgroups were up-regulated and the rest were down-regulated. Thus, the function of miR-322/503 on vascular formation was bidirectional. (Figure 9)

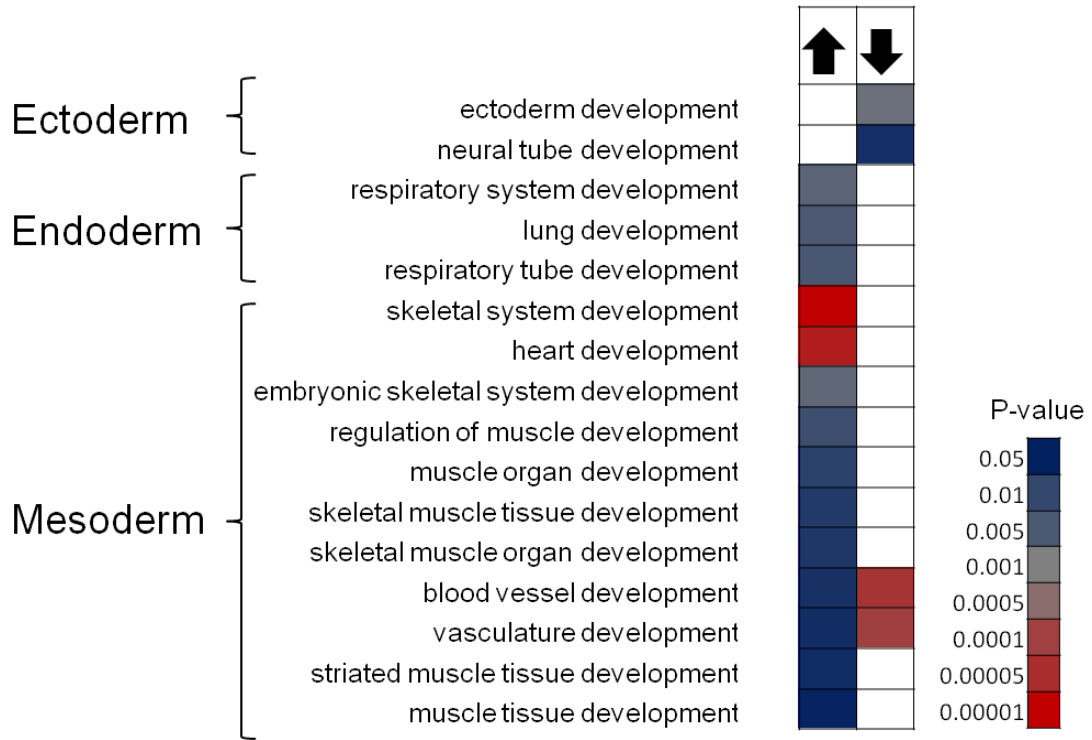


Figure 9. Microarray analysis of ectopic miR-322/503 expression's effect on differentiation. Microarray followed by GO analysis was performed on total RNA samples of differentiation day 4 cells of doxycycline-treated and non-treated groups (doxycycline treatment was at day 3). Differentiation was performed as described in Figure 6A. Up and down arrows meant up-regulated and down-regulated terms in doxycycline-treated group verse non-treated groups. Different colors stands for corresponding p-values.

3.3 Inhibitors of miR-322 and miR-503 blocked cardiac differentiation

To study whether loss of miR-322/503 would cause defects in cardiac differentiation, we employed “miRZip” microRNA inhibitors against miR-322 and miR-503. Stable miR-322-inhibitor and miR-503-inhibitor transfected E14 cell lines were established, as well as a stable scramble transfected E14 cell line through lentiviral infection followed by puromycin selection. We performed monolayer differentiation with the three cell lines listed. Total RNAs was collected for RT-qPCR and cells were gathered for immunostaining at differentiation day 8. When staining for α -actinin, miR-322-inhibitor and miR-503-inhibitor groups showed a remarkable decrease in expression of α -actinin. (Figure 10A) Through RT-qPCR of cardiac factors (Nkx2-5, Tbx5, Mef2C, α -MHC), miR-322-inhibitor and miR-503-inhibitor groups showed significantly repressed expression levels of the cardiac factors. (Figure 10B) In conclusion, inhibitors of miR-322 and miR-503 blocked cardiac differentiation.

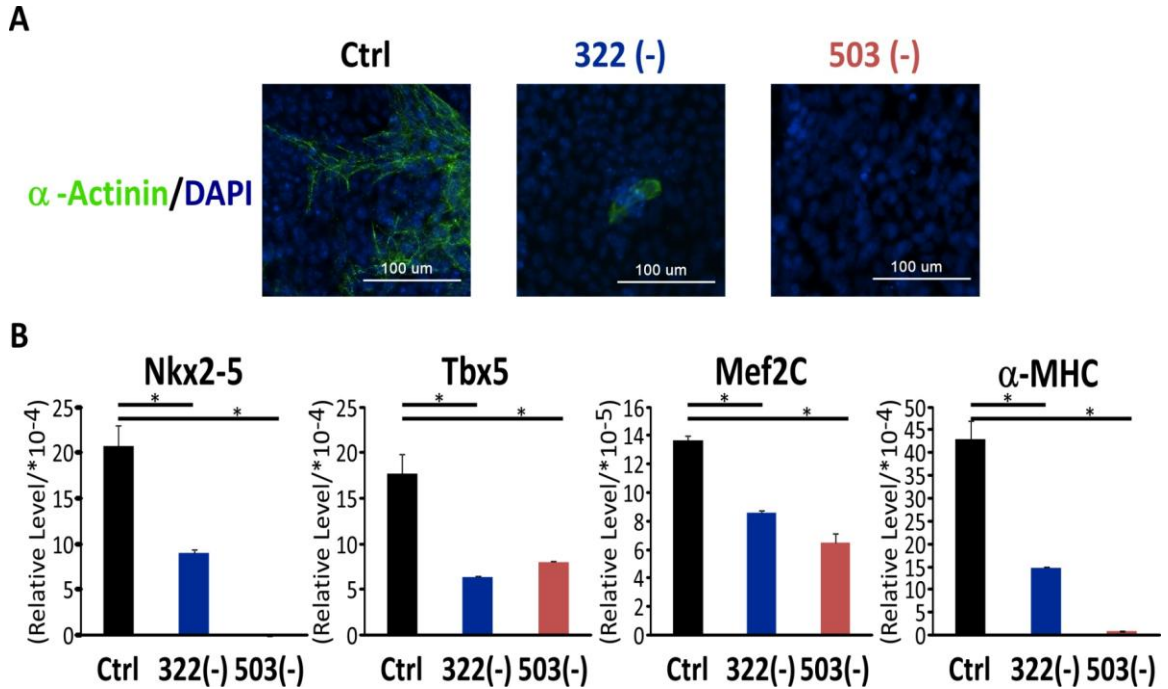


Figure 10. Inhibitors of miR-322 and miR-503 blocked cardiac differentiation. Ctrl: scramble control; 322(-): miR-322-inhibitor; 503(-): miR-503-inhibitor. **(A)** Immunostaining of α -actinin on differentiation day 8 cells of Ctrl, 322(-) and 503(-) groups. Green stands for α -actinin; Blue stands for DAPI. **(B)** RT-qPCR of cardiac factors (Nkx2-5, Tbx5, Mef2C, α -MHC) on differentiation day 8 samples of Ctrl, 322(-) and 503(-). *: $p < 0.05$ in t test.

3.4 Celf1 is a target of miR-322/503 cluster

3.4.1 miR-322/503 repressed Celf1 expression

We have shown that miR-322/503 is an important regulator in cardiac differentiation through cardiac driving screening, gain-of-function and loss-of-function studies. We then attempted to determine how miR-322/503 regulated cardiac differentiation. By studying the microarray data of ectopic miR-322/503 expression, we found that an interesting gene, CUG-binding Protein 1 (Celf1), was down-regulated by miR-322/503 induction (data not shown). Celf1 was reported to be closely related to myotonic dystrophy type1 (DM1), a disease that displayed remarkable skeletal muscle and some extent of heart defects (148). Putting those information and the important regulatory role of miR-322/503 in cardiac differentiation we just discovered together, we proposed a hypothetical pathway for how miR-322/503 regulates cardiac differentiation. We proposed that miR-322/503 potentially promotes cardiac differentiation by targeting Celf1, which might inhibit cardiac differentiation. We then tested Celf1 expression changes after miR-322/503 overexpression. By transfecting 293FT cells with p13.8-miR-322/503 plasmid, we identified dose-dependent decreases of endogenous Celf1 expression with increases of p13.8-miR-322/503 plasmid amount transfected. (Figure 11A) E14/ Tet-On Advanced/ pLVX-miR-322/503 cells were used in inducible miR-322/503 overexpression studies to study the effect of ectopic miR-

322/503 expression on differentiation. We found an obvious decrease of Celf1 expression at differentiation day 4 following doxycycline treatment at day 3 in E14/ Tet-On Advanced/ pLVX-miR-322/503 cells in differentiation as described in Figure 6A. (Figure 11B)



Figure 11. miR-322/503 repressed Celf1 expression. (A) Western blots test of Celf1 in 293FT cells transfected with increasing amount pLL3.8-miR-322/503 plasmid. Among all groups, total plasmid amount transfected were maintained the same and the differences of pLL3.8-miR-322/503 were compensated by pLL3.8 vector. “-” stands for original pLL3.8 vector transfection. (B) Western blots test of Celf1 in doxycycline-treated and non-treated differentiation day 4 E14/ Tet-On Advanced/ pLVX-miR-322/503 cells. Doxycycline treatment and differentiation process were described in figure 6A. β -actin is used as internal control.

3.4.2 miR-322/503 verse Celf1 in various tissues

After confirming miR-322/503 repressed Celf1 *in vitro*, we attempted to study whether the same reverse correlation between miR-322/503 and Celf1 was observed *in vivo*. We performed RT-qPCR of miR-322, miR-503, and Celf1 on total RNAs from tongue, stomach, brain, liver, heart, kidney, lung, and bladder of E15.5 mouse embryos. After the relative levels of miR-322, miR-503, and Celf1 were established, we introduced two formulas $-\text{Log}(\text{miR-322/Celf1})$ and $\text{Log}(\text{miR-503/Celf1})$ to display the correlation between miR-322 and miR-503 verses Celf1 in various tissues. According to these two formulas, miR-322 or miR-503 was enriched and Celf1 was expressed at low levels if values were positive; miR-322 or miR-503 was expressed at low levels and Celf1 was enriched if values were negative. After plotting the results as bar graphs, we easily established that tongue and heart for both graphs were consistently found to be the most positive, while the brain was consistently found to be the most negative. Thus, miR-322 and miR-503 were highly enriched in tongue and heart but expressed at low levels in brain, matching Figure 4B. Conversely, Celf1 was enriched in the brain but expressed at low values in the tongue and heart. (Figure 12)

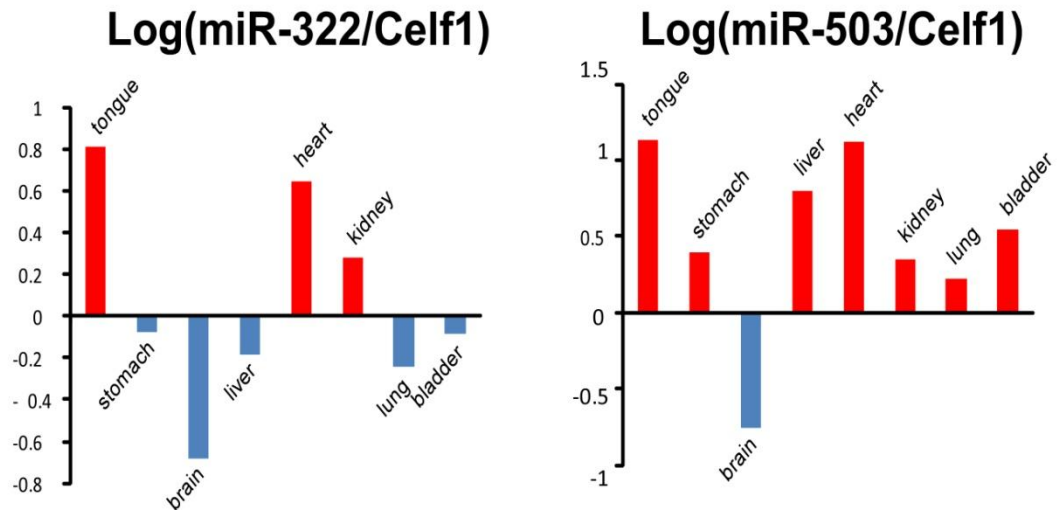


Figure 12. miR-322/503 verse Celf1 in various tissues. RT-qPCR of miR-322, miR-503 and Celf1 was performed on total RNAs extracted from various tissues of E15.5 embryos. Expression levels of miR-322 and miR-503 were related to 18s rRNA; expression levels of Celf1 was related to Gapdh. Log(miR-322/Celf1) or Log(miR-503/Celf1) were used to show correlations between of miR-322 or miR-503 and Celf1.

3.4.3 miR-322/503 verse Celf1 during wild type ES differentiation

We studied the expression pattern of Celf1 during wild type ES differentiation, through execution of RT-qPCR on total RNAs collected. Celf1 expression levels were consistently high and stable until differentiation day 4. Celf1 expression initially decreased at differentiation day 4 and reached its lowest levels at differentiation day 6. After day 6, Celf1 expression started to increase again, and reached relatively high levels at day 8. Concurrently, miR-322 and miR-503 levels displayed inverse patterns. miR-322 and miR-503 started to increase at day 3 and reached peak expression levels at day 5. Following day 5, their expressions returned to relatively low levels. (Figure 13) Therefore, Celf1 displayed a reverse pattern when compared to miR-322 and miR-503; Celf1 expression changes were on a one-day delay compared to expression changes of miR-322 and miR-503.

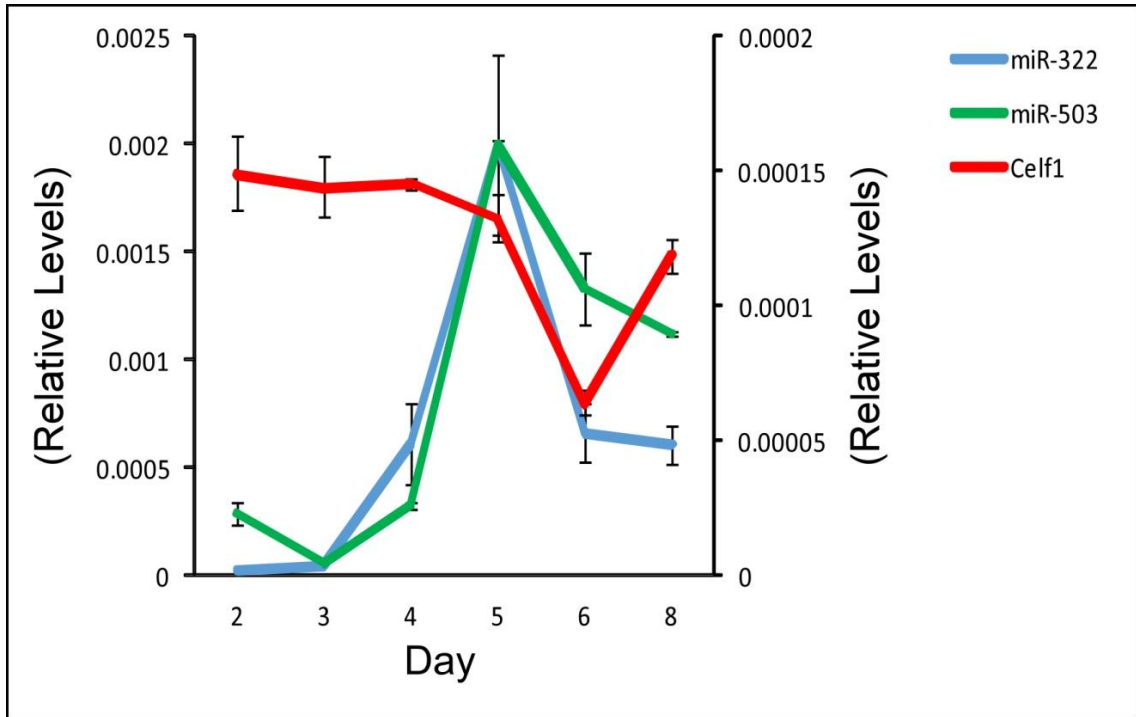


Figure 13. miR-322/503 versus Celf1 during wild type ES differentiation. RT-qPCR of miR-322, miR-503 and Celf1 during wild type E14 differentiation. Expression levels of miR-322 and miR-503 were related to 18s rRNA; expression level of Celf1 was related to GAPDH.

3.4.4 Celf1 is proven to be a miR-322/503 target by luciferase assay

We found that Celf1 expression was repressed by miR-322/503 in 293FT cells and E14 cells and that Celf1 displayed the reverse pattern compared to miR-322/503 in E15.5 mouse embryo tissues and wild type E14 cell differentiation. In order to prove that Celf1 was a true target of miR-322/503, we performed a luciferase assay. We employed the RNA-22 program to predict potential target sites of miR-322/503 on Celf1 mRNA. Six predicted sites for miR-322 and three predicted sites for miR-503 were found on Celf1 mRNA. (Figure 14A, 14B) We then copied 3 regions of Celf1 mRNA into pmirGLO vector to construct the luciferase vectors: Luc1 (including site 678, 919), Luc2 (including site 1401, 1499, 1500, 1559, 1560), Luc3 (including site 2122, 2123). (Figure 14A) We also discovered that miR-322 and miR-503 had nearly identical seed sequences, with only one nucleotide difference. (Figure 14B) That could cause miR-322 and miR-503 to share many target sites. By co-transfecting the luciferase vectors with pLL3.8-miR322/503 or blank pLL3.8 plamid, we found that miR-322/503 targeted Celf1 mRNA at site 2123 (2122). In conclusion, Celf1 was a target of miR-322/503; the target site was 2123 (2122) on Celf1 mRNA. (Figure 14C)

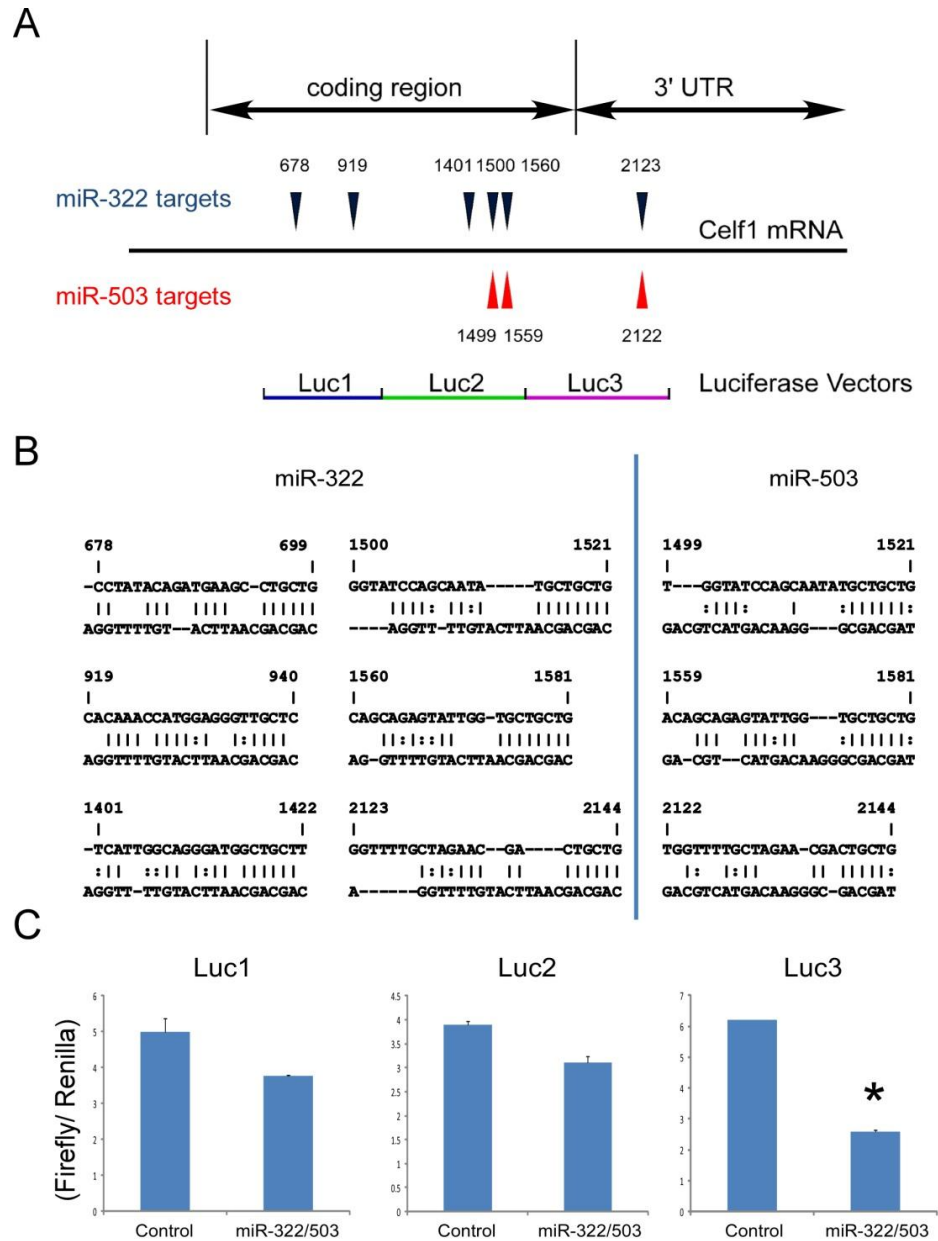


Figure 14. Celf1 was proven to be a miR-322/503 target. (A, B) Schematic diagram of predicted miR-322/503 sites on Celf1 mRNA and the regions that were cloned into pmirGLO luciferase vector for luciferase assay. There were 6 predicted sites for miR-322 and 3 predicted sites for miR-503 on Celf1 mRNA. The regions copied for luciferase assay were Luc1 (including site 678, 919), Luc2 (including site 1401, 1499, 1500, 1559, 1560) and Luc3 (including site 2122, 2123). **(C)** Luciferase assay of Luc1, Luc2 or Luc3 contained luciferase vectors with co-transfection of p13.8-miR-322/503 or blank p13.8 plasmid. Firefly activity was normalized to Renilla activity. *: $p < 0.05$ in t-test.

3.4.5 Celf family expression patterns during embryo development

After confirming that Celf1 was targeted by miR-322/503, we studied the expression patterns of Celf1 during murine embryo development. As Celf1 belongs to the Celf family, we performed *in situ* hybridization assays of Celf1, Celf2, Celf4 and Celf6 on E7.5, E8.5, E9.5, and E10.5 embryos. As to E15.5 embryos, we performed RT-qPCR test of Celf1, Celf2, Celf4, and Celf6 on total RNAs of various tissues. In E7.5 embryos, we identified the expressions of Celf1, Celf2, and Celf4, indicating potential functions for the Celf family in early embryo development. From E7.5 to E10.5, all four Celf members were expressed and finally enriched in neural parts, especially the brain, but the least expressed in the heart region. (Figure 15A) In E15.5 embryos, the four Celf members displayed the highest expressions in brain and the lowest in heart and tongue. (Figure 15B) In conclusion, Celf1, Celf2, Celf4, and Celf6 were highly enriched in neural parts and the lowest expressed in the heart and tongue during murine embryo development. This finding indicated the four Celf members might promote neural differentiation and inhibit heart differentiation.

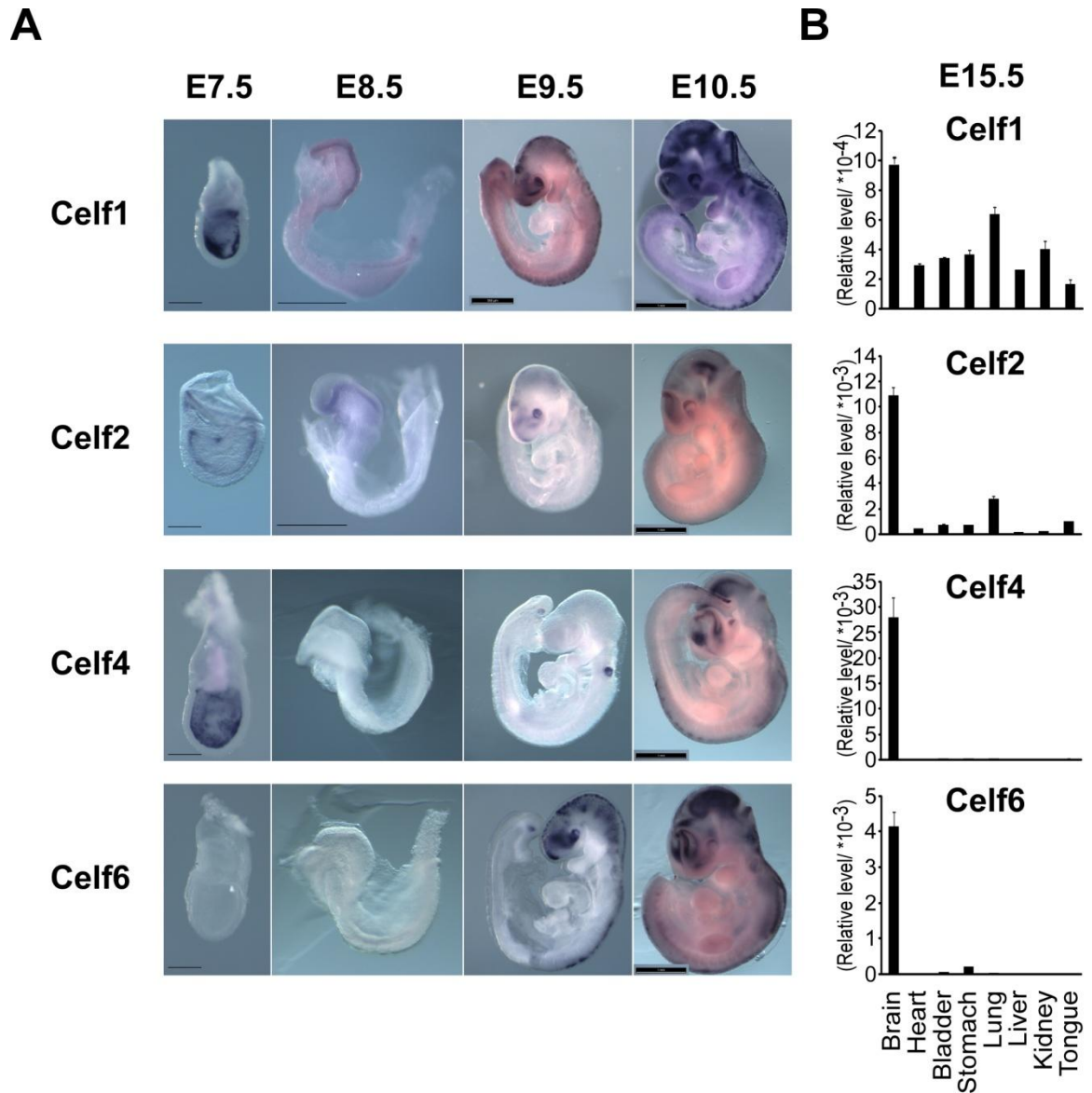


Figure 15. Celf family expression patterns during embryo development. (A) *In situ* hybridization assays of Celf1, Celf2, Celf4, and Celf6 on E7.5, E8.5, E9.5, and E10.5 mouse embryos. **(B)** RT-qPCR of Celf1, Celf2, Celf4, and Celf6 on total RNAs extracted from various tissues of E15.5 mouse embryos.

3.5 Celf1 knockdown mimicked the function of ectopic miR-322/503 expression on differentiation

It was previously shown that ectopic miR-322/503 expression promoted cardiac differentiation and Celf1 was a shared target of miR-322 and miR-503. It was logical for us to then hypothesize that Celf1 knockdown would mimic the function of ectopic miR-322/503 expression on differentiation, promoting cardiac differentiation. We first constructed E14 Celf1 knockdown (Celf1-KD) cell line with Celf1-shRNA and verified Celf1 knockdown through Western blots. (Figure 16A) Next we did monolayer differentiation with Celf1-KD and scramble shRNA transfected E14 cells, collected total RNA samples during differentiation and performed RT-qPCR for several differentiation makers. Pluripotency markers (Oct4 and Sox2) and mesoderm markers (Eomes, T, Gsc, and Mesp1) displayed identical expression patterns between Celf1-KD and scramble shRNA groups. Cardiac factors (Tbx5, Mef2C, Nkx2-5, and α -MHC) showed significant increases in the Celf1-KD group. (Figure 16B) Moreover, the expression patterns of the cardiac markers in the Celf1-KD group were identical to their expression patterns in the ectopic miR-322/503 expression group. (Figure 7A) Therefore, Celf1 knockdown mimicked the function of ectopic miR-322/503 expression on differentiation; miR-322/503 promoted cardiac differentiation by targeting Celf1.

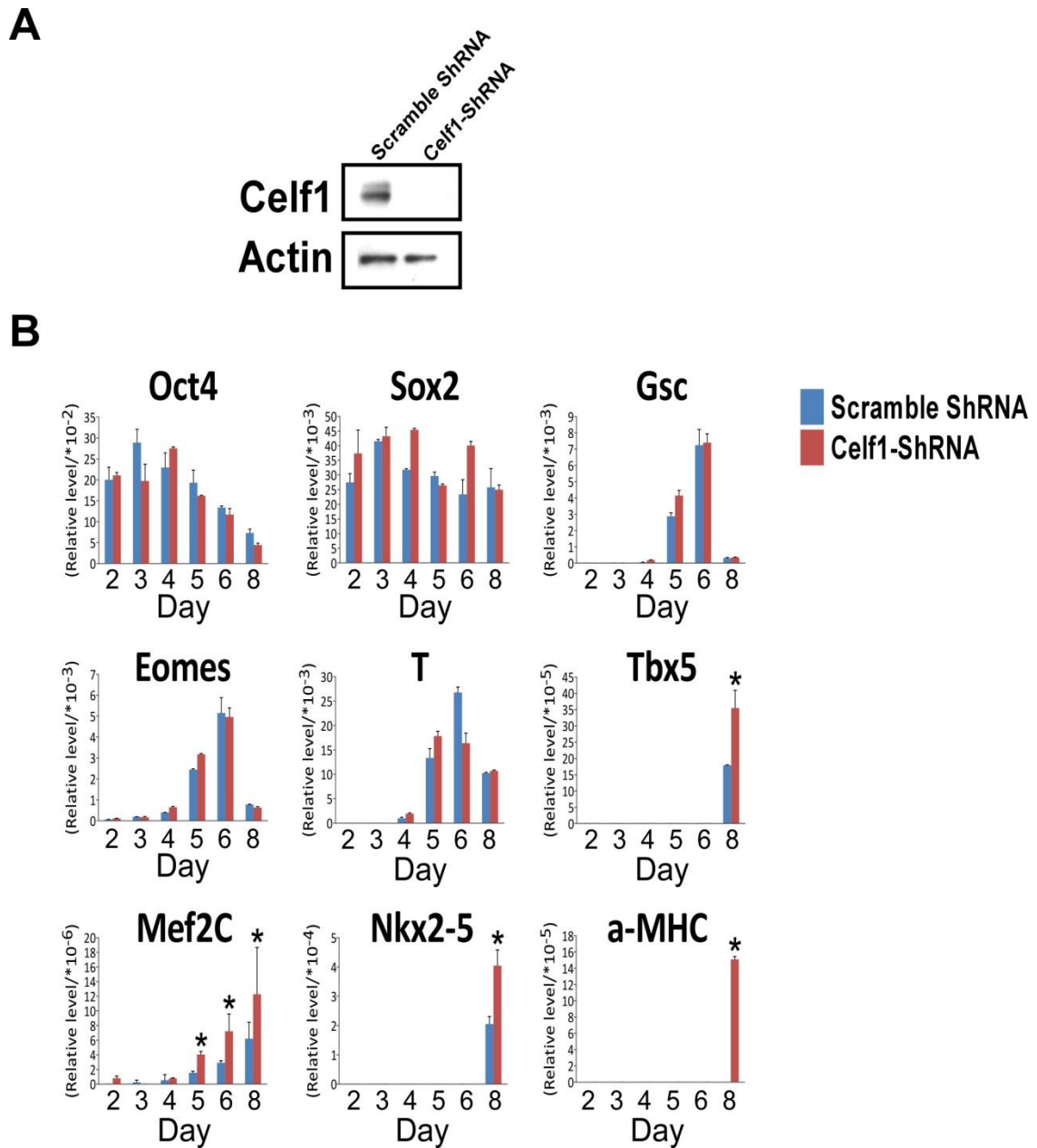


Figure 16. Celf1 knockdown mimicked the function of ectopic miR-322/503 expression on differentiation. (A) Western blots verification of Celf1 knockdown. Celf1-shRNA was used for constructing E14 Celf1 knockdown cell line; scramble shRNA is used for constructing E14 control cell line. β -actin was used as internal control for Western blots. (B) RT-qPCR of pluripotency markers (Oct4 and Sox2), mesoderm markers (Eomes, T, Gsc and Mesp1) and cardiac factors (Tbx5, Mef2C, Nkx2-5 and α -MHC) during differentiations of E14 Celf1 knockdown and E14 scramble shRNA cells. *: $p < 0.05$ in t-test.

3.6 Ectopic Celf1 expression inhibited cardiac and promoted neural differentiation

3.6.1 Inducible Celf1 overexpression ES cell line

In order to make Celf1 overexpression time controllable, we constructed E14 /Tet-On Advanced/ pLVX-FLAG-Celf1 Cell line (FLAG was fused to the N-terminus of Celf1). FLAG-Celf1 was induced with doxycycline treatment on E14 /Tet-On Advanced/ pLVX-FLAG-Celf1 Cells. (Figure 17A) We then performed monolayer differentiation of E14 /Tet-On Advanced/ pLVX-FLAG-Celf1 Cells and divided the resulting cells into 6 groups: non-treated, doxycycline treatment from day 0, doxycycline treatment from day1, doxycycline treatment from day 2, doxycycline treatment from day 3, and doxycycline treatment from day 4. We performed RT-qPCR of Nkx2-5, Sox1, Pax6, and Nestin on the differentiation day 8 samples of the above six groups. In the group of doxycycline treatment from day 4, cardiac factor (Nkx2-5) was the most significantly repressed and early neural factors (Sox1, Pax6, Nestin) were the most significantly enhanced. (Figure 17B, 17C) Previously, we have shown that Celf1 was the highly enriched in neural parts and the lowest expressed in the heart. Celf1 levels initially decreased at differentiation day 4 in wild type E14 differentiation. Therefore, inducing Celf1 overexpression at day 4 reversed the expression pattern in wild type E14 differentiation; Celf1 overexpression inhibited cardiac and promoted

neural differentiation. In our following studies of ectopic Celf1 expression, we performed monolayer differentiation of E14 /Tet-On Advanced/ pLVX-FLAG-Celf1 Cells and gave doxycycline treatment from differentiation day 4. (Figure 17D)

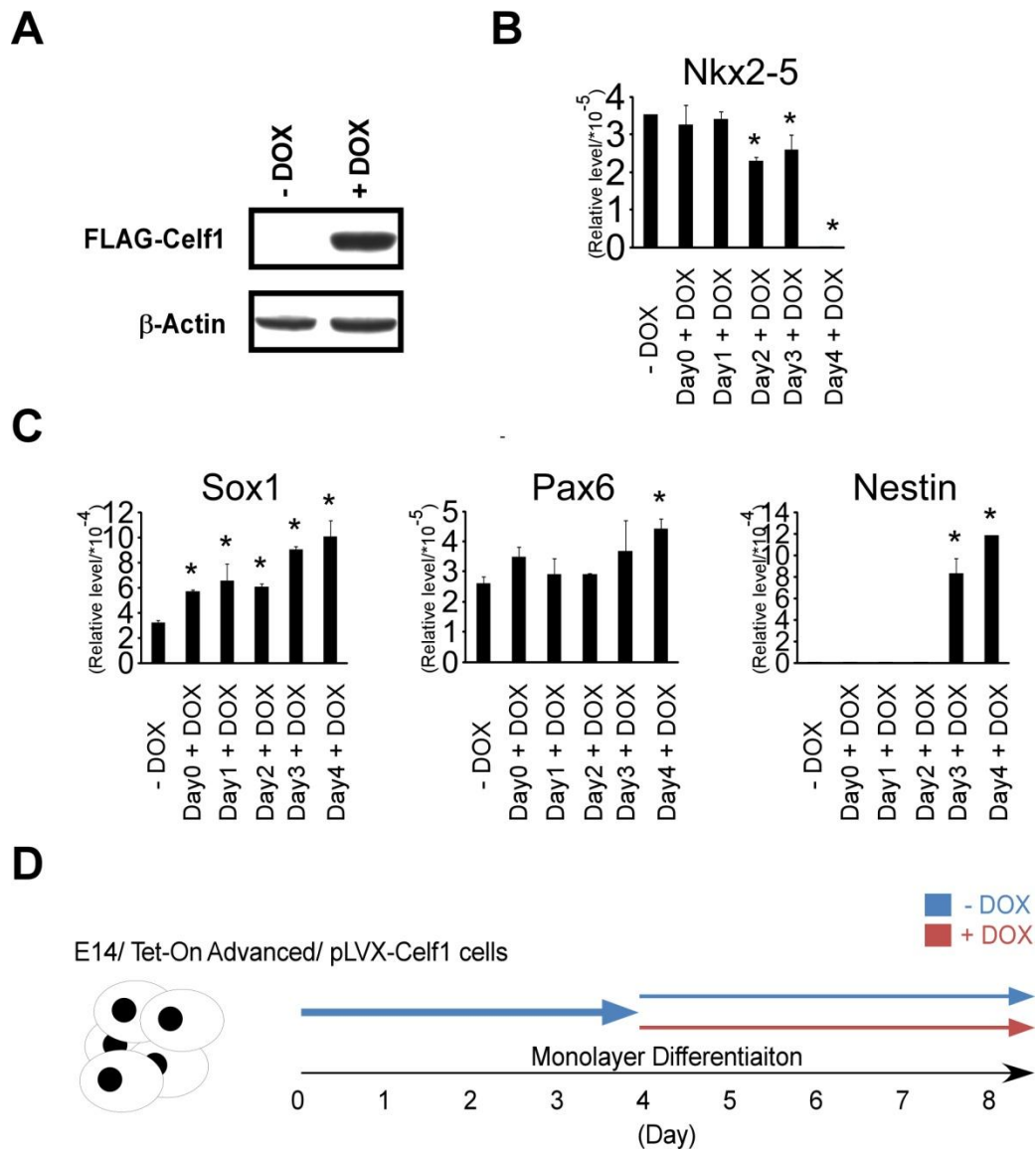


Figure 17. Inducible Celf1 overexpression cell line. We constructed E14/Tet-On Advanced/pLVX-FLAG-Celf1 Cell line as inducible Celf1 overexpression cell line. (A) Western blots verification of inducible Celf1 overexpression cells. FLAG was fused to the N-terminus of Celf1. β -actin was used as internal control. (B, C) RT-qPCR of Nkx2-5, Sox1, Pax6, and Nestin was performed on differentiation day 8 samples of the inducible Celf1 overexpression cells. Doxycycline treatment start time varied from day 0 to day 4. Untreated group served as negative control. Expression levels were related to GAPDH. (D) Schematic diagram of monolayer differentiation process in the following studies of Celf1 overexpression function.

3.6.2 Ectopic Celf1 expression inhibited cardiac differentiation

We performed monolayer differentiation of E14 /Tet-On Advanced/ pLVX-FLAG-Celf1 cells and induced ectopic Celf1 expression by doxycycline treatment from day 4. We collected total RNA samples during differentiation and prepared differentiation day 8 cells for immunostaining. By immunostaining for α -actinin, we found remarkable decreases in α -actinin expression after doxycycline treatment. (Figure 18A) During differentiation, pluripotency markers (Oct4, Sox2) and cardiac mesoderm marker (Mesp1) were not significantly affected following the induction of Celf1 overexpression from differentiation day 4. However, cardiac factors (Tbx5, Mef2C, Nkx2-5, α -MHC) were significantly repressed with Celf1 overexpression. (Figure 18B) Therefore, Celf1 inhibited cardiac differentiation without affecting pluriopotency stage and mesoderm formation.

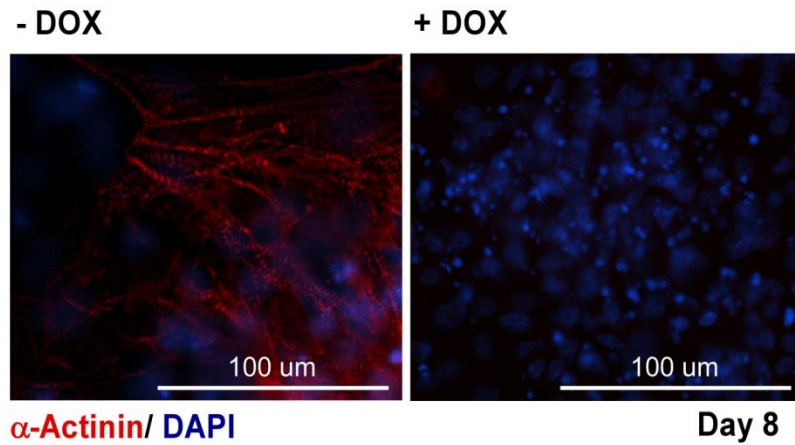
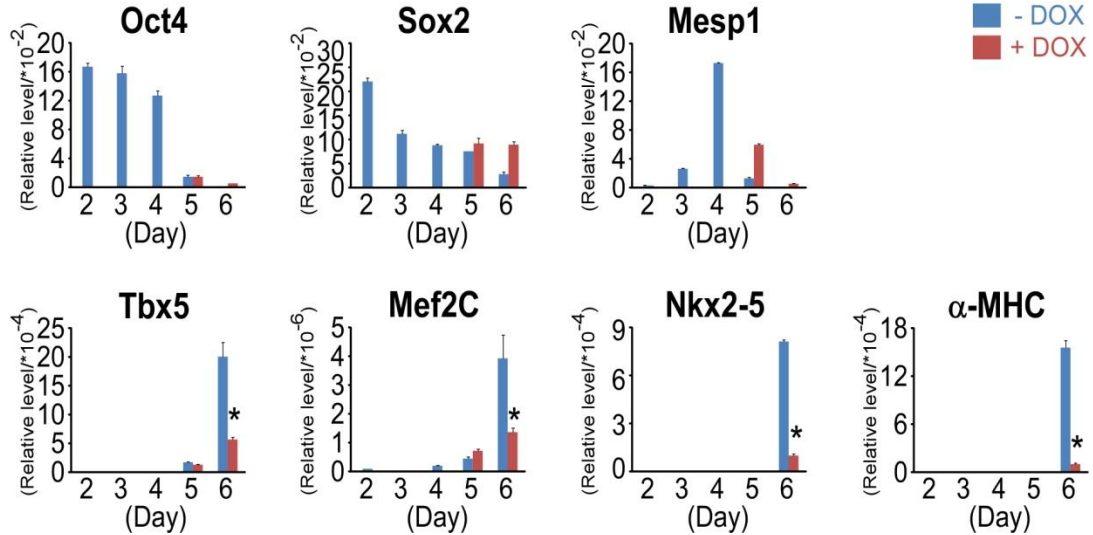
A**B**

Figure 18. Ectopic Celf1 expression inhibited cardiac differentiation. We performed monolayer differentiation of E14 /Tet-On Advanced/ pLVX-FLAG-Celf1 cells with activin supplement and induced ectopic Celf1 expression with doxycycline treatment from differentiation day 4. **(A)** Immunostaining of α -actinin was performed on differentiation day 8 cells. **(B)** RT-qPCR of Oct4, Sox2, Mesp1, Tbx5, Mef2C, Nkx2-5, and α -MHC was performed on total RNAs during the differentiation. *: $p < 0.05$ in t-test.

3.6.3 Ectopic Celf1 expression promoted neural differentiation

In order to study whether ectopic Celf1 overexpression affects neural differentiation, we performed monolayer differentiation of E14 /Tet-On Advanced/ pLVX-FLAG-Celf1 cells with SB431542 and FGF2 supplements and induced ectopic Celf1 expression by doxycycline treatment from day 4. We then collected total RNA samples during the differentiation process for RT-qPCR. Cells were collected at differentiation day 8.5 for immunostaining. By immunostaining for TuJ1, we found remarkable increases in mature TuJ1 expression following doxycycline treatment, whereas little expression of immature TuJ1 expression was found in non-treated group (Figure 19A) During differentiation, three neural factors (Notch3, Sox1, and Pax6) displayed remarkable increase after Celf1 overexpression, while nestin did not show significant change (Figure 19B) Nestin is reported to function in both neural differentiation and regeneration of damaged muscle (149) and Celf1 might affect both processes to diminish Nestin change. Therefore, ectopic Celf1 expression promoted neural differentiation.

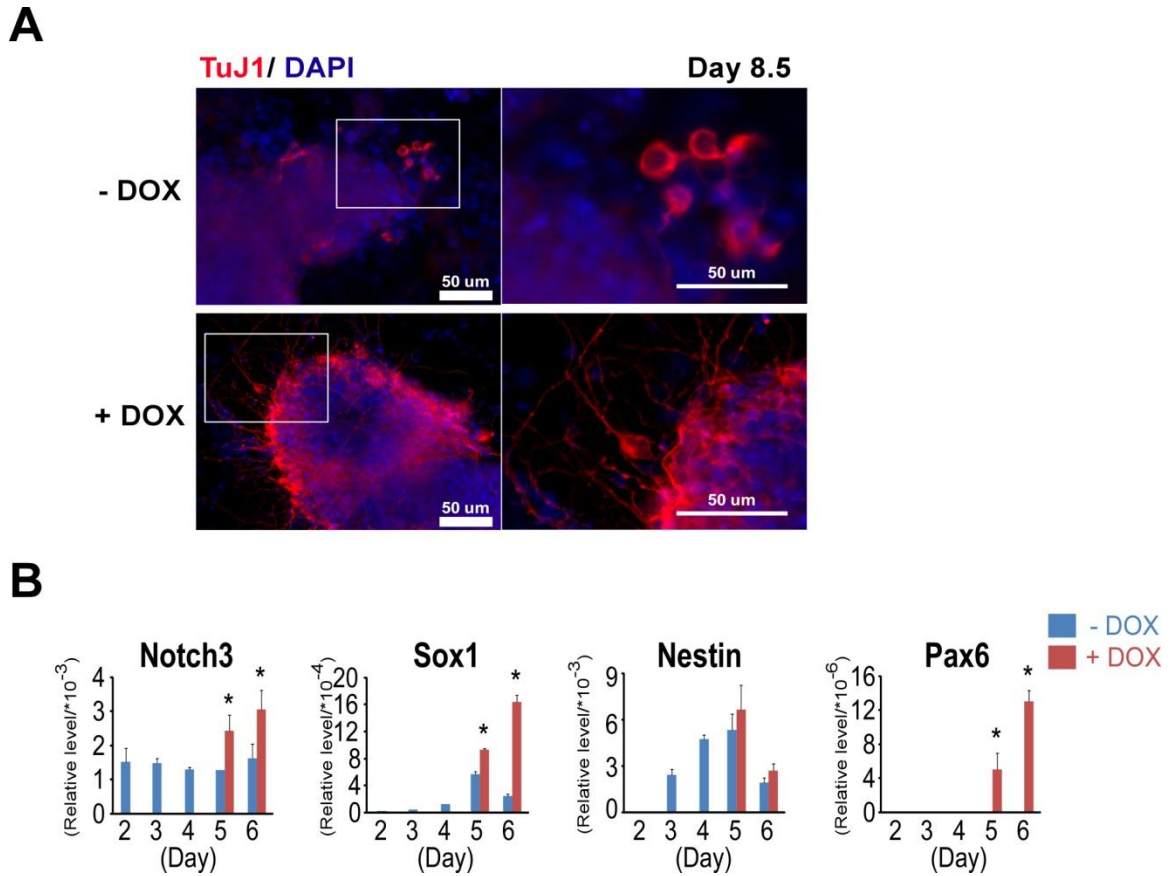


Figure 19. Ectopic Celf1 expression promoted neural differentiation. We performed monolayer differentiation of E14 /Tet-On Advanced/ pLVX-FLAG-Celf1 cells with medium containing SB431542 and FGF2 supplements and induced ectopic Celf1 expression by doxycycline treatment from day 4. **(A)** Immunostaining of TuJ1 was performed on differentiation day 8.5 cells. **(B)** RT-qPCR of Notch3, Sox1, Nestin, and Pax6 was performed on total RNAs during the differentiation. *: $p < 0.05$ in t-test.

3.6.4 Celf1 promoted mRNA decay of several cardiac factors

Celf1, as an mRNA binding protein, was reported to have two functions: one was regulating mRNA alternative splicing (150); the other was facilitating mRNA decay (151). For mRNA decay, the consensus sequences of Celf1 to mRNA 3'UTR are the GRE sequence (UGUUUGUUUGU) and GU-repeat sequence (UGUGUGUGUGU) (152). We executed a bioinformatics study to search for mRNAs with the two listed consensus sequences in their 3'UTRs. In the parameters for the bioinformatics search, we allowed, at most, 2 mismatches. Among the mRNAs containing either of the two consensus sequences, we selected several cardiac differentiation related genes for mRNA decay assay. In the mRNA decay assay, we performed monolayer differentiation of E14 /Tet-On Advanced/ pLVX-FLAG-Celf1 cells with activin supplement, induced ectopic Celf1 expression with doxycycline treatment from differentiation day 4, added 10 ug/mL Actinomycin D at day 5 and collected total RNAs at 0 hours, 2.5 hours, 8 hours, and 12 hours post-actinomycin D treatment. The control group followed the same procedure excluding doxycycline treatment. After RT-qPCR, relative expression levels were all normalized to their corresponding 0 hour levels. We found that the decay of Wnt5A, Myocd, and Hdac5 mRNAs were remarkably promoted with Celf1 overexpression, while Tbx3 was not significantly affected. (Figure 20) In conclusion, ectopic Celf1 expression promoted mRNA decay of several cardiac factors, which thereby inhibited cardiac differentiation.

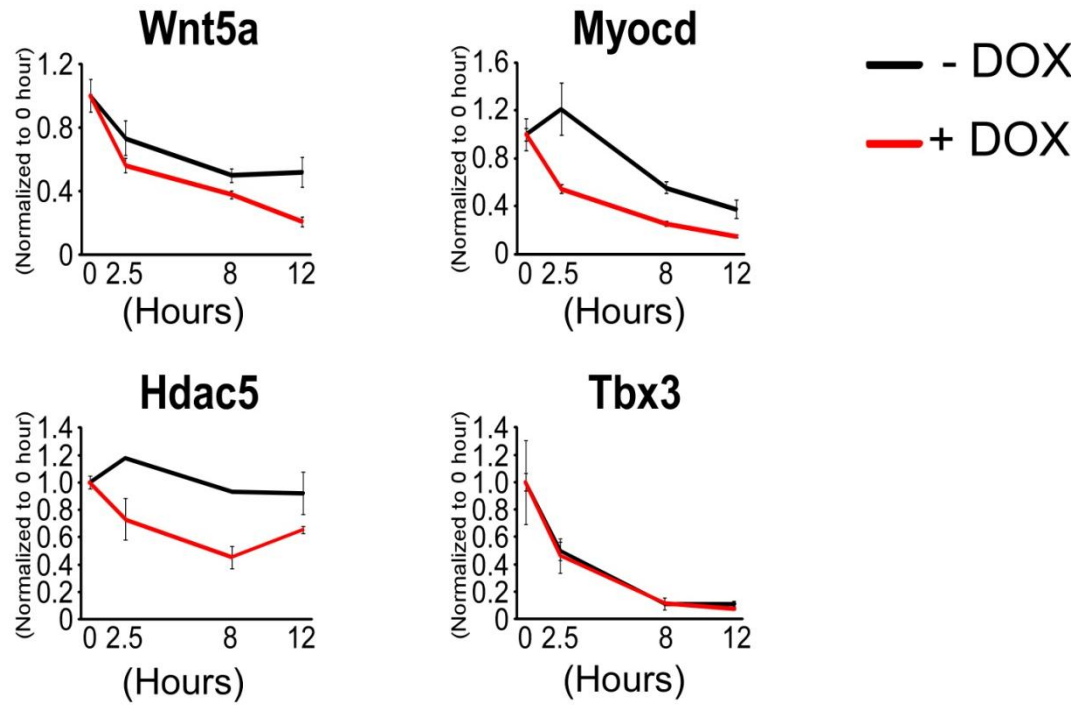


Figure 20. Celf1 promoted mRNA decay of several cardiac factors. mRNA decay assay was performed on E14 /Tet-On Advanced/ pLVX-FLAG-Celf1 cells. RT-qPCR of Wnt5A, Myocd, Hdac5, and Tbx3 was performed on total RNAs collected in mRNA decay assay. Expression levels were related to GAPDH. Relative expression levels were then normalized to the genes' 0 hour relative levels.

4 DISCUSSION AND CONCLUSION

4.1 Discussion

4.1.1 Cardiac-driving microRNA screening

In this study, we performed screening of cardiac-driving microRNA to discover novel microRNAs that promoted cardiac differentiation. To perform the screening, we had to initially generate a microRNA list for screening. Presently, thousands of microRNAs have been discovered. It is unpractical for us to screen all microRNAs. To make the screening library small enough for screening, we generated a screening library of microRNAs enriched in Mesp1 positive progenitor cells. Mesp1 is a pivotal transcription factor and marker of cardiac mesoderm (52). Therefore, Mesp1 positive progenitor cells were also cells of cardiac mesoderm. It was straightforward for us to think that microRNAs enriched in cardiac mesoderm during development should facilitate cardiac differentiation. To discover the microRNAs enriched in Mesp1 positive progenitor cells, we used Mesp1 lineage tracing ES cells and separated Mesp1 positive and negative cells after 3 days differentiation by FACS sorting. Through RNA sequencing and comparing microRNA expressions between Mesp1 positive and negative cells, we were able to generate a list of microRNAs that were enriched in Mesp1 positive cells. We constructed overexpression clones of enriched microRNAs in Mesp1 positive cells and performed cardiac-driving screening using the VALA

kinetic image cytometry microscope. With the microscope, we monitored calcium flux activities of E14 cells infected with each microRNA overexpression lentiviruses after 5 days differentiation. Calcium flux, as a phenotype of cardiomyocytes, was utilized as an indicator of cardiac differentiation. We introduced “+++”, “++”, “+” and “-” to mark calcium flux intensity from the highest to lowest as described in Figure 2B. From the results, we found miR-322/503 and miR-17/92 were labeled as “+++”. miR-17/92 were reported to be crucial in cardiac differentiation (134). miR-322/503 showed comparable calcium flux activity to miR-17/92, which suggested its potential role in cardiac differentiation.

In published references, miR-322 and miR-503 were mainly described to regulate tumor growth and angiogenesis, which included smooth muscle and endothelia cell formations. In cancer, miR-322 and miR-503 were mostly described as tumor suppressor microRNAs. In hepatocarcinoma and breast cancer cells, miR-322 and miR-503, induced by thyroid hormone receptors, repressed proliferation and invasion (153). In hepatocarcinoma, another paper showed that miR-322 repressed cell migration and invasion at least partially by targeting c-Myb (154). In colon cancer, repression of miR-322/503 caused formation and activation of mTORC2, which promoted tumorigenesis and invasion (155). In hepatocellular carcinoma and gastric cancer cells, miR-322 and miR-503 repressed epithelial-to-mesenchymal transition (EMT) (156, 157). However, miR-322-5p was up-regulated in pancreatic cancer and promoted proliferation and invasion by

regulating ERK1/2 pathway (158). In angiogenesis, miR-322 and miR-503 mainly promoted smooth muscle and endothelia cell formations, but repressed their proliferations. miR-322 was induced after vascular injury (159). miR-322/503 were downregulated in pulmonary arterial hypertension, and the ectopic miR-322/503 expression ameliorated pulmonary arterial hypertension in vivo (160). miR-322 and miR-503 promoted muscle differentiation by targeting Cdc25A to induce G1 cell-cycle arrest (161), in which the expressions of miR-322 and miR-503 are induced by TGF β induction (162). miR-503 was remarkably up-regulated in endothelial cells of diabetes mellitus and limb ischemia and inhibited endothelial cells's proliferation and migration (163). miR-322 inhibited the abilities of proliferation, migration and cord formation of endothelia cells in cell-autonomous mode (164). The repression of miR-322 in the human dermal microvascular endothelia cells leads to up-regulated MEK1 or cyclin E1 and increased cell proliferation (165). In hypoxia conditions, miR-322 is up-regulated and promotes angiogenesis (166). In conclusions, miR-322 and miR-503 inhibit proliferation and promote further differentiation of endothelia and smooth muscle cells in most conditions. However, the functions of miR-322 and miR-503 in promoting cardiac differentiation were not reported.

We then studied the miR-322/503 coding area on the genome. We found that miR-322 and miR-503 are located within the longest exon region of long non-coding RNA (lncRNA) C430049B03Rik (Figure 21). By performing evolutionary

conservation study of their upstream region, we identified one 6.5 kb highly conserved promoter region shared by miR-322/503 and C430049B03Rik. This was used for constructing miR-322/503 promoter-LacZ reporter to test the expression of miR-322/503 in mouse embryos. In Figure 4A, we found that miR-322/503 was highly enriched in the heart region of E8.5 murine embryos. As C430049B03Rik is regulated by the same promoter, C430049B03Rik may also be highly expressed at heart region during embryo development, suggesting that C430049B03Rik may also function in heart development. Although miR-322 and miR-503 are in the same transcript of C430049B03Rik and may be transcribed together with C430049B03Rik, how miR-322 and miR-503 are released from C430049B03Rik transcript is still unknown. In this project, we identified Celf1, a post-transcription regulator of both mRNA decay and alternative splicing, as a target of miR-322/503. It is possible that the release of miR-322 and miR-503 from C430049B03Rik is a mRNA alternative splicing process and is regulated by Celf1 or other Celf family members; meanwhile, miR-322/503 might regulate mRNA alternative splicing process by targeting Celf1. That hypothesis needs to be verified through studying mRNA splicing patterns with ectopic miR-322/503 or Celf1 expression in differentiation.

After studying sequences downstream of miR-322/503, we found that miR-542 is located roughly 4kb downstream of miR-322/503. In our screening, miR-542 was labeled as “++”, suggesting a role for miR-542 in cardiac differentiation. In

addition, miR-351, miR-450b, miR450-1 and miR-450-2 are all located within 5.5 kb downstream of miR-322/503 as well. Those microRNAs were also enriched in Mesp1 positive progenitor cells. (Data not shown) Putting the above information together, the whole locus, including miR-322/503, miR-542, miR-351, miR-450b, miR450-1, miR-450-2, and C430049B03Rik, may be very important for cardiac differentiation and heart development. As the locus is on X chromosome, if we could find heart development defects with knockout or mutation of this locus, we might be able to explain why some heart diseases show incidence differences between male and female.

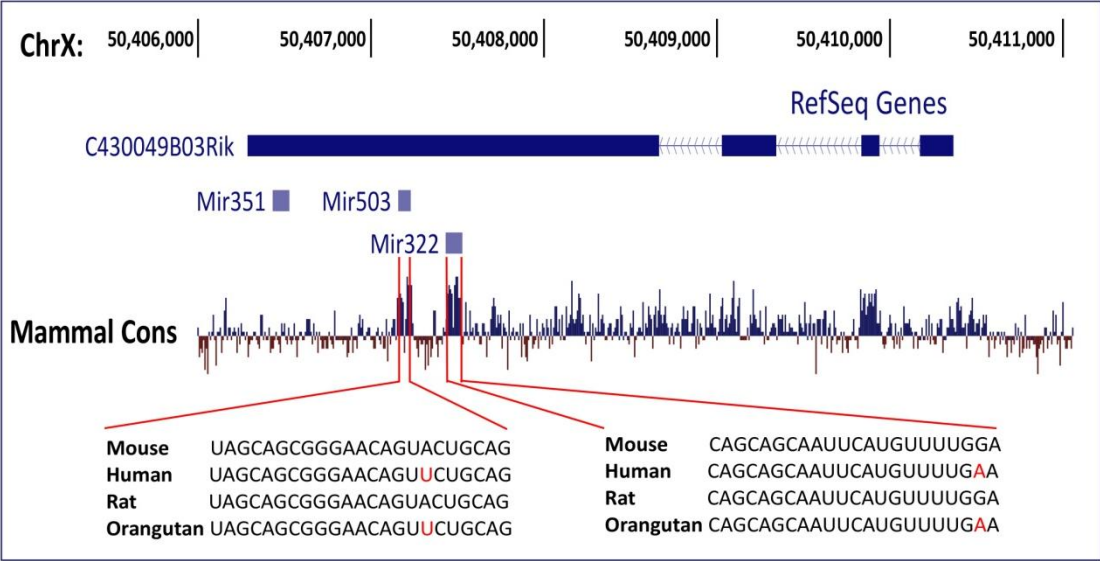


Figure 21. miR-322 and miR-503 on mouse genome. miR-322 and miR-503 are located within the transcript of C430049B03Rik on X chromosome. Coding region of miR-322, miR-503, and C430049B03Rik are on the minus strand. Both miR-322 and miR-503 are highly conserved. Bar graph shows the conservation level among mammalian animals. 'ChrX' stands for chromosome X; 'Mammal Cons' stands for conservation level among mammalian animals. Red characters in sequences indicate the differences of corresponding sequences when compared to mouse sequences.

4.1.2 Effect of ectopic miR-322/503 expression on differentiation

Our studies indicated that miR-322/503 displayed the highest cardiac-driving potential in the screening. We next studied the effect of ectopic miR-322/503 expression on differentiation. Since miR-322 and miR-503 are in a cluster and regulated by a shared promoter, we cloned the miR-322 and miR-503 coding regions together into an inducible overexpression vector and overexpressed them together. We found expressions of miR-322 and miR-503 along wild type E14 differentiation concurrently started to increase at differentiation day 3 and reached peaks at day 5. As most differentiation regulatory factors function properly at their suitable time frames and might function differently or even reversely when expressed at other time points, for example Wnts, we used the inducible miR-322/503 overexpression system and induced the overexpression with doxycycline treatment at day 3 to let miR-322/503 overexpress when it was highly expressed along wild type ES differentiation. As a result of ectopic miR-322/503 expression, differentiation towards cardiac, skeletal, endothelia, and endoderm was enhanced, whereas smooth muscle differentiation was unaffected. By studying the gene expression pattern changes with microarray on the total RNAs collected at 24 hours after induction of miR-322/503 overexpression, we found a significant percentage of mesoderm and endoderm genes, especially cardiac and skeletal muscle-related genes, were significantly up-regulated, while ectoderm genes were significantly down-regulated, which suggested miR-

322/503's importance in promoting cardiac and skeletal muscle differentiation as well as inhibiting neural differentiation.

After confirming that miR-322/503 promoted cardiac differentiation of ES cells, we speculated as to whether or not miR-322/503 could be applied into therapies against several heart diseases, for example heart failure. The underlying cause contributing to heart failure is cardiomyocytes lack of regenerative. Currently, interest in recent cell therapy techniques, which utilize induced cardiomyocytes to repair injured cardiomyocytes, is growing. miR-322/503's function in driving cardiac differentiation lends itself as a potential therapeutic target for heart failure therapy. Moreover, we were also trying to deliver synthetic miR-322/503 directly into bodies to test if miR-322/503 could improve heart function and repair heart injury in heart failure.

Apart from miR-322/503's function in cardiac differentiation, we also noticed miR-322/503's function in neural differentiation. Following induction of miR-322/503 overexpression at 24 hours, genes involved in ectoderm formation were significantly down-regulated. Therefore, miR-322/503 may inhibit neural differentiation. This conclusion concurs with the discovery of Celf1's role in neural differentiation. Celf1 was proven to be a target of miR-322/503. We have discovered Celf1 promotes neural differentiation. It is possible that miR-322/503 regulates neural differentiation through targeting Celf1.

4.1.3 Losses of miR-322 and miR-503 impair cardiac differentiation

After ascertaining that ectopic miR-322/503 expression promoted cardiac differentiation, we attempted to study whether loss of miR-322/503 would result in reduced cardiac differentiation. The initial challenge for us was to find an approach to repress miR-322/503 expression in ES cells. For protein-coding genes, people usually use shRNA or a recently discovered system, CRISPR, to do gene knockdown (KD) (167). In our study, it was unpractical for us to use both shRNA and CRISPR. The miR-322/503 cluster is located within the transcript of LncRNA C430049B03Rik. C430049B03Rik would be knockdown as well no matter we used either shRNA or CRISPR system to knockdown miR-322/503. As C430049B03Rik LncRNA's function was not yet determined, we could not distinguish whether it is because of miR-322/503 knockdown or C430049B03Rik knockdown if there were some defects of differentiation by using shRNA or CRISPR for miR-322/503 knockdown. Therefore, we had to find other approaches to repress miR-322/503. We then found two ways to achieve that purpose, which were miR sponges and "miRZip". The mechanism for both miR sponges and miRZip was through absorbing corresponding microRNAs and reducing working microRNA concentrations. Finally, we chose lentiviral based miRZip for constructing stable miR-322 or miR-503 repressed ES cell lines – miRZip-322 ES cell line or miRZip-503 cell line. However, there were two pitfalls when using miRZip. First, we could just construct miRZip-322 ES cell line and miRZip-503

ES cell line separately but could not construct miRZip-322&miRZip-503 ES cell line, the cell line in which miR-322 and miR-503 were both repressed, since they had the same drug selection markers. Second, it was hard for us to verify whether miR-322/503 was repressed or not. As previously described, both miR sponges and miRZip obtain knockdown through absorbing microRNAs rather than degrading them. In other words, the functional single strand microRNA levels were lowered but total microRNA levels might not be affected by absorbing. Currently, RT-qPCR and northern blots were usually used for microRNA measurements. However, both RT-qPCR and northern blots detected the total amount of microRNA rather than functional single strand microRNA. We referred to miRZip's company manual and found the only approach to check whether miRZip worked or not was to measure level changes of microRNA targeted genes. For our experiment, we need to check Celf1 level changes with miRZip-322 or miRZip-503 transfection to verify the repression of miR-322 or miR-503.

After studying the differentiation of miRZip-322 ES cells and miRZip-503 ES cells, we found remarkable repression of cardiac differentiation from both cell lines when compared to control group. This indicated that loss of miR-322/503 would impair cardiac differentiation. That led us to think whether knockout of miR-322/503 would block heart development. We purchased miR-322/503 KO cells from Sanger Institute and generated miR-322/503 KO heterozygous female mice. We obtained one litter of mice from mating the miR-322/503 KO heterozygous

female mouse with a wild type male mouse. In the resulting litter, two male mice were homozygous knockout and one died at post-natal day 1 (P1). We dissected the mouse and found hypertrophy of the heart. (Data not shown) As the knockout is located on the X chromosome and potentially affect reproduction, the female mice failed to become pregnant following the initial pregnancy. Therefore, statistically significant numbers of homozygous null mice were unable to be collected to conclusively prove that miR-322/503 KO causes hypertrophy of the developing heart. To address this difficulty, we purchased miR-322/503 conditional knockout (CKO) male mice from Jackson Lab. We are currently using the miR-322/503 CKO mice for loss of miR-322/503 *in vivo* study.

4.1.4 Celf1 as a direct target of miR-322/503 in regulating cardiac differentiation

By studying the microarray data of ectopic miR-322/503 expression, we found that Celf1 was down-regulated by miR-322/503 induction. Celf1 was reported to be closely related to myotonic dystrophy type1 (DM1), a disease that displayed remarkable skeletal muscle and some extent of heart defects (148). We then used RNA22 to predict target sites of miR-322 and miR-503 on Celf1 mRNA. We happened to notice that miR-322 and miR-503 had highly identical seed sequences and most predicted target sites for miR-322 and miR-503 were the same. Through application of luciferase assays, we confirmed that miR-322/503 targeted Celf1 at a predicted site on Celf1 mRNA 3'UTR, which was shared by miR-322 and miR-503. This result also partially explained why we studied miR-322 and miR-503 together. The shared miR-322/503 target Celf1 was also confirmed by the inverse expression correlation between miR-322/503 and Celf1. In 293FT cells, Celf1 was repressed by miR-322/503 in a dose-dependent pattern; in E14 cells, Celf1 was down-regulated by the induction of miR-322/503 overexpression. This finding agreed with a previously reported paper, which stated that miR-503 could drive Celf1 into processing bodies (P-bodies) to repress Celf1 (168).

We then studied expression patterns of Celf1 during wild type E14 cells differentiation and murine embryo development. We then compared the patterns

of Celf1 expression levels to miR-322/503's expression levels. During wild type E14 cells differentiation, Celf1 maintained a relatively high level for the first 4 days. At day 4, Celf1 expression started to decrease and reached their lowest expression levels at day 6. Following day 6, Celf1 returned to relatively high expression levels. This expression pattern was opposite to the expression patterns of miR-322 and miR-503 but had a one-day delay, confirming miR-322/503 targeting Celf1. During murine embryo development, Celf1 was finally enriched in neural parts and least expressed in heart, which was also opposite to miR-322/503's expression patterns in murine embryos. Therefore, miR-322/503 and Celf1 also displayed an inverse expression level correlation during mouse embryo development.

Celf1's expression pattern during wild type E14 cells differentiation was maintained at relatively high levels from day 0 to day 4, but needed to be down-regulated from day 4 to day 6. Since Celf1 level was maintained relatively high at the early stage of differentiation, we hypothesize that Celf1 is necessary for pluripotency or mesoderm formation. While we were studying Celf1 knockdown's effect on differentiation, we noticed delayed differentiation and weakened beating despite knockdown of Celf1 mostly reproduced the effect of miR-322/503 overexpression on cardiac differentiation. Similarly, while studying Celf1 overexpression, we noticed a weakened effect on cardiac and neural differentiation if overexpression of Celf1 was induced before day 4. From the

expression patterns of markers of the pluripotency (Oct4, Sox2) and mesoderm (T, Emos, Gsc, Mesp1), we could tell that differentiation process before day 4 were pluripotent stage and mesoderm formation process. Thus, Celf1 may be important for pluripotency or mesoderm formation at early stages of differentiation.

Celf1's expression patterns during mouse embryo development provided us with the idea that Celf1 might promote neural differentiation and inhibit cardiac differentiation. In the developmental field, researchers prefer to study when and where genes were expressed and then propose hypotheses as to how the genes affected development. Here, we not only studied Celf1 but also other Celf family members. The four members of the Celf were all enriched in neural parts with expressions levels lowest in the heart, which indicated the possible roles Celf family members played in neural and cardiac differentiation.

4.1.5 Celf1 inhibits cardiac differentiation and promotes neural differentiation

We used inducible Celf1 overexpression E14 cells to study the effect of Celf1 overexpression on differentiation. By inducing Celf1 at different days, we found that Celf1 displayed the highest potential for inhibiting cardiac differentiation and promoting neural differentiation when Celf1 overexpression was induced from day 4. These findings agreed with the time point when Celf1 expression started to decrease during wild type E14 cells differentiation. These results indicate that the reduction of Celf1 expression during ES cell differentiation is potentially important in cardiac differentiation. We performed RT-qPCR and immunostaining to verify Celf1's role in cardiac and neural differentiation. After induction of Celf1 overexpression at day 4, cardiac differentiation was repressed and neural differentiation was promoted.

We then attempted to study the mechanism through which Celf1 functioned. Celf1 has been reported to have two functions: one is facilitating mRNA decay; the other is regulating RNA alternative splicing. Here, we tested how Celf1 regulated cardiac differentiation through mediation of mRNA decay. By bioinformatics study, we generated a list of predicted Celf1 mediated mRNA decay targets. We selected Wnt5a, Myocd, Hdac5, and Tbx3 for RNA decay assays and found mRNA decay speed of Wnt5a, Myocd, and Hdac5 were significantly increased while Tbx3 mRNA levels were unaffected with Celf1

overexpression. Therefore, Celf1 potentially inhibits cardiac differentiation through promoting mRNA decay of cardiac factors. We are also studying how Celf1 regulates differentiations of cardiac and neural through regulating RNA alternative splicing. As is known to all, most mRNAs have isoforms. Among isoforms, some are tissue specific (169, 170). Thus, we proposed that Celf1 might facilitate the RNA alternative splicing process towards neural specific isoforms and inhibit the RNA alternative splicing process towards cardiac specific isoforms. In this way, Celf1 can inhibit cardiac differentiation and promote neural differentiation. In conclusion, Celf1 may inhibit cardiac differentiation and promote neural differentiation by promoting mRNA decay and regulating RNA alternative splicing.

Excessive Celf1 expression has also been reported to promote myotonic dystrophy 1 (DM1) and cause defects in skeletal muscle, suggesting a function for Celf1 in skeletal muscle differentiation (148, 171). There are two types of DMs, DM1 and DM2. Celf1 functioned in DM1 but not in DM2, which is milder in symptoms than DM1 (172). DM1, a disease of muscular dystrophy, is caused by expanded poly (CTG) repeats at the 3' UTR region of DM protein kinase (DMPK) gene. The RNA transcribed from the mutant DMPK gene caused muscleblind-like (MBNL) protein depletion and Celf1 expression increase. Both MBNL and Celf1 are RNA alternative splicing regulatory factors. The loss of MBNL and increase of Celf1 in DM1 lead to dysregulated RNA alternative splicing and finally cause

neural and muscular defects. For example, the mRNA of myomesin 1 (MYOM1) did not include exon 17a in wild type 293T cells after splicing but included the exon 17a in expanded CUG repeat overexpressing 293T cells (173). The Celf1 increase in DM1 was reported to be facilitated by PKC pathway involved hyperphosphorylation and the activation of PKC pathway was dependent on expanded CUG repeats at 3'UTR of DMPK gene (171). Knockout of Celf1 in DM1 mice did not correct splicing defects but lowered Celf1's translational targets, MEF2A and C/EBP β , which relieved the symptoms of DM1 (174). Another paper stated that the inhibition of Celf1 could correct Celf1-mediated dysregulated splicing but did not correct MBNL-mediated splicing defects (175). Moreover, skeletal muscle cells need correct synapse connections between them and their connecting neurons not only for skeletal muscle contraction but to support their growth. Abnormal synapse connections could lead to muscle atrophy (176). It was recently reported that the differentiation of DM1 stem cells gives rise to excessive neurite growth and abnormal synapse formation during stem cell differentiation (177). Thus, Celf1 might promote DM1 not only through inhibiting skeletal muscle differentiation but also by inducing abnormal formation of skeletal connecting neurons. As we have already shown that Celf1 is targeted by miR-322/503, we plan to apply miR-322/503 into the therapy against DM1.

4.2 Conclusion

In order to discover novel microRNA involved cardiac differentiation regulatory pathway, we performed cardiac driving screening on the microRNAs enriched in Mesp1 positive progenitor cells. miR-322 and miR-503 were the top two enriched microRNAs in Mesp1 positive progenitor cells. In cardiac driving screening, miR-322/503 induced the strongest calcium flux activity and precocious beating. After performing LacZ staining and RT-qPCR on murine embryos, we found that miR-322/503 was highly enriched in heart and skeletal muscle during murine embryo development. With ectopic miR-322/503 expression in E14 cells, differentiation towards cardiac, skeletal muscle, endothelia, and endoderm were significantly enhanced. By microarray assays and GO analysis, genes involved in promoting ectoderm differentiation were significantly down-regulated and genes involved in promoting mesoderm and endoderm differentiation, especially heart and skeletal muscle, were significantly up-regulated with miR-322/503 overexpression. The microarray results not only proved that miR-322/503 promoted differentiations towards heart and skeletal muscle but also indicated the possible inhibitory function of miR-322/503 in neural differentiation. By treating E14 cells with inhibitors of miR-322 and miR-503, cardiac differentiation was remarkably inhibited, which suggested the necessity of miR-322/503 in cardiac differentiation. We then tried to find targets of miR-322/503 in regulating differentiation. Through studying references and doing bioinformatics research, we identified and focused

on Celf1. Celf1 expression was repressed with miR-322/503 overexpression in both 293FT cells and E14 cells. During wild type E14 cells differentiation and murine embryo development, Celf1 displayed an inverse correlation to miR-322/503. Through luciferase assays, Celf1 was proved to be a miR-322/503 target. Celf1 knockdown utilizing shRNA mimicked the function of ectopic miR-322/503 expression, further proving that miR-322/503 promoted cardiac differentiation through repression of Celf1. Ectopic Celf1 expression inhibited cardiac differentiation and promoted neural differentiation, which agreed with Celf1's expression pattern during murine embryo development. In conclusion, miR-322/503 promoted cardiac differentiation by targeting Celf1; Celf1 inhibited cardiac differentiation and promoted neural differentiation. (Figure 22)

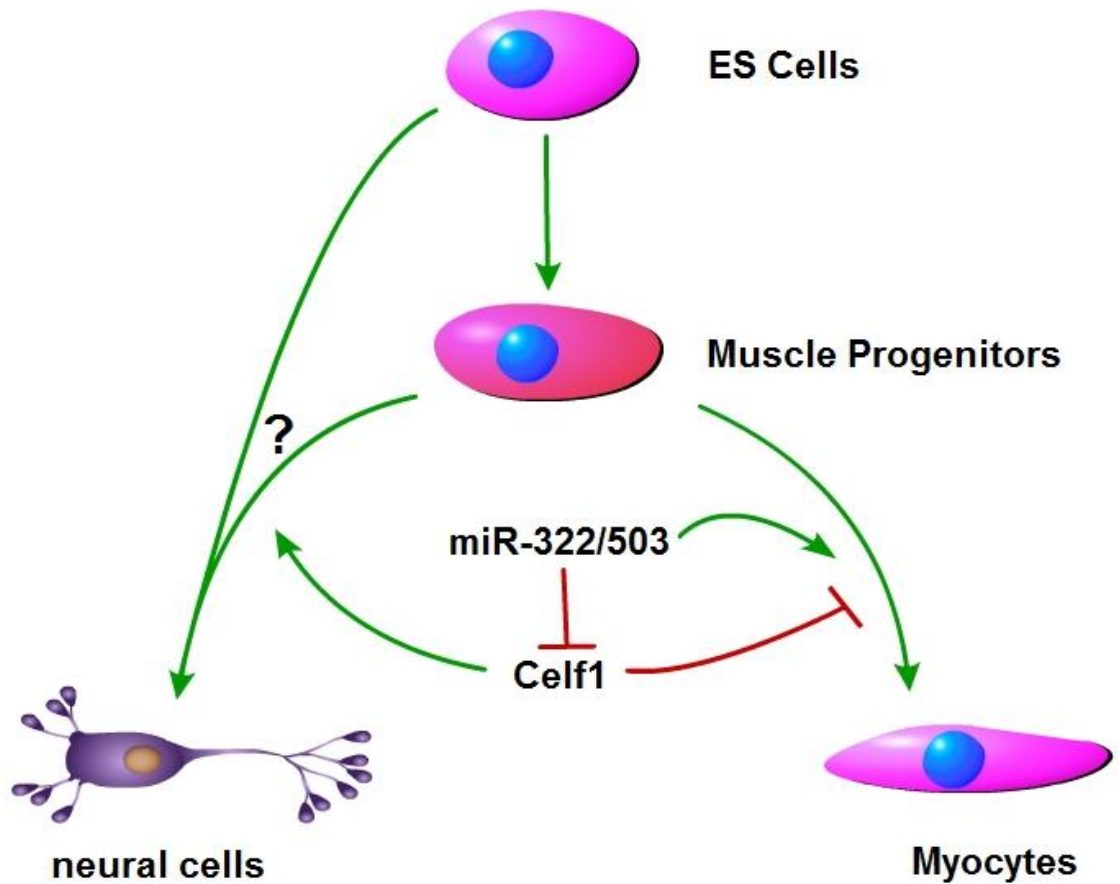


Figure 22. Working model of miR-322/503 in regulating cardiac and neural differentiations. As the microRNA(s) that displayed the highest cardiac driving potential in the screening, miR-322/503 cluster promotes cardiac differentiation by targeting Celf1. Celf1, as a post-transcription RNA regulator, inhibits cardiac differentiation and promotes neural differentiation. Celf1 was proved to inhibit cardiac differentiation by promoting mRNA decays of several cardiac factors (including Wnt5a, Myocd, and Hdac5).

BIBLIOGRAPHY

1. J. Rossant, Investigation of the determinative state of the mouse inner cell mass. I. Aggregation of isolated inner cell masses with morulae. *J Embryol Exp Morphol* **33**, 979 (Jul, 1975).
2. A. C. Enders, K. C. Lantz, S. Schlafke, Differentiation of the inner cell mass of the baboon blastocyst. *Anat Rec* **226**, 237 (Feb, 1990).
3. P. Maddox-Hyttel *et al.*, Immunohistochemical and ultrastructural characterization of the initial post-hatching development of bovine embryos. *Reproduction* **125**, 607 (Apr, 2003).
4. C. S. Minot, Primitive streak of vertebrates. *Science* **2**, 105 (Jul 27, 1883).
5. F. L. Conlon *et al.*, A primary requirement for nodal in the formation and maintenance of the primitive streak in the mouse. *Development* **120**, 1919 (Jul, 1994).
6. V. Wilson, R. S. Beddington, Cell fate and morphogenetic movement in the late mouse primitive streak. *Mech Dev* **55**, 79 (Mar, 1996).
7. C. C. Lu, E. J. Robertson, Multiple roles for Nodal in the epiblast of the mouse embryo in the establishment of anterior-posterior patterning. *Dev Biol* **273**, 149 (Sep 1, 2004).
8. P. P. Tam, M. Parameswaran, S. J. Kinder, R. P. Weinberger, The allocation of epiblast cells to the embryonic heart and other mesodermal lineages: the role of ingression and tissue movement during gastrulation. *Development* **124**, 1631 (May, 1997).
9. A. Moorman, S. Webb, N. A. Brown, W. Lamers, R. H. Anderson, Development of the heart: (1) formation of the cardiac chambers and arterial trunks. *Heart* **89**, 806 (Jul, 2003).
10. T. Brade, L. S. Pane, A. Moretti, K. R. Chien, K. L. Laugwitz, Embryonic heart progenitors and cardiogenesis. *Cold Spring Harb Perspect Med* **3**, a013847 (Oct, 2013).
11. S. M. Meilhac, F. Lescroart, C. Blanpain, M. E. Buckingham, Cardiac cell lineages that form the heart. *Cold Spring Harb Perspect Med* **4**, a013888 (Sep, 2014).
12. F. Herrmann, A. Gross, D. Zhou, H. A. Kestler, M. Kuhl, A boolean model of the cardiac gene regulatory network determining first and second heart field identity. *Plos One* **7**, e46798 (2012).
13. M. Buckingham, S. Meilhac, S. Zaffran, Building the mammalian heart from two sources of myocardial cells. *Nat Rev Genet* **6**, 826 (Nov, 2005).
14. K. L. Laugwitz, A. Moretti, L. Caron, A. Nakano, K. R. Chien, Islet1 cardiovascular progenitors: a single source for heart lineages? *Development* **135**, 193 (Jan, 2008).
15. L. Bu *et al.*, Human ISL1 heart progenitors generate diverse multipotent cardiovascular cell lineages. *Nature* **460**, 113 (Jul 2, 2009).

16. S. J. Kattman, T. L. Huber, G. M. Keller, Multipotent flk-1+ cardiovascular progenitor cells give rise to the cardiomyocyte, endothelial, and vascular smooth muscle lineages. *Dev Cell* **11**, 723 (Nov, 2006).
17. J. A. Epstein *et al.*, Migration of cardiac neural crest cells in Splotch embryos. *Development* **127**, 1869 (May, 2000).
18. X. Jiang, D. H. Rowitch, P. Soriano, A. P. McMahon, H. M. Sucov, Fate of the mammalian cardiac neural crest. *Development* **127**, 1607 (Apr, 2000).
19. A. C. Gittenberger-de Groot *et al.*, The arterial and cardiac epicardium in development, disease and repair. *Differentiation* **84**, 41 (Jul, 2012).
20. T. C. Katz *et al.*, Distinct compartments of the proepicardial organ give rise to coronary vascular endothelial cells. *Dev Cell* **22**, 639 (Mar 13, 2012).
21. M. R. Hutson, M. L. Kirby, Model systems for the study of heart development and disease. Cardiac neural crest and conotruncal malformations. *Semin Cell Dev Biol* **18**, 101 (Feb, 2007).
22. A. Keyte, M. R. Hutson, The neural crest in cardiac congenital anomalies. *Differentiation* **84**, 25 (Jul, 2012).
23. S. Zaffran, R. G. Kelly, S. M. Meilhac, M. E. Buckingham, N. A. Brown, Right ventricular myocardium derives from the anterior heart field. *Circ Res* **95**, 261 (Aug 6, 2004).
24. C. H. Mjaatvedt *et al.*, The outflow tract of the heart is recruited from a novel heart-forming field. *Dev Biol* **238**, 97 (Oct 1, 2001).
25. K. L. Waldo *et al.*, Conotruncal myocardium arises from a secondary heart field. *Development* **128**, 3179 (Aug, 2001).
26. C. Kelley, H. Blumberg, L. I. Zon, T. Evans, GATA-4 is a novel transcription factor expressed in endocardium of the developing heart. *Development* **118**, 817 (Jul, 1993).
27. R. G. Kelly, M. E. Buckingham, A. F. Moorman, Heart Fields and Cardiac Morphogenesis. *Cold Spring Harb Perspect Med* **4**, (2014).
28. J. Manner, J. M. Perez-Pomares, D. Macias, R. Munoz-Chapuli, The origin, formation and developmental significance of the epicardium: a review. *Cells Tissues Organs* **169**, 89 (2001).
29. O. M. Martinez-Estrada *et al.*, Wt1 is required for cardiovascular progenitor cell formation through transcriptional control of Snail and E-cadherin. *Nat Genet* **42**, 89 (Jan, 2010).
30. A. von Gise *et al.*, WT1 regulates epicardial epithelial to mesenchymal transition through beta-catenin and retinoic acid signaling pathways. *Dev Biol* **356**, 421 (Aug 15, 2011).
31. J. Lim, J. P. Thiery, Epithelial-mesenchymal transitions: insights from development. *Development* **139**, 3471 (Oct, 2012).
32. M. R. Hutson *et al.*, Cardiac arterial pole alignment is sensitive to FGF8 signaling in the pharynx. *Dev Biol* **295**, 486 (Jul 15, 2006).
33. S. E. Senyo, R. T. Lee, B. Kuhn, Cardiac regeneration based on mechanisms of cardiomyocyte proliferation and differentiation. *Stem Cell Res*, (Sep 28, 2014).

34. D. Kimelman, Mesoderm induction: from caps to chips. *Nat Rev Genet* **7**, 360 (May, 2006).
35. M. Nosedá, T. Peterkin, F. C. Simoes, R. Patient, M. D. Schneider, Cardiopoietic factors: extracellular signals for cardiac lineage commitment. *Circ Res* **108**, 129 (Jan 7, 2011).
36. C. Showell, O. Binder, F. L. Conlon, T-box genes in early embryogenesis. *Dev Dyn* **229**, 201 (Jan, 2004).
37. V. Kouskoff, G. Lacaud, S. Schwantx, H. J. Fehling, G. Keller, Sequential development of hematopoietic and cardiac mesoderm during embryonic stem cell differentiation. *Proc Natl Acad Sci U S A* **102**, 13170 (Sep 13, 2005).
38. L. Yang *et al.*, Human cardiovascular progenitor cells develop from a KDR+ embryonic-stem-cell-derived population. *Nature* **453**, 524 (May 22, 2008).
39. Y. Li, W. Yu, A. J. Cooney, R. J. Schwartz, Y. Liu, Brief report: Oct4 and canonical Wnt signaling regulate the cardiac lineage factor Mesp1 through a Tcf/Lef-Oct4 composite element. *Stem Cells* **31**, 1213 (Jun, 2013).
40. I. Costello *et al.*, The T-box transcription factor Eomesodermin acts upstream of Mesp1 to specify cardiac mesoderm during mouse gastrulation. *Nat Cell Biol* **13**, 1084 (Sep, 2011).
41. J. van den Aamele *et al.*, Eomesodermin induces Mesp1 expression and cardiac differentiation from embryonic stem cells in the absence of Activin. *EMBO Rep* **13**, 355 (Apr, 2012).
42. Y. Saga *et al.*, MesP1: a novel basic helix-loop-helix protein expressed in the nascent mesodermal cells during mouse gastrulation. *Development* **122**, 2769 (Sep, 1996).
43. Y. Saga *et al.*, MesP1 is expressed in the heart precursor cells and required for the formation of a single heart tube. *Development* **126**, 3437 (Aug, 1999).
44. F. Lescroart *et al.*, Early lineage restriction in temporally distinct populations of Mesp1 progenitors during mammalian heart development. *Nat Cell Biol* **16**, 829 (Sep, 2014).
45. Y. Saga, Genetic rescue of segmentation defect in MesP2-deficient mice by MesP1 gene replacement. *Mech Dev* **75**, 53 (Jul, 1998).
46. R. David *et al.*, MesP1 drives vertebrate cardiovascular differentiation through Dkk-1-mediated blockade of Wnt-signalling. *Nat Cell Biol* **10**, 338 (Mar, 2008).
47. A. Bondue *et al.*, Mesp1 acts as a master regulator of multipotent cardiovascular progenitor specification. *Cell Stem Cell* **3**, 69 (Jul, 2008).
48. R. C. Lindsley *et al.*, Mesp1 coordinately regulates cardiovascular fate restriction and epithelial-mesenchymal transition in differentiating ESCs. *Cell Stem Cell* **3**, 55 (Jul 3, 2008).
49. R. P. Harvey, Patterning the vertebrate heart. *Nat Rev Genet* **3**, 544 (Jul, 2002).

50. J. Han, J. D. Molkenin, Regulation of MEF2 by p38 MAPK and its implication in cardiomyocyte biology. *Trends Cardiovasc Med* **10**, 19 (Jan, 2000).
51. T. J. Lints, L. M. Parsons, L. Hartley, I. Lyons, R. P. Harvey, Nkx-2.5: a novel murine homeobox gene expressed in early heart progenitor cells and their myogenic descendants. *Development* **119**, 969 (Nov, 1993).
52. A. Bondue *et al.*, Mesp1 acts as a master regulator of multipotent cardiovascular progenitor specification. *Cell Stem Cell* **3**, 69 (Jul 3, 2008).
53. T. M. Schultheiss, J. B. Burch, A. B. Lassar, A role for bone morphogenetic proteins in the induction of cardiac myogenesis. *Genes Dev* **11**, 451 (Feb 15, 1997).
54. F. Reifers, E. C. Walsh, S. Leger, D. Y. Stainier, M. Brand, Induction and differentiation of the zebrafish heart requires fibroblast growth factor 8 (fgf8/acerebellar). *Development* **127**, 225 (Jan, 2000).
55. M. J. Marvin, G. Di Rocco, A. Gardiner, S. M. Bush, A. B. Lassar, Inhibition of Wnt activity induces heart formation from posterior mesoderm. *Genes Dev* **15**, 316 (Feb 1, 2001).
56. R. J. Arceci, A. A. King, M. C. Simon, S. H. Orkin, D. B. Wilson, Mouse GATA-4: a retinoic acid-inducible GATA-binding transcription factor expressed in endodermally derived tissues and heart. *Mol Cell Biol* **13**, 2235 (Apr, 1993).
57. S. W. Kubalak, W. C. Miller-Hance, T. X. O'Brien, E. Dyson, K. R. Chien, Chamber specification of atrial myosin light chain-2 expression precedes septation during murine cardiogenesis. *J Biol Chem* **269**, 16961 (Jun 17, 1994).
58. M. P. Gupta, M. Gupta, A. Stewart, R. Zak, Activation of alpha-myosin heavy chain gene expression by cAMP in cultured fetal rat heart myocytes. *Biochem Biophys Res Commun* **174**, 1196 (Feb 14, 1991).
59. S. D. Vincent, M. E. Buckingham, How to make a heart: the origin and regulation of cardiac progenitor cells. *Curr Top Dev Biol* **90**, 1 (2010).
60. R. G. Kelly, The second heart field. *Curr Top Dev Biol* **100**, 33 (2012).
61. E. D. Cohen, Y. Tian, E. E. Morrisey, Wnt signaling: an essential regulator of cardiovascular differentiation, morphogenesis and progenitor self-renewal. *Development* **135**, 789 (Mar, 2008).
62. E. Tzahor, Wnt/beta-catenin signaling and cardiogenesis: timing does matter. *Dev Cell* **13**, 10 (Jul, 2007).
63. O. W. Prall *et al.*, An Nkx2-5/Bmp2/Smad1 negative feedback loop controls heart progenitor specification and proliferation. *Cell* **128**, 947 (Mar 9, 2007).
64. A. Moretti *et al.*, Multipotent embryonic isl1+ progenitor cells lead to cardiac, smooth muscle, and endothelial cell diversification. *Cell* **127**, 1151 (Dec 15, 2006).

65. S. M. Wu *et al.*, Developmental origin of a bipotential myocardial and smooth muscle cell precursor in the mammalian heart. *Cell* **127**, 1137 (Dec 15, 2006).
66. C. L. Cai *et al.*, A myocardial lineage derives from Tbx18 epicardial cells. *Nature* **454**, 104 (Jul 3, 2008).
67. B. Zhou *et al.*, Epicardial progenitors contribute to the cardiomyocyte lineage in the developing heart. *Nature* **454**, 109 (Jul 3, 2008).
68. B. Zhou, A. von Gise, Q. Ma, J. Rivera-Feliciano, W. T. Pu, Nkx2-5- and Isl1-expressing cardiac progenitors contribute to proepicardium. *Biochem Biophys Res Commun* **375**, 450 (Oct 24, 2008).
69. J. J. McMurray, M. A. Pfeffer, Heart failure. *Lancet* **365**, 1877 (May 28-Jun 3, 2005).
70. K. Dickstein *et al.*, ESC guidelines for the diagnosis and treatment of acute and chronic heart failure 2008: the Task Force for the diagnosis and treatment of acute and chronic heart failure 2008 of the European Society of Cardiology. Developed in collaboration with the Heart Failure Association of the ESC (HFA) and endorsed by the European Society of Intensive Care Medicine (ESICM). *Eur J Heart Fail* **10**, 933 (Oct, 2008).
71. T. O. Cheng, Definition of heart failure. *Eur J Heart Fail* **1**, 433 (Dec, 1999).
72. , (Aug in Primary and Secondary Care: Partial Update, 2010).
73. J. M. Perez-Pomares, J. L. de la Pompa, Signaling during epicardium and coronary vessel development. *Circ Res* **109**, 1429 (Dec 9, 2011).
74. K. Kikuchi, K. D. Poss, Cardiac regenerative capacity and mechanisms. *Annu Rev Cell Dev Biol* **28**, 719 (2012).
75. P. W. Burridge, G. Keller, J. D. Gold, J. C. Wu, Production of de novo cardiomyocytes: human pluripotent stem cell differentiation and direct reprogramming. *Cell Stem Cell* **10**, 16 (Jan 6, 2012).
76. A. Aguirre, I. Sancho-Martinez, J. C. Izpisua Belmonte, Reprogramming toward heart regeneration: stem cells and beyond. *Cell Stem Cell* **12**, 275 (Mar 7, 2013).
77. V. F. Segers, R. T. Lee, Stem-cell therapy for cardiac disease. *Nature* **451**, 937 (Feb 21, 2008).
78. A. N. Patel *et al.*, Surgical treatment for congestive heart failure with autologous adult stem cell transplantation: a prospective randomized study. *J Thorac Cardiovasc Surg* **130**, 1631 (Dec, 2005).
79. B. E. Strauer, R. Kornowski, Stem cell therapy in perspective. *Circulation* **107**, 929 (Feb 25, 2003).
80. M. A. Laflamme, C. E. Murry, Heart regeneration. *Nature* **473**, 326 (May 19, 2011).
81. R. R. Miller, N. A. Awan, K. S. Maxwell, D. T. Mason, Sustained reduction of cardiac impedance and preload in congestive heart failure with the antihypertensive vasodilator prazosin. *N Engl J Med* **297**, 303 (Aug 11, 1977).

82. J. N. Cohn *et al.*, Effect of vasodilator therapy on mortality in chronic congestive heart failure. Results of a Veterans Administration Cooperative Study. *N Engl J Med* **314**, 1547 (Jun 12, 1986).
83. D. T. Mason, Afterload reduction and cardiac performance. Physiologic basis of systemic vasodilators as a new approach in treatment of congestive heart failure. *Am J Med* **65**, 106 (Jul, 1978).
84. J. Bayliss, M. Norell, R. Canepa-Anson, G. Sutton, P. Poole-Wilson, Untreated heart failure: clinical and neuroendocrine effects of introducing diuretics. *Br Heart J* **57**, 17 (Jan, 1987).
85. R. N. Doughty, A. Rodgers, N. Sharpe, S. MacMahon, Effects of beta-blocker therapy on mortality in patients with heart failure. A systematic overview of randomized controlled trials. *Eur Heart J* **18**, 560 (Apr, 1997).
86. B. E. Jaski, M. A. Fifer, R. F. Wright, E. Braunwald, W. S. Colucci, Positive inotropic and vasodilator actions of milrinone in patients with severe congestive heart failure. Dose-response relationships and comparison to nitroprusside. *J Clin Invest* **75**, 643 (Feb, 1985).
87. A. A. Matar, J. J. Chong, Stem cell therapy for cardiac dysfunction. *Springerplus* **3**, 440 (2014).
88. C. L. Mummery *et al.*, Differentiation of human embryonic stem cells and induced pluripotent stem cells to cardiomyocytes: a methods overview. *Circ Res* **111**, 344 (Jul 20, 2012).
89. P. Menasche, Stem cell therapy for heart failure: are arrhythmias a real safety concern? *Circulation* **119**, 2735 (May 26, 2009).
90. H. Song, S. K. Chung, Y. Xu, Modeling disease in human ESCs using an efficient BAC-based homologous recombination system. *Cell Stem Cell* **6**, 80 (Jan 8, 2010).
91. T. M. Jayawardena *et al.*, MicroRNA-mediated in vitro and in vivo direct reprogramming of cardiac fibroblasts to cardiomyocytes. *Circ Res* **110**, 1465 (May 25, 2012).
92. L. Qian *et al.*, In vivo reprogramming of murine cardiac fibroblasts into induced cardiomyocytes. *Nature* **485**, 593 (May 31, 2012).
93. Y. Zhang, Z. Wang, R. A. Gemeinhart, Progress in microRNA delivery. *J Control Release* **172**, 962 (Dec 28, 2013).
94. V. Ambros, The functions of animal microRNAs. *Nature* **431**, 350 (Sep 16, 2004).
95. D. P. Bartel, MicroRNAs: genomics, biogenesis, mechanism, and function. *Cell* **116**, 281 (Jan 23, 2004).
96. Y. Lee *et al.*, MicroRNA genes are transcribed by RNA polymerase II. *EMBO J* **23**, 4051 (Oct 13, 2004).
97. X. Cai, C. H. Hagedorn, B. R. Cullen, Human microRNAs are processed from capped, polyadenylated transcripts that can also function as mRNAs. *RNA* **10**, 1957 (Dec, 2004).

98. R. I. Gregory, T. P. Chendrimada, R. Shiekhattar, MicroRNA biogenesis: isolation and characterization of the microprocessor complex. *Methods Mol Biol* **342**, 33 (2006).
99. E. P. Murchison, G. J. Hannon, miRNAs on the move: miRNA biogenesis and the RNAi machinery. *Curr Opin Cell Biol* **16**, 223 (Jun, 2004).
100. E. Lund, J. E. Dahlberg, Substrate selectivity of exportin 5 and Dicer in the biogenesis of microRNAs. *Cold Spring Harb Symp Quant Biol* **71**, 59 (2006).
101. X. Ji, The mechanism of RNase III action: how dicer dices. *Curr Top Microbiol Immunol* **320**, 99 (2008).
102. T. M. Rana, Illuminating the silence: understanding the structure and function of small RNAs. *Nat Rev Mol Cell Biol* **8**, 23 (Jan, 2007).
103. D. S. Schwarz, P. D. Zamore, Why do miRNAs live in the miRNP? (vol 16, pg 1025, 2002). *Gene Dev* **16**, 1582 (Jun 15, 2002).
104. B. P. Lewis, I. H. Shih, M. W. Jones-Rhoades, D. P. Bartel, C. B. Burge, Prediction of mammalian microRNA targets. *Cell* **115**, 787 (Dec 26, 2003).
105. P. Maziere, A. J. Enright, Prediction of microRNA targets. *Drug Discov Today* **12**, 452 (Jun, 2007).
106. L. P. Lim *et al.*, Microarray analysis shows that some microRNAs downregulate large numbers of target mRNAs. *Nature* **433**, 769 (Feb 17, 2005).
107. M. Selbach *et al.*, Widespread changes in protein synthesis induced by microRNAs. *Nature* **455**, 58 (Sep 4, 2008).
108. D. Baek *et al.*, The impact of microRNAs on protein output. *Nature* **455**, 64 (Sep 4, 2008).
109. V. Ambros, MicroRNAs: genetically sensitized worms reveal new secrets. *Curr Biol* **20**, R598 (Jul 27, 2010).
110. N. Liu *et al.*, An intragenic MEF2-dependent enhancer directs muscle-specific expression of microRNAs 1 and 133. *Proc Natl Acad Sci U S A* **104**, 20844 (Dec 26, 2007).
111. Y. Zhao, E. Samal, D. Srivastava, Serum response factor regulates a muscle-specific microRNA that targets Hand2 during cardiogenesis. *Nature* **436**, 214 (Jul 14, 2005).
112. K. N. Ivey *et al.*, MicroRNA regulation of cell lineages in mouse and human embryonic stem cells. *Cell Stem Cell* **2**, 219 (Mar 6, 2008).
113. G. Zheng, Y. Tao, W. Yu, R. J. Schwartz, Brief report: SRF-dependent MiR-210 silences the sonic hedgehog signaling during cardiopoiesis. *Stem Cells* **31**, 2279 (Oct, 2013).
114. T. E. Callis *et al.*, MicroRNA-208a is a regulator of cardiac hypertrophy and conduction in mice. *J Clin Invest* **119**, 2772 (Sep, 2009).
115. Z. Lin *et al.*, miR-23a functions downstream of NFATc3 to regulate cardiac hypertrophy. *Proc Natl Acad Sci U S A* **106**, 12103 (Jul 21, 2009).

116. T. Thum *et al.*, MicroRNA-21 contributes to myocardial disease by stimulating MAP kinase signalling in fibroblasts. *Nature* **456**, 980 (Dec 18, 2008).
117. E. van Rooij *et al.*, Dysregulation of microRNAs after myocardial infarction reveals a role of miR-29 in cardiac fibrosis. *Proc Natl Acad Sci U S A* **105**, 13027 (Sep 2, 2008).
118. S. Nicoli *et al.*, MicroRNA-mediated integration of haemodynamics and Vegf signalling during angiogenesis. *Nature* **464**, 1196 (Apr 22, 2010).
119. E. M. Small, L. B. Sutherland, K. N. Rajagopalan, S. Wang, E. N. Olson, MicroRNA-218 regulates vascular patterning by modulation of Slit-Robo signaling. *Circ Res* **107**, 1336 (Nov 26, 2010).
120. K. R. Cordes *et al.*, miR-145 and miR-143 regulate smooth muscle cell fate and plasticity. *Nature* **460**, 705 (Aug 6, 2009).
121. R. Ji *et al.*, MicroRNA expression signature and antisense-mediated depletion reveal an essential role of MicroRNA in vascular neointimal lesion formation. *Circ Res* **100**, 1579 (Jun 8, 2007).
122. L. Elia *et al.*, The knockout of miR-143 and -145 alters smooth muscle cell maintenance and vascular homeostasis in mice: correlates with human disease. *Cell Death Differ* **16**, 1590 (Dec, 2009).
123. S. Albinsson *et al.*, MicroRNAs are necessary for vascular smooth muscle growth, differentiation, and function. *Arterioscler Thromb Vasc Biol* **30**, 1118 (Jun, 2010).
124. S. Ikeda *et al.*, Altered microRNA expression in human heart disease. *Physiol Genomics* **31**, 367 (Nov 14, 2007).
125. S. J. Matkovich *et al.*, Reciprocal regulation of myocardial microRNAs and messenger RNA in human cardiomyopathy and reversal of the microRNA signature by biomechanical support. *Circulation* **119**, 1263 (Mar 10, 2009).
126. T. Thum *et al.*, MicroRNAs in the human heart: a clue to fetal gene reprogramming in heart failure. *Circulation* **116**, 258 (Jul 17, 2007).
127. C. Voellenkle *et al.*, MicroRNA signatures in peripheral blood mononuclear cells of chronic heart failure patients. *Physiol Genomics* **42**, 420 (Aug, 2010).
128. S. Fichtlscherer *et al.*, Circulating microRNAs in patients with coronary artery disease. *Circ Res* **107**, 677 (Sep 3, 2010).
129. X. Ji *et al.*, Plasma miR-208 as a biomarker of myocardial injury. *Clin Chem* **55**, 1944 (Nov, 2009).
130. J. Elmen *et al.*, LNA-mediated microRNA silencing in non-human primates. *Nature* **452**, 896 (Apr 17, 2008).
131. R. E. Lanford *et al.*, Therapeutic silencing of microRNA-122 in primates with chronic hepatitis C virus infection. *Science* **327**, 198 (Jan 8, 2010).
132. N. Cloonan *et al.*, MicroRNAs and their isomiRs function cooperatively to target common biological pathways. *Genome Biol* **12**, R126 (2011).

133. Y. Hayashita *et al.*, A polycistronic microRNA cluster, miR-17-92, is overexpressed in human lung cancers and enhances cell proliferation. *Cancer Res* **65**, 9628 (Nov 1, 2005).
134. J. Wang *et al.*, Bmp signaling regulates myocardial differentiation from cardiac progenitors through a MicroRNA-mediated mechanism. *Dev Cell* **19**, 903 (Dec 14, 2010).
135. E. Dirkx *et al.*, Nfat and miR-25 cooperate to reactivate the transcription factor Hand2 in heart failure. *Nat Cell Biol* **15**, 1282 (Nov, 2013).
136. A. Eulalio *et al.*, Functional screening identifies miRNAs inducing cardiac regeneration. *Nature* **492**, 376 (Dec 20, 2012).
137. L. T. Bish *et al.*, Adeno-associated virus (AAV) serotype 9 provides global cardiac gene transfer superior to AAV1, AAV6, AAV7, and AAV8 in the mouse and rat. *Hum Gene Ther* **19**, 1359 (Dec, 2008).
138. A. B. Katwal *et al.*, Adeno-associated virus serotype 9 efficiently targets ischemic skeletal muscle following systemic delivery. *Gene Ther* **20**, 930 (Sep, 2013).
139. S. T. Pleger *et al.*, Cardiac AAV9-S100A1 gene therapy rescues post-ischemic heart failure in a preclinical large animal model. *Sci Transl Med* **3**, 92ra64 (Jul 20, 2011).
140. Y. Ying *et al.*, Heart-targeted adeno-associated viral vectors selected by in vivo biopanning of a random viral display peptide library. *Gene Ther* **17**, 980 (Aug, 2010).
141. K. D. Foust *et al.*, Intravascular AAV9 preferentially targets neonatal neurons and adult astrocytes. *Nat Biotechnol* **27**, 59 (Jan, 2009).
142. A. Geisler *et al.*, microRNA122-regulated transgene expression increases specificity of cardiac gene transfer upon intravenous delivery of AAV9 vectors. *Gene Ther* **18**, 199 (Feb, 2011).
143. N. Chirmule *et al.*, Immune responses to adenovirus and adeno-associated virus in humans. *Gene Ther* **6**, 1574 (Sep, 1999).
144. A. D. Judge *et al.*, Sequence-dependent stimulation of the mammalian innate immune response by synthetic siRNA. *Nat Biotechnol* **23**, 457 (Apr, 2005).
145. M. F. Lu, C. Pressman, R. Dyer, R. L. Johnson, J. F. Martin, Function of Rieger syndrome gene in left-right asymmetry and craniofacial development. *Nature* **401**, 276 (Sep 16, 1999).
146. S. Sundararajan, M. Wakamiya, R. R. Behringer, J. A. Rivera-Perez, A fast and sensitive alternative for beta-galactosidase detection in mouse embryos. *Development* **139**, 4484 (Dec 1, 2012).
147. A. Bondue *et al.*, Defining the earliest step of cardiovascular progenitor specification during embryonic stem cell differentiation. *J Cell Biol* **192**, 751 (Mar 7, 2011).
148. M. Koshelev, S. Sarma, R. E. Price, X. H. Wehrens, T. A. Cooper, Heart-specific overexpression of CUGBP1 reproduces functional and molecular

- abnormalities of myotonic dystrophy type 1. *Hum Mol Genet* **19**, 1066 (Mar 15, 2010).
149. K. Michalczyk, M. Ziman, Nestin structure and predicted function in cellular cytoskeletal organisation. *Histol Histopathol* **20**, 665 (Apr, 2005).
 150. A. N. Ladd, N. Charlet-B, T. A. Cooper, The CELF family of RNA binding proteins is implicated in cell-specific and developmentally regulated alternative splicing. *Mol Cell Biol* **21**, 1285 (Feb, 2001).
 151. I. Vlasova-St Louis, P. R. Bohjanen, Coordinate regulation of mRNA decay networks by GU-rich elements and CELF1. *Curr Opin Genet Dev* **21**, 444 (Aug, 2011).
 152. B. Rattenbacher *et al.*, Analysis of CUGBP1 targets identifies GU-repeat sequences that mediate rapid mRNA decay. *Mol Cell Biol* **30**, 3970 (Aug, 2010).
 153. L. Ruiz-Llorente, S. Ardila-Gonzalez, L. F. Fanjul, O. Martinez-Iglesias, A. Aranda, microRNAs 424 and 503 are mediators of the anti-proliferative and anti-invasive action of the thyroid hormone receptor beta. *Oncotarget* **5**, 2918 (May 30, 2014).
 154. L. Yu *et al.*, MicroRNA-424 is down-regulated in hepatocellular carcinoma and suppresses cell migration and invasion through c-Myb. *Plos One* **9**, e91661 (2014).
 155. J. F. Mouillet *et al.*, The unique expression and function of miR-424 in human placental trophoblasts. *Biol Reprod* **89**, 25 (Aug, 2013).
 156. Y. Peng, Y. M. Liu, L. C. Li, L. L. Wang, X. L. Wu, microRNA-503 inhibits gastric cancer cell growth and epithelial-to-mesenchymal transition. *Oncol Lett* **7**, 1233 (Apr, 2014).
 157. Y. Zhang *et al.*, MiR-424-5p reversed epithelial-mesenchymal transition of anchorage-independent HCC cells by directly targeting ICAT and suppressed HCC progression. *Sci Rep* **4**, 6248 (2014).
 158. K. Wu *et al.*, MicroRNA-424-5p suppresses the expression of SOCS6 in pancreatic cancer. *Pathol Oncol Res* **19**, 739 (Oct, 2013).
 159. E. Merlet *et al.*, miR-424/322 regulates vascular smooth muscle cell phenotype and neointimal formation in the rat. *Cardiovasc Res* **98**, 458 (Jun 1, 2013).
 160. J. Kim *et al.*, An endothelial apelin-FGF link mediated by miR-424 and miR-503 is disrupted in pulmonary arterial hypertension. *Nat Med* **19**, 74 (Jan, 2013).
 161. S. Sarkar, B. K. Dey, A. Dutta, MiR-322/424 and -503 are induced during muscle differentiation and promote cell cycle quiescence and differentiation by down-regulation of Cdc25A. *Mol Biol Cell* **21**, 2138 (Jul 1, 2010).
 162. D. Llobet-Navas *et al.*, The miR-424/503 cluster reduces CDC25A expression during cell cycle arrest imposed by TGFbeta in mammary epithelial cells. *Mol Cell Biol*, (Sep 29, 2014).

163. A. Caporali *et al.*, Deregulation of microRNA-503 contributes to diabetes mellitus-induced impairment of endothelial function and reparative angiogenesis after limb ischemia. *Circulation* **123**, 282 (Jan 25, 2011).
164. A. Chamorro-Jorganes *et al.*, MicroRNA-16 and microRNA-424 regulate cell-autonomous angiogenic functions in endothelial cells via targeting vascular endothelial growth factor receptor-2 and fibroblast growth factor receptor-1. *Arterioscler Thromb Vasc Biol* **31**, 2595 (Nov, 2011).
165. T. Nakashima *et al.*, Down-regulation of mir-424 contributes to the abnormal angiogenesis via MEK1 and cyclin E1 in senile hemangioma: its implications to therapy. *Plos One* **5**, e14334 (2010).
166. G. Ghosh *et al.*, Hypoxia-induced microRNA-424 expression in human endothelial cells regulates HIF-alpha isoforms and promotes angiogenesis. *J Clin Invest* **120**, 4141 (Nov, 2010).
167. L. S. Qi *et al.*, Repurposing CRISPR as an RNA-guided platform for sequence-specific control of gene expression. *Cell* **152**, 1173 (Feb 28, 2013).
168. Y. H. Cui *et al.*, miR-503 represses CUG-binding protein 1 translation by recruiting CUGBP1 mRNA to processing bodies. *Mol Biol Cell* **23**, 151 (Jan, 2012).
169. J. Orłowski, J. B. Lingrel, Tissue-specific and developmental regulation of rat Na,K-ATPase catalytic alpha isoform and beta subunit mRNAs. *J Biol Chem* **263**, 10436 (Jul 25, 1988).
170. E. T. Wang *et al.*, Alternative isoform regulation in human tissue transcriptomes. *Nature* **456**, 470 (Nov 27, 2008).
171. A. J. Ward, M. Rimer, J. M. Killian, J. J. Dowling, T. A. Cooper, CUGBP1 overexpression in mouse skeletal muscle reproduces features of myotonic dystrophy type 1. *Hum Mol Genet* **19**, 3614 (Sep 15, 2010).
172. R. Cardani *et al.*, Overexpression of CUGBP1 in skeletal muscle from adult classic myotonic dystrophy type 1 but not from myotonic dystrophy type 2. *Plos One* **8**, e83777 (2013).
173. M. Koebis *et al.*, Alternative splicing of myomesin 1 gene is aberrantly regulated in myotonic dystrophy type 1. *Genes Cells* **16**, 961 (Sep, 2011).
174. Y. K. Kim, M. Mandal, R. S. Yadava, L. Paillard, M. S. Mahadevan, Evaluating the effects of CELF1 deficiency in a mouse model of RNA toxicity. *Hum Mol Genet* **23**, 293 (Jan 15, 2014).
175. D. S. Berger, A. N. Ladd, Repression of nuclear CELF activity can rescue CELF-regulated alternative splicing defects in skeletal muscle models of myotonic dystrophy. *PLoS Curr* **4**, RRN1305 (2012).
176. L. Kong *et al.*, Impaired synaptic vesicle release and immaturity of neuromuscular junctions in spinal muscular atrophy mice. *J Neurosci* **29**, 842 (Jan 21, 2009).
177. A. Marteyn *et al.*, Mutant human embryonic stem cells reveal neurite and synapse formation defects in type 1 myotonic dystrophy. *Cell Stem Cell* **8**, 434 (Apr 8, 2011).